Summer 8-15-2016

Molecular Mechanisms Mediating the Effects of Acute Dietary Vitamin A Deficiency on a Defined Model Human Gut Microbiota

Matthew Charles Hibberd
Washington University in St. Louis

WASHINGTON UNIVERSITY IN ST. LOUIS

Division of Biology and Biomedical Sciences

Molecular Microbiology and Microbial Pathogenesis

Dissertation Examination Committee:
Jeffrey I. Gordon, Chair
Gautam Dantas
Daniel E. Goldberg
Jeffrey P. Henderson
Scott J. Hultgren
Lora L. Iannotti
Clay F. Semenkovich

Molecular Mechanisms Mediating the Effects of Acute Dietary Vitamin A Deficiency on a Defined Model Human Gut Microbiota

by

Matthew Charles Hibberd

A dissertation presented to the
Graduate School of Arts and Sciences
of Washington University in
partial fulfillment of the
requirements for the degree
of Doctor of Philosophy

August 2016

St. Louis, Missouri

Table of Contents

Chapter 3

Future directions

Acknowledgments

We, though individuals, are products of the collective influences of our environment, and I count myself fortunate to be a product of a number of incredibly supportive and inspiring environments over the course of my personal and professional life. I am proud to count myself a product of the Gordon Lab and the steadfast and enthusiastic guidance of my thesis advisor Jeffrey Gordon. In reflecting on my time in the lab, I am awed by Jeff's ability to maintain in the lab an ecosystem populated with individuals who possess the professional qualities of creativity, intelligence, and enthusiasm and the personal qualities of empathy, graciousness, and generosity. Jeff leads these traits truly by example and expects that we hold ourselves to the same standard. In return, we are rewarded by an environment full of opportunity and support at a scale it takes (at least) the length of a PhD to truly comprehend. I feel incredibly fortunate to have had the opportunity to train under Jeff's guidance and learn alongside and from the extraordinarily talented individuals with whom I have shared the last many years in the lab.

I would also like to thank my thesis committee, in particular Daniel Goldberg, who deserves special gratitude for serving as my committee chair. I will always be grateful to my entire committee for their patient guidance and for the time each member devoted to attending my committee meetings and advising my work.

The opportunity to learn from a number of former and current CGS_SB and Gordon Lab affiliated individuals was formative in my early time in the lab. In particular, I would like to acknowledge Federico Rey, who mentored me on my rotation project, Mark Gonzalez, my first and longest-tenured bay-mate, and Jeremiah Faith, who contributed to many of the techniques I utilized in the work described in this dissertation. The current CGS_SB and Gordon Lab staff are truly a resource deserving of acknowledgement. Although so many individuals have been incredibly giving of their time and support, I would like to acknowledge in particular Sabrina Wagoner, Janaki Lelwala-Guruge, Maria Karlsson, David O'Donnell, Justin Serugo, Eric Martin, Brian Koebbe, Jessica Hoisington-Lopez, Su Deng, and Laura Kyro.

Collaborators outside the lab have played important roles in the development of my project from initiation to present. In particular, I must acknowledge Barb Mickelson at Envigo for assistance in research animal nutrition and diet formulation, Rich Giannone and Bob Hettich at Oak Ridge National Labs for work with bacterial proteomics, and Dmitry Rodionov and Andrei Osterman for comparative genomics and biochemical contributions.

None of my work would have been possible without support in part from the National Institutes of Health and the Bill & Melinda Gates Foundation.

I have also been fortunate enough to count many of my labmates and classmates as close friends outside the lab. I owe a special debt of gratitude to Vitas Wagner, Joe Planer, Nick Semenkovich, and Andy Kau for making the lab fun place to work and for sharing many good times outside the lab as well. My classmate Robin Cutler has been my closest friend since we met during orientation, and I would like to acknowledge Robin's constant support, patience as a cycling partner, and wise perspective as a colleague.

My parents Chuck and Janel Hibberd and my sister Katie have all contributed to my personal and professional life in distinct and important ways. My sister Katie has often provided a different perspective to my own but has always been supportive of my personal and professional choices. My mother Janel, a teacher by training and at heart, is a born inquisitor of the natural world, always insists on hearing my most recent developments (in the lab and otherwise), and constantly challenges me to find joy in whatever I do. My father, Chuck, has set an example, both personally and professionally, of high ethics and character, that I constantly aspire to achieve. My first exposure to science (and, though unappreciated at the time, both nutrition and intestinal microbes) was playing with toys hidden in a bottom drawer of his beef cattle nutrition lab and watching television projections of microscope images of bacteria from rumen fluid samples. My family, both immediate and extended (and in-law), has been a constant source of love and support – I do not possess the eloquence required to appropriately express my thanks.

More than any other individual, I owe my deepest gratitude to my wife, Ashley. She spans the roles of colleague, soulmate, and partner in adventure, and provides a constant source of love and support. I imagine all spouses make sacrifices for partners in graduate school, but I feel Ashley's willingness to move multiple states to support me in my educational pursuits and to support me through the challenges of life in graduate school go above and beyond. I am so very excited for what the future holds for us. It is to her that I dedicate this work.

Matthew C. Hibberd

Washington University in St. Louis

August 2016

ABSTRACT OF THE DISSERTATION

Molecular mechanisms mediating the effects of acute dietary vitamin A deficiency on a defined model human gut microbiota

by

Matthew Charles Hibberd

Doctor of Philosophy in Biology and Biomedical Sciences

Molecular Microbiology and Microbial Pathogenesis

Washington University in St. Louis, 2016

Professor Jeffrey I. Gordon, Chair

Micronutrient deficiencies represent a form of "hidden hunger" that afflict two billion people worldwide. To test the hypothesis that dietary micronutrient deficiency has differential effects on members of the human gut microbiota, a consortium containing 92 sequenced phylogenetically diverse bacterial strains was introduced into germ-free mice. Recipient animals were subjected to a diet oscillation that began with highly defined micronutrient-sufficient diet followed by a derivative diet with one of four types of single micronutrient deficiency, or a diet representing combined deficiencies, followed by return to the original sufficient diet. Times-series studies of microbial community structure and transcriptome revealed that acute vitamin A deficiency had the largest effects. *Bacteroides vulgatus*, a member of the developing microbiota associated with healthy growth of children, was a prominent responder, increasing its abundance in the absence of dietary vitamin A, and manifesting robust changes in gene expression affecting a number of metabolic and other pathways. *In vitro* studies of different retinoids revealed that retinol was the most potent inhibitor of *B. vulgatus* growth. Applying retinol selection to a library of 30,300 *B. vulgatus* transposon mutants revealed that disruption of AcrR, a member of the TetR family of transcriptional repressors, abrogated retinol sensitivity. Genetic complementation studies, *in vitro* RNA-Seq analysis, and transcription factor binding assays disclosed that AcrR (i) functions as a repressor

of an adjacent AcrAB-TolC efflux system (and of dispersed genes comprising a larger regulon) and (ii) mediates retinol sensitivity. Measurement of retinol efflux from wild-type, *acrR*-mutant, and complemented *acrR* mutant strains of *B. vulgatus*, combined with studies of the effects of a pharmacologic inhibitor of this efflux system and of bile acids on growth provided additional support that members of the AcrR regulon, including AcrAB-TolC, function as determinants of retinol and bile acid sensitivity in gut *Bacteroides*. Our findings raise the possibility that dietary retinol availability, bile acids generated by microbial biotransformation, and this efflux system interact to influence the fitness of *B. vulgatus* and perhaps other gut bacterial species.

Chapter 1

Introduction

The microbiota and micronutrient deficiencies in the context of global health

Humans are an amalgamation of human and microbial cells and genes. Our population of microbial cells is equal to or exceeds our population of human cells (Sender et al. 2016). The gut contains our largest community of microbes (the microbiota) and microbial genes (the microbiome), and is composed of members of all three domains of life – Eukarya, Archaea and Bacteria (and their viruses). Bacteria dominate the gut environment and are the best studied while the identities and activities of the eukaryotic and archaeal members of the microbiota are less well defined (Reyes et al. 2010; Marchesi 2010; Dutilh et al. 2014; Ogilvie et al. 2013; Parfrey et al. 2014). Bacteria in the gut are represented primarily by two phyla, the Bacteroidetes and the Firmicutes (Qin et al. 2010; HMP Consortium, 2012; Walker et al. 2011; G. D. Wu et al. 2011; Eckburg et al. 2005). A healthy adult living in the USA harbors ~100 species-level bacterial taxa and ≥200 strain-level taxa as judged by low-error sequencing of 16S rRNA amplicons (Faith et al. 2013). Significant interpersonal variations exist in bacterial community composition. Although many host-derived factors influence the configuration of the gut microbiota, arguably the most significant environmental determinant of microbial community structure is diet (Muegge et al. 2011; Faith et al. 2011; Walker et al. 2011; Carmody et al. 2015; Ussar et al. 2015).

Malnutrition, specifically undernutrition, is a significant global health challenge (Black et al. 2013; Bryce et al. 2005). An estimated 45% of all childhood deaths worldwide can be attributed directly or indirectly to various forms of undernutrition (Black et al. 2013). Moreover, the long term sequelae of childhood undernutrition - stunting, neurodevelopmental and immune defects - persist and are refractory to current therapies. Although food insecurity is an important factor in disease pathogenesis, it is not the only one; other factors, including enteropathogen burden, environmental enteric dysfunction, and perturbed postnatal development (maturation) of the gut microbiota appear to play causal roles (Blanton et al. 2016).

Dietary macronutrient deficiencies often produce more overt disease (Ahmed et al. 2014; Ahmed et al. 2009; Williams et al. 2003) than micronutrient (vitamin and mineral) deficiencies.

Thus, micronutrient deficiencies represent a form of "hidden hunger" (Muthayya et al. 2013). Epidemiologists estimate that micronutrient deficiencies afflict two billion people worldwide, with the greatest prevalence occurring in pregnant women and children under the age of five (Institute of Medicine (US) Committee on Micronutrient Deficiencies 1998; Bailey et al. 2015). It is clear that micronutrient deficiencies are highly prevalent in the developing world, are associated with poverty, and are part of an intergenerational cycle that involves pregnant mothers and their children (Bailey et al. 2015). Deficiencies of iron, vitamin A, folate, and zinc are of particular concern to global health organizations such as the World Health Organization, the United Nations Children's Fund, and the Bill & Melinda Gates Foundation due to their high prevalence and severity of morbidity and mortality associated with these deficiencies.

Iron deficiency

Iron is critically important for oxygen transport in the blood and cellular respiration in muscle. Dietary iron is derived from plant and animal sources in non-heme and heme forms, respectively (Stipanuk and Caudill 2013). In the body, iron resources are highly conserved (only 0.05% of body stores lost per day in humans) and iron access is tightly controlled by host iron transport and storage systems. High iron loss occurs during menstruation, pregnancy, and lactation, and during infections (Stipanuk and Caudill 2013); the combination of chronic dietary iron deficiency and iron loss due these factors can lead to iron deficiency. Iron deficiency, as evidenced primarily by high rates of microcytic anemia, is the most common nutritional disorder worldwide, afflicting some 30% of the world's population (McLean et al. 2009). Iron-deficiency anemia contributes to adverse pregnancy outcomes and maternal mortality; the offspring of iron deficient mothers begin life with iron deficiency, which has a significant negative impact on a variety of biological processes including immune function and psychomotor development (Baynes and Bothwell 1990).

Zinc deficiency

Zinc is an essential cofactor for a large number of enzymes and for the DNA binding activity of a variety of transcription factors; as such, it is important for healthy growth and development (Shankar and Prasad 1998; King 2011). Zinc is obtained in the diet primarily from animal products and whole grain cereals. A recent survey of zinc availability in national food supplies estimates a global prevalence of zinc inadequacy of 17% (Wessells and Brown 2012). Zinc bioavailability is also affected by dietary components that limit its absorption such as phytates (Brnić et al. 2014). The involvement of zinc in myriad cellular processes, combined with a lack of a specialized zinc storage system in the human body, makes zinc deficiency a significant impairment, with manifestations that include immune dysfunction and increased rates of diarrheal disease (Shankar and Prasad 1998; Rink and Gabriel 2000).

Vitamin A deficiency

Vitamin A is a class of essential fat-soluble compounds whose activities are important for vision, immune function, reproduction, and signal transduction cascades that are key to normal development (Stipanuk and Caudill 2013). Vitamin A is present in the diet in the form of retinyl esters from animal sources and provitamin A carotenoids from plant sources; both require additional metabolic processing before they can exert their biological functions. The fat solubility and storage characteristics of re-esterified vitamin A make it difficult for an individual who once had adequate vitamin A stores to become deficient due to dietary insufficiency alone. However, chronic exposure to rice-based diets with little fat to aid in or stimulate absorption can potentiate deficiency (Roels et al. 1958). Furthermore, the vitamin A status of mothers and their nursing infants is connected via breast milk, with the result that deficiency can also be transmitted intergenerationally (Stoltzfus and Underwood 1995). Vitamin A deficiency is the leading cause of blindness in children, impairs immune responses to infection, and can lead to significant mortality (Bailey et al. 2015; The World Health Organization 2009).

Folate deficiency

Folate is a water soluble B vitamin (B9) involved in the many facets of one-carbon metabolism, including DNA synthesis, repair, and methylation (Stipanuk and Caudill 2013). Folate is present primarily in plant-derived components of diet and is synthesized by members of the gut microbiota. Folate deficiency causes macrocytic anemia in children and can lead to significant developmental defects in the offspring of deficient mothers (Krishnaswamy and Nair 2007); moreover, epigenetic changes in the offspring of deficient mothers may contribute to some of the more chronic sequelae of deficiency (Guéant et al. 2013).

Multiple micronutrient deficiencies

Micronutrient deficiencies rarely exist in isolation; rather, the socioeconomic and cultural factors that contribute to food insecurity often lead to clustered deficiencies of multiple micronutrients (Muthayya et al. 2013; Bailey, West, and Black 2015). Furthermore, certain single micronutrient deficiencies can interact physiologically to potentiate other deficiencies and increase associated morbidities. Perhaps the most significant and best-studied examples of such an interaction occurs when iron deficiency anemia is potentiated by deficiencies in vitamin A or folic acid (Fishman, Christian, and West 2000; Schultink and Gross 1998). Additionally, zinc is required for proper mobilization of vitamin A stores in the liver (Smith et al. 1973).

Just as micronutrient deficiencies do not exist in isolation, these complex, nutritionally-propagated conditions are also not easily treated in isolation, as illustrated by treatment strategies for zinc deficiency (Solomons, Ruz, and Gibson 1999). The most direct method for treatment of micronutrient deficiency (or deficiencies) is administration of micronutrient supplements. Challenges associated with the production, distribution, and administration of purified supplements have led to more socially 'acceptable' and sustainable therapeutic efforts based on direct fortification of foods and dietary diversification (Bailey et al. 2015). Importantly, supplementation does not treat the dietary or cultural origins of a given deficiency (or deficiencies); hence, public health efforts have been directed at obtaining more holistic treatment and the need for deeper understanding

of the root causes of specific deficiencies. Fortification is an attractive method for creating foods with added nutritional value; however, the cultural acceptance of enhanced foods like β-carotene biofortified "Golden Rice" are limited due to local food traditions, political issues, and acceptance of genetically-modified crops (Ye et al. 2000).

The complex nature of multiple micronutrient deficiencies, interpersonal differences in dietary requirements, coupled with technical aspects of formulation and production of a "one size fits all" multiple micronutrient supplement, can lead to over-supplementation of one or more micronutrients. For example, the WHO-recommended maternal prophylactic dose of 300,000-400,000 international units (IU) of vitamin A (either in a single or two equal doses administered >24 hr apart), while intended to reduce maternal and infant vitamin A deficiencies, meets the criterion for acute toxicity in humans (Penniston and Tanumihardjo 2006). The efficacy and safety of high-dose vitamin A supplementation strategies have not been adequately studied. Moreover, strong evidence suggests that iron supplementation in the developing world can potentiate multiple infections, most notably malaria (Soofi et al. 2013; Veenemans et al. 2011; Sazawal et al. 2006). Thus, responsible and effective treatment of such deficiencies, without associated negative consequences, represents a challenging active problem in global public health.

Studies of micronutrient deficiency in gnotobiotic animal models

Gnotobiotic animal research has been a powerful tool for nutrition research since the inception of methods for rearing animals under germ-free conditions. More specifically, much of what is known currently about interactions between the gut microbiota and host micronutrient metabolism has been derived from historical gnotobiotic animal studies. An 'eternal' challenge of nutrition research is the paradox between studying humans directly, and systematically manipulating (and controlling) variables that are hypothesized to impact the interrelationships between diet, (gut) microbial community configuration, and host biological features/processes. Gnotobiotic animal models provide perhaps the best avenue for controlling experimental variables in an *in vivo* system. Highly-defined research diets can be formulated and administered. The composition of the

microbiota introduced into these animals can be manipulated. Replication is possible through the use of animals with defined genetic backgrounds and the capacity to control environmental conditions. Lines of conventionally-raised animals (e.g., rodents) can be re-derived as germ-free either by embryo transfer or by caesarian section. Gnotobiotic isolators are typically composed of clear, flexible vinyl with sealed gloved ports for within-isolator manipulations, HEPA-filtered inlets and outlets for circulation of room air, and a chambered docking port for bringing supplies into and biospecimens out of isolators. Both diets and water are sterilized by autoclaving or irradiation, along with any other experimental supplies (some heat-sensitive supplies require chemical sterilization by ethylene oxide gas treatment) before placement in the isolator.

B vitamins

Vitamins B1 (thiamine), B6 (pyridoxine), B7 (biotin), B9 (folic acid), and B12 (cobalamin) are synthesized by the small intestinal and colonic microbiota and absorbed to varying extent from these regions of the gut (Klipstein and Samloff 1966; Stevens and Hume 1998). The dietary B vitamin requirements of gnotobiotic animals are linked to their ability to scavenge microbiota-derived B vitamins by coprophagy (and cecotrophy in the case of rabbits) (National Research Council (US). Subcommittee on Laboratory Animal Nutrition 1995). Experimental folate deficiency has been shown to depend on both dietary deficiency and perturbation of the gut microbiota with antibiotics (Klipstein et al. 1973). Furthermore, experimental folate deficiency in gnotobiotic animals can be ameliorated by the introduction of an intact microbiota.

Bacterially-derived, labeled folate can be found in the tissues of human hosts (Camilo et al. 1996; Klipstein and Samloff 1966; Klipstein and Lipton 1970). Some have suggested that the ability of Lactobacillus spp. and Bifidobacterium spp. to produce B vitamins may contribute to their purported probiotic activities (O'Connor 2013).

Vitamins K and A

Early studies identified a requirement for dietary vitamin K (primarily K_2) in germfree but not conventionally-raised (CONV-R) animals (Wostmann 1981). Germfree rats consuming very low levels of dietary vitamin A survive four times longer than their CONV-R counterparts when fed the same diets (>40 weeks versus 8-10 weeks), even in the presence of outright symptoms of deficiency (Bieri et al. 1969; Rogers et al. 1971). More recent studies have linked vitamin A deficiency to enteric infections, suggesting an interaction between this vitamin, the immune system, and opportunistic or overt pathogens in the intestine (Curtale et al. 1995; Sommer et al. 1987). Additional indirect interactions between vitamin A, gut microbes, and the immune system may exist, as vitamin A deficiency has been linked to decreases in Th17 cells in the small intestine with concurrent reduction in the abundance of segmented filamentous bacteria (Cha et al. 2010).

Minerals

Intestinal microbes possess sophisticated direct and small molecule-mediated transport systems for iron and zinc. CONV-R rats and rabbits exhibit enhanced iron uptake and storage, and the presence of an intact gut microbiota ameliorates anemia on low-iron diets (Reddy et al. 1965; Reddy et al. 1972). Germfree rats also lose more iron in feces than CONV-R animals (Reddy et al. 1972). Germfree animals fed zinc-deficient diets exhibit lower dietary zinc requirements than CONV-R controls, suggesting a detrimental effect of the microbiota on zinc metabolism (Smith et al. 1972). More recent studies of germfree mice and chickens, colonized with microbiota of varying complexity, have shown the ecological importance of bacterial zinc acquisition systems: the effects are dependent on community context and host inflammatory state (Gielda and DiRita 2012; Pesciaroli et al. 2011; Liu et al. 2012).

Controlled manipulation of interactions between diet, the gut microbiota, and host: gnotobiotics, defined communities, and assay methods

At the time that many of the gnotobiotic animal studies described above were performed, multi-omic methods for mechanistic analyses of the effects of micronutrient deficiency on the microbiota (and host) were not available. Just as the use of defined experimental diets for gnotobiotic animals allows control over micronutrient exposure, defined communities of sequenced human gut bacteria provide an opportunity for hypothesis-generating and hypothesis-based experiments devoted to characterizing interactions between micronutrients and members of the microbiota. The popularity of defined microbial community experiments has grown with the expansion of gnotobiotic facilities, although the idea is certainly not new. In fact, early efforts by Schaedler and colleagues resulted in the generation and broad adoption of an early defined gut microbiota ("altered Schaedler flora" or ASF) (Schaedler et al. 1965; Dewhirst et al. 1999). The traditional use of the ASF was as a standardized microbial "background" introduced at birth in order to allow confirmation of specific pathogen-free status in animals residing in barrier facilities. More modern implementations of the defined community concept allow researchers to assemble well-characterized bacteria from strain repositories, such as the American Type Culture Collection (ATCC) and its German equivalent, the Deutsche Sammlung von Mikroorganismen und Zellkulturen GmbH (DSMZ). The use of organisms from these curated collections for defined community experiments was particularly attractive during the earlier years of microbial genome sequencing when generating a deep draft or finished genome was a very exhaustive and elaborate process. More recently, the dramatic increase in sequencing capacity and concurrent decrease in sequencing costs, improvements in genome assembly and annotation tools, and advances in the ability to culture bacterial members of a given human's gut microbiota have allowed defined communities to be assembled from sets of primary rather than 'domesticated' isolates (Goodman et al. 2011). Researchers can now assemble defined communities to complexities approaching the estimated complexity of the human communities they are intended to represent and introduce them into germfree recipient animals fed defined diets (Faith et al. 2011).

Regardless of the origin of defined community members, the ability to manipulate community membership is powerful for many reasons. On the technical side, such control allows for colonization of experimental animals with known organisms, and like the intended use of the ASF, enhances researchers' ability to detect contaminants. On the experimental side, hypothesis testing is potentiated by the ability to perform "add one (or more) in" or "leave one (or more) out" experiments, providing direct proof of an organisms' ability to influence the biological properties of other community members, the overall community, and/or host (Faith et al. 2014). The ability to interrogate defined microbial communities hinges on the possession or generation of draft quality or better genome sequences for all community members. Genome sequences allow *in silico* metabolic reconstructions to be performed and prototrophies and auxotrophies to be predicted. Methods such as short read shotgun sequencing of community DNA (Community Profiling by Sequencing; COPRO-Seq), microbial RNA-Seq, whole genome transposon mutagenesis (INSeq), and targeted or non-targeted mass spectrometry can be applied to characterize community structure and expressed functions in specified community and dietary contexts. COPRO-Seq avoids biases common to 16S rRNA sequencing (McNulty et al. 2011; McNulty et al., 2013; Faith et al., 2011), further, using the regions of the genome of each community member that discriminates it from other members in a defined community permits quantification of organism abundances at strain-level resolution. The low cost of sequencing and easy scalability of COPRO-Seq enables accurate detection of low abundance members. Microbial RNA-Seq allows the metatranscriptome of a microbial community or community members to be delineated using the same high-throughput short-read sequencing methods employed for COPRO-Seq (Rey et al. 2010). Possessing a defined set of sequenced genomes allows accurate mapping of short transcript reads to their genes of origin and more precise definition of gene and operon boundaries. Depth of interrogation is scalable, as it is for COPRO-Seq. Short-read transcriptional data can be normalized and analyzed at the level of a single community member, allowing a 'bottom-up' approach for delineating that member's responses and contribution to the community meta-transcriptome. These bottom-up analyses can complement top-down analyses of the entire community's metatranscriptomic response to ma-

nipulation of membership and/or diet. INsertion Sequencing (INSeq) is a method that marries genome-wide transposon mutagenesis with short-read sequencing technology and allows identification of the genetic determinants of fitness for members of a defined artificial human gut microbiota installed in gnotobiotic mice. Each INSeq library is composed of tens of thousands of transposon (Tn) mutants (single site of Tn insertion/strain; 10-25 Tn insertions/gene; typically >80% genes covered/genome). The *mariner* Tn vector contains MmeI sites positioned at each end, and digestion of microbial DNA prepared from the gut contents or feces of recipient gnotobiotic mice with this enzyme cleaves genomic DNA at a site 20-21 bp distal to the restriction enzyme's recognition site. The site of Tn insertion and the relative abundance of each Tn mutant in the input libraries introduced into mice and in the 'output' (e.g., fecal) communities recovered from these animals is defined using a protocol developed previously in our lab (Wu et al. 2015). Alternatively, the library can be subjected to *in vitro* selections and selected libraries analyzed as above, or arrayed to obtain individual mutants for further study.

Overview of the dissertation and hypotheses

I have created a gnotobiotic mouse model of acute dietary micronutrient deficiencies. Animals were colonized with a defined community of cultured, sequenced human gut-derived bacterial strains obtained from ATCC and DSMZ. The size and diversity of this model human gut community were unprecedented (92 organisms gavaged, of which 45.5 ± 1.8 colonize each mouse; 348,843 total annotated coding sequences). I hypothesized that Fe, Zn, folate and/or vitamin A deficiencies would have differential effects on the community that could impact the fitness and niche of its members. I also hypothesized that these effects of micronutrient deficiency may persist, particularly if the deficiency is experienced as the microbiota executes its developmental program during the first 2-3 years of postnatal life and impacts host development: under these circumstances the biological effects of micronutrient insufficiency may be felt even after the deficiency is 'corrected' by a dietary intervention.

I pursued my hypotheses by first introducing the defined community into germfree mice and subjecting the mice to a sequence of diet oscillations where a period of micronutrient sufficiency was followed by deficiency followed by a return to sufficiency. Groups of animals experienced either a single deficiency (Fe, Zn, folate, or vitamin A) or combined deficiencies (all four). A control group was maintained on a micronutrient sufficient diet throughout. The deficient diets were very well defined, with protein represented only by amino acids to avoid the potentially confounding problem of having to vary protein type between different experimental diets due to differences in baseline micronutrient content. Microbial responses to diet oscillations were initially defined using COPRO-Seq and microbial RNA-Seq. Analyses of the resulting large datasets revealed that vitamin A deficiency had the greatest impact on defined community structure and on the meta-transcriptome, with the strongest and most consistent response represented by an inverse correlation between dietary vitamin A content and the abundance of *Bacteroides vulgatus*. Follow-up INSeq, pharmacologic, genetic complementation, transcription factor binding and mass spectrometry-based proteomic and metabolic studies revealed a *B. vulgatus* regulon controlled by AcrR that included an AcrAB efflux system, which mediates the effects of vitamin A on the fitness of this organism. Together, these studies provide an unanticipated view of the effects of vitamin A on bacterial members of the human gut microbiota.

References

Ahmed, T, D Auble, J A Berkley, R Black, P P Ahern, M Hossain, A Hsieh, S Ireen, M Arabi, and J I Gordon. 2014. "An Evolving Perspective About the Origins of Childhood Undernutrition and Nutritional Interventions That Includes the Gut Microbiome." *Annals of the New York Academy of Sciences* 1332 (1): 22–38. doi:10.1111/nyas.12487.

Ahmed, T, S Rahman, and Al Cravioto. 2009. "Oedematous Malnutrition." *Indian J. Med. Res.* 130 (November): 651–54.

Bailey, R L, K P West Jr, and R E Black. 2015. "The Epidemiology of Global Micronutrient Deficiencies." *Annals of Nutrition and Metabolism* 66 (2): 22–33. doi:10.1159/000371618.

Baynes, R D, and T H Bothwell. 1990. "Iron Deficiency.." *Annual Review of Nutrition* 10: 133–48. doi:10.1146/annurev.nu.10.070190.001025.

Bieri, J G, E G McDaniel, and W E Rogers. 1969. "Survival of Germfree Rats Without Vitamin a.." *Science* 163 (3867): 574–75.

Black, R E, C G Victora, S P Walker, Z A Bhutta, P Christian, M de Onis, M Ezzati, et al. 2013. "Maternal and Child Undernutrition and Overweight in Low-Income and Middle-Income Countries.." *Lancet (London, England)* 382 (9890): 427–51. doi:10.1016/S0140-6736(13)60937-X.

Blanton, L V, M R Charbonneau, T Salih, M J Barratt, S Venkatesh, O Ilkaveya, S Subramanian, et al. 2016. "Gut Bacteria That Prevent Growth Impairments Transmitted by Microbiota From Malnourished Children.." *Science* 351 (6275): aad3311. doi:10.1126/science.aad3311.

Brnić, M, R Wegmüller, C Zeder, Gabriela Senti, and R F Hurrell. 2014. "Influence of Phytase, EDTA, and Polyphenols on Zinc Absorption in Adults From Porridges Fortified with Zinc Sulfate or Zinc Oxide.." *Journal of Nutrition* 144 (9). American Society for Nutrition: 1467–73. doi:10.3945/jn.113.185322.

Bryce, J, C Boschi-Pinto, K Shibuya, R E Black, WHO Child Health Epidemiology Reference Group. 2005. “WHO Estimates of the Causes of Death in Children..” *Lancet (London, England)* 365 (9465): 1147–52. doi:10.1016/S0140-6736(05)71877-8.

Camilo, E, J Zimmerman, J B Mason, B Golner, R Russell, J Selhub, and I H Rosenberg. 1996. “Folate Synthesized by Bacteria in the Human Upper Small Intestine Is Assimilated by the Host..” *Gastroenterology* 110 (4): 991–98.

Carmody, R N, G K Gerber, J M Luevano Jr, D M Gatti, L Somes, K L Svenson, and P J Turnbaugh. 2015. “Diet Dominates Host Genotype in Shaping the Murine Gut Microbiota.” *Cell Host and Microbe* 17 (1). Elsevier Inc.: 72–84. doi:10.1016/j.chom.2014.11.010.

Cha, H-R, S-Y Chang, J-H Chang, J-O Kim, J-Y Yang, C-H Kim, and M-N Kweon. 2010. “Downregulation of Th17 Cells in the Small Intestine by Disruption of Gut Flora in the Absence of Retinoic Acid..” *The Journal of Immunology* 184 (12). American Association of Immunologists: 6799–6806. doi:10.4049/jimmunol.0902944.

Charbonneau, M R, D O’Donnell, LV Blanton, SM Totten, J C C Davis, M J Barratt, J Cheng, et al. 2016. “Sialylated Milk Oligosaccharides Promote Microbiota-Dependent Growth in Models of Infant Undernutrition..” *Cell* 164 (5): 859–71. doi:10.1016/j.cell.2016.01.024.

Consortium, The Human Microbiome Project. 2012. “Structure, Function and Diversity of the Healthy Human Microbiome.” *Nature* 486: 207–14. doi:10.1038/nature11234.

Curtale, F, R P Pokhrel, R L Tilden, and G Higashi. 1995. “Intestinal Helminths and Xerophthalmia in Nepal. a Case-Control Study..” *Journal of Tropical Pediatrics* 41 (6): 334–37.

Dewhirst, F E, C C Chien, B J Paster, R L Ericson, R P Orcutt, D B Schauer, and J G Fox. 1999. “Phylogeny of the Defined Murine Microbiota: Altered Schaedler Flora..” *Applied and Environmental Microbiology* 65 (8): 3287–92.

Dutilh, B E, N Cassman, K McNair, SE Sanchez, Genivaldo G Z Silva, L Boling, J J Barr, et al. 2014. “A Highly Abundant Bacteriophage Discovered in the Unknown Sequences of Human Faecal Metagenomes..” *Nature Communications* 5: 4498. doi:10.1038/ncomms5498.

Eckburg, P B, E M Bik, C N Bernstein, E Purdom, L Dethlefsen, M Sargent, S R Gill, K E Nelson, and D A Relman. 2005. "Diversity of the Human Intestinal Microbial Flora.." *Science* 308 (5728). 1635–38. doi:10.1126/science.1110591.

Faith, J J, N P McNulty, F E Rey, and J I Gordon. 2011. "Predicting a Human Gut Microbiota's Response to Diet in Gnotobiotic Mice." *Science* 333 (6038). NIH Public Access: 101–4. doi:10.1126/science.1206025.

Faith, Jeremiah J, Janaki L Guruge, Mark Charbonneau, Sathish Subramanian, Henning Seedorf, Andrew L Goodman, Jose C Clemente, et al. 2013. "The Long-Term Stability of the Human Gut Microbiota.." *Science* 341 (6141). American Association for the Advancement of Science: 1237439. doi:10.1126/science.1237439.

Faith, J J, P P Ahern, V K Ridaura, J Cheng, and J I Gordon. 2014. "Identifying gut microbe-host phenotype relationships using combinatorial communities in gnotobiotic mice." *Science Translational Medicine*, *6*(220), 220ra11–220ra11. http://doi.org/10.1126/scitranslmed.3008051

Fishman, S M, P Christian, and K P West. 2000. "The Role of Vitamins in the Prevention and Control of Anaemia.." *Public Health Nutrition* 3 (2): 125–50.

Gielda, Lindsay M, and Victor J DiRita. 2012. "Zinc Competition Among the Intestinal Microbiota.." *mBio* 3 (4): e00171–12. doi:10.1128/mBio.00171-12.

Goodman, A L, G Kallstrom, J J Faith, A Reyes, A Moore, G Dantas, and J I Gordon. 2011. "Extensive Personal Human Gut Microbiota Culture Collections Characterized and Manipulated in Gnotobiotic Mice.." *Proceedings of the National Academy of Sciences USA* 108 (15): 6252–57. doi:10.1073/pnas.1102938108.

Guéant, J-L, F Namour, R-M Guéant-Rodriguez, and J-L Daval. 2013. "Folate and Fetal Programming: a Play in Epigenomics?." *Trends in Endocrinology and Metabolism: TEM* 24 (6): 279–89. doi:10.1016/j.tem.2013.01.010.

Institute of Medicine (US) Committee on Micronutrient Deficiencies, Howson, C. P., Kennedy, E. T., & Horwitz, A. (1998). Prevention of Micronutrient Deficiencies: Tools for Policymakers and Public Health Workers. http://doi.org/10.17226/5962

King, J C. 2011. “Zinc: an Essential but Elusive Nutrient..” In, 94:679S–84S. American Society for Nutrition. doi:10.3945/ajcn.110.005744.

Klipstein, F A, and I M Samloff. 1966. “Folate Synthesis by Intestinal Bacteria..” *The American Journal of Clinical Nutrition* 19 (4): 237–46.

Klipstein, F A, and S D Lipton. 1970. “Intestinal Flora of Folate-Deficient Mice..” *The American Journal of Clinical Nutrition* 23 (2): 132–40.

Klipstein, F A, S D Lipton, and E A Schenk. 1973. “Folate Deficiency of the Intestinal Mucosa..” *The American Journal of Clinical Nutrition* 26 (7): 728–37.

Krishnaswamy, Kamala, and K Madhavan Nair. 2007. “Importance of Folate in Human Nutrition.” *British Journal of Nutrition* 85 (S2). Cambridge University Press: S115–24. doi:10.1079/BJN2000303.

Liu, J Z, S Jellbauer, A J Poe, V Ton, M Pesciaroli, T E Kehl-Fie, N A Restrepo, et al. 2012. “Zinc Sequestration by the Neutrophil Protein Calprotectin Enhances Salmonella Growth in the Inflamed Gut.” *Cell Host and Microbe* 11 (3): 227–39. doi:10.1016/j.chom.2012.01.017.

Marchesi, J R. 2010. “Prokaryotic and Eukaryotic Diversity of the Human Gut..” *Advances in Applied Microbiology* 72: 43–62. doi:10.1016/S0065-2164(10)72002-5.

McLean, E, M Cogswell, I Egli, D Wojdyla, and Bde Benoist. 2009. “Worldwide Prevalence of Anaemia, WHO Vitamin and Mineral Nutrition Information System, 1993-2005..” *Public Health Nutrition* 12 (4). Cambridge University Press: 444–54. doi:10.1017/S1368980008002401.

McNulty, N P, T Yatsunenko, A Hsiao, J J Faith, B D Muegge, A L Goodman, B Henrissat, et al. 2011. “The Impact of a Consortium of Fermented Milk Strains on the Gut Microbiome of Gnotobiotic Mice and Monozygotic Twins..” *Science Translational Medicine* 3 (106): 106ra106. doi:10.1126/scitranslmed.3002701.

McNulty, N P, M Wu, A R Erickson, C Pan, B K Erickson, E C Martens, et al. 2013. “Effects of Diet on Resource Utilization by a Model Human Gut Microbiota Containing Bacteroides cellulosilyticus WH2, a Symbiont with an Extensive Glycobiome.” *PLOS Biology*, *11*(8), e1001637. http://doi.org/10.1371/journal.pbio.1001637.s023

Muegge, B D, J Kuczynski, D Knights, J C Clemente, A Gonzalez, L Fontana, B Henrissat, R Knight, and J I Gordon. 2011. “Diet Drives Convergence in Gut Microbiome Functions Across Mammalian Phylogeny and Within Humans..” *Science* 332 (6032). American Association for the Advancement of Science: 970–74. doi:10.1126/science.1198719.

Muthayya, S, J H Rah, J D Sugimoto, F F Roos, K Kraemer, and R E Black. 2013. “The Global Hidden Hunger Indices and Maps: an Advocacy Tool for Action..” *PLoS ONE* 8 (6). Public Library of Science: e67860. doi:10.1371/journal.pone.0067860.

National Research Council (US). Subcommittee on Laboratory Animal Nutrition. 1995. *Nutrient Requirements of Laboratory Animals*. National Academies Press.

Ogilvie, Lesley A, Lucas D Bowler, Jonathan Caplin, Cinzia Dedi, David Diston, Elizabeth Cheek, Huw Taylor, James E Ebdon, and Brian V Jones. 2013. “Genome Signature-Based Dissection of Human Gut Metagenomes to Extract Subliminal Viral Sequences..” *Nature Communications* 4: 2420. doi:10.1038/ncomms3420.

O’Connor, E M. 2013. “The Role of Gut Microbiota in Nutritional Status.” *Current Opinion in Clinical Nutrition and Metabolic Care* 16 (5): 509–16. doi:10.1097/MCO.0b013e3283638eb3.

Parfrey, L W, W A Walters, C L Lauber, J C Clemente, D Berg-Lyons, C Teiling, C Kodira, et al. 2014. “Communities of Microbial Eukaryotes in the Mammalian Gut Within the Context of Environmental Eukaryotic Diversity..” *Frontiers in Microbiology* 5. Frontiers: 298. doi:10.3389/fmicb.2014.00298.

Penniston, K L, and S A Tanumihardjo. 2006. “The Acute and Chronic Toxic Effects of Vitamin a..” *The American Journal of Clinical Nutrition* 83 (2): 191–201.

Pesciaroli, M, F Aloisio, S Ammendola, C Pistoia, P Petrucci, M Tarantino, M Francia, A Battistoni, and P Pasquali. 2011. “An Attenuated Salmonella Enterica Serovar Typhimurium Strain Lacking the ZnuABC Transporter Induces Protection in a Mouse Intestinal Model of Salmonella Infection..” *Vaccine* 29 (9): 1783–90. doi:10.1016/j.vaccine.2010.12.111.

Qin, J, R Li, J Raes, M Arumugam, K Solvsten Burgdorf, C Manichanh, T Nielsen, et al. 2010. “A Human Gut Microbial Gene Catalogue Established by Metagenomic Sequencing..” *Nature* 464 (7285): 59–65. doi:10.1038/nature08821.

Reddy, B S, J R Pleasants, and B S Wostmann. 1972. “Effect of Intestinal Microflora on Iron and Zinc Metabolism, and on Activities of Metalloenzymes in Rats..” *The Journal of Nutrition* 102 (1): 101–7.

Reddy, B S, J R Pleasants, D R Zimmerman, and B S Wostmann. 1965. “Iron and Copper Utilization in Rabbits as Affected by Diet and Germfree Status..” *The Journal of Nutrition* 87 (2): 189–96.

Rey, F E, J J Faith, J Bain, M J Muehlbauer, R D Stevens, C B Newgard, and J I Gordon. 2010. “Dissecting the in Vivo Metabolic Potential of Two Human Gut Acetogens.” *Journal of Biological Chemistry* 285 (29): 22082–90. doi:10.1074/jbc.M110.117713.

Reyes, A, M Haynes, N Hanson, F E Angly, A C Heath, F Rohwer, and J I Gordon. 2010. “Viruses in the Faecal Microbiota of Monozygotic Twins and Their Mothers.” *Nature* 466 (7304). Nature Publishing Group: 334–38. doi:10.1038/nature09199.

Rink, L, and P Gabriel. 2000. “Zinc and the Immune System..” *The Proceedings of the Nutrition Society* 59 (4): 541–52.

Roels, O A, M Trout, and R Dujacquier. 1958. “Carotene Balances in Boys in Ruanda Where Vitamin a Deficiency Is Prevalent..” *The Journal of Nutrition* 65 (1): 115–27.

Rogers, W E, J G Bieri, and E G McDaniel. 1971. “Vitamin a Deficiency in the Germfree State..” *Federation Proceedings* 30 (6): 1773–78.

Sazawal, S, R E Black, M Ramsan, H M Chwaya, R J Stoltzfus, A Dutta, U Dhingra, et al. 2006. “Effects of Routine Prophylactic Supplementation with Iron and Folic Acid on Admission to Hospital and Mortality in Preschool Children in a High Malaria Transmission Setting: Community-Based, Randomised, Placebo-Controlled Trial..” *Lancet)* 367 (9505): 133–43. doi:10.1016/S0140-6736(06)67962-2.

Schaedler, R W, R Dubos, and R Costello. 1965. “Association of Germfree Mice with Bacteria Isolated From Normal Mice.” *The Journal of Experimental Medicine* 122 (1). The Rockefeller University Press: 77–82.

Schultink, W, and R Gross. 1998. *The Influence of Vitamin a on Iron Status and Possible Consequences for Micronutrient Deficiency Alleviation Programs. Micronutrient Interactions: Impact ….* International Life Sciences Institute. Washington.

Sender, R, S Fuchs, and R Milo. 2016. “Are We Really Vastly Outnumbered? Revisiting the Ratio of Bacterial to Host Cells in Humans..” *Cell* 164 (3): 337–40. Shankar, A H, and A S Prasad. 1998. “Zinc and Immune Function: the Biological Basis of Altered Resistance to Infection..” *The American Journal of Clinical Nutrition* 68 (2 Suppl): 447S–463S.

Smith, J C, E G McDaniel, F F Fan, and J A Halsted. 1973. “Zinc: a Trace Element Essential in Vitamin a Metabolism..” *Science* 181 (4103): 954–55.

Smith, J C, E G McDaniel, L D McBean, F S Doft, and J A Halsted. 1972. “Effect of Microorganisms Upon Zinc Metabolism Using Germfree and Conventional Rats.” *The Journal of Nutrition* 102 (6): 711–19.

Solomons, N W, M Ruz, and R S Gibson. 1999. “Single-Nutrient Interventions with Zinc..” *The American Journal of Clinical Nutrition* 70 (1): 111–13.

Sommer, A, I Tarwotjo, and J Katz. 1987. “Increased Risk of Xerophthalmia Following Diarrhea and Respiratory Disease..” *The American Journal of Clinical Nutrition* 45 (5): 977–80.

Soofi, S, S Cousens, S P Iqbal, T Akhund, J Khan, I Ahmed, A K M Zaidi, and ZA Bhutta. 2013. “Effect of Provision of Daily Zinc and Iron with Several Micronutrients on Growth and Morbidity Among Young Children in Pakistan: a Cluster-Randomised Trial..” *Lancet* 382 (9886): 29–40. doi:10.1016/S0140-6736(13)60437-7.

Stevens, C E, and I D Hume. 1998. “Contributions of Microbes in Vertebrate Gastrointestinal Tract to Production and Conservation of Nutrients..” *Physiological Reviews* 78 (2): 393–427.

Stipanuk, M H, and M A Caudill. 2013. *Biochemical, Physiological, and Molecular Aspects of Human Nutrition*. Elsevier Health Sciences.

Stoltzfus, R J, and B A Underwood. 1995. “Breast-Milk Vitamin a as an Indicator of the Vitamin a Status of Women and Infants..” *Bulletin of the World Health Organization* 73 (5). World Health Organization: 703–11.

Subramanian, S, S Huq, T Yatsunenko, R Haque, M Mahfuz, M A Alam, A Benezra, et al. 2014. “Persistent Gut Microbiota Immaturity in Malnourished Bangladeshi Children..” *Nature* 510 (7505): 417–21. doi:10.1038/nature13421.

The World Health Organization. 2009. “Global Prevalence of Vitamin a Deficiency in Populations at Risk 1995-2005,” pp. 1–68.

Ussar, S, N W Griffin, O Bezy, S Fujisaka, S Vienberg, Sr Softic, L Deng, L Bry, J I Gordon, and C R Kahn. 2015. “Interactions Between Gut Microbiota, Host Genetics and Diet Modulate the Predisposition to Obesity and Metabolic Syndrome.” *Cell Metabolism* 22 (3). Elsevier: 516–30. doi:10.1016/j.cmet.2015.07.007.

Veenemans, J, P Milligan, A M Prentice, L R A Schouten, N Inja, Aafke C van der Heijden, L C C de Boer, et al. 2011. “Effect of Supplementation with Zinc and Other Micronutrients on Malaria in Tanzanian Children: a Randomised Trial.” *PLoS Medicine* 8 (11). Public Library of Science: e1001125. doi:10.1371/journal.pmed.1001125.

Walker, A W, J Ince, S H Duncan, L M Webster, G Holtrop, X Ze, D Brown, et al. 2011. “Dominant and Diet-Responsive Groups of Bacteria Within the Human Colonic Microbiota..” *The ISME Journal* 5 (2): 220–30. doi:10.1038/ismej.2010.118.

Wessells, K R, and K H Brown. 2012. “Estimating the Global Prevalence of Zinc Deficiency: Results Based on Zinc Availability in National Food Supplies and the Prevalence of Stunting..” *PLoS ONE* 7 (11). Public Library of Science: e50568. doi:10.1371/journal.pone.0050568.

Williams, C D, B M Oxon, and H Lond. 2003. *Kwashiorkor: a Nutritional Disease of Children Associated with a Maize Diet. 1935. Bulletin of the World Health Organization*. Vol. 81. World Health Organization.

Wostmann, B S. 1981. The Germfree Animal in Nutritional Studies. *Annual Review of Nutrition* 1: 257–79. doi:10.1146/annurev.nu.01.070181.001353.

Wu, G D, J Chen, C Hoffmann, KBittinger, Y-Yu Chen, S A Keilbaugh, M Bewtra, et al. 2011. “Linking Long-Term Dietary Patterns with Gut Microbial Enterotypes.” *Science* 334 (6052): 105–8. doi:10.1126/science.1208344.

Wu, M, N P McNulty, D A Rodionov, M S Khoroshkin, N W Griffin, J Cheng, P Latreille, et al. 2015. “Genetic Determinants of in Vivo Fitness and Diet Responsiveness in Multiple Human Gut Bacteroides..” *Science* 350 (6256). American Association for the Advancement of Science: aac5992. doi:10.1126/science.aac5992.

Ye, X, S Al-Babili, A Klöti, J Zhang, P Lucca, P Beyer, and I Potrykus. 2000. “Engineering the Provitamin a (Beta-Carotene) Biosynthetic Pathway Into (Carotenoid-Free) Rice Endosperm..” *Science* 287 (5451): 303–5.

Chapter 2

Molecular mechanisms mediating the effects of acute dietary vitamin A deficiency on a model human gut microbiota

Molecular mechanisms mediating the effects of acute dietary vitamin A deficiency on a model human gut microbiota

Matthew C. Hibberd[1,2], Meng Wu[1], Dmitry A. Rodionov[3,4], Xiaoqing Li[3], Jiye Cheng[1,2], Nick Griffin[1,2], Ansel Hsaio[1,2], Michael Barratt[1,2], Andrei L. Osterman[4], and Jeffrey I. Gordon[1,2*]

[1]Center for Genome Sciences and Systems Biology and [2]Center for Gut Microbiome and Nutrition Research, Washington University, St. Louis, MO 63108 USA.

[3]A. A. Kharkevich Institute for Information Transmission Problems, Russian Academy of Sciences, Moscow 127994, Russia

[4]Infectious and Inflammatory Disease Center, Sanford Burnham Prebys Medical Discovery Institute, La Jolla, 92037 CA USA.

*Correspondence to: jgordon@wustl.edu

Abstract

Micronutrient deficiencies represent a form of "hidden hunger" that afflict two billion people worldwide. To test the hypothesis that dietary micronutrient deficiency has differential effects on members of the human gut microbiota, a consortium containing 92 sequenced phylogenetically diverse bacterial strains was introduced into germ-free mice. Recipient animals were subjected to a diet oscillation that began with highly defined micronutrient-sufficient diet followed by a derivative diet with one of four types of single micronutrient deficiency, or a diet representing combined deficiencies, followed by return to the original sufficient diet. Times-series studies of microbial community structure and transcriptome revealed that acute vitamin A deficiency had the largest effects. *Bacteroides vulgatus*, a member of the developing microbiota associated with healthy growth of children, was a prominent responder, increasing its abundance in the absence of dietary vitamin A, and manifesting robust changes in gene expression affecting a number of metabolic and other pathways. *In vitro* studies of different retinoids revealed that retinol was the most potent inhibitor of *B. vulgatus* growth. Applying retinol selection to a library of 30,300 *B. vulgatus* transposon mutants revealed that disruption of AcrR, a member of the TetR family of transcriptional repressors, abrogated retinol sensitivity. Genetic complementation studies, *vitro* RNA-Seq analysis, and transcription factor binding assays disclosed that AcrR (i) functions as a repressor of an adjacent AcrAB-TolC efflux system (and of dispersed genes comprising a larger regulon) and (ii) mediates retinol sensitivity. Measurement of retinol efflux from wild-type, *acrR*-mutant, and complemented *acrR* mutant strains of *B. vulgatus*, combined with studies of the effects of a pharmacologic inhibitor of this efflux system and of bile acids on growth provided additional support that members of the AcrR regulon, including AcrAB-TolC, function as determinants of retinol and bile acid sensitivity in gut *Bacteroides*. Our findings raise the possibility that dietary retinol availability, bile acids generated by microbial biotransformation, and this efflux system interact to influence the fitness of *B. vulgatus* and perhaps other gut bacterial species.

Introduction

Dietary micronutrients (vitamins and minerals) are cofactors for many enzymes whose functions are essential for health. The "hidden hunger" of micronutrient deficiencies represents a global health challenge, affecting 2 billion individuals, with inadequate iron, zinc, folate and vitamin A representing the major contributors to this problem (Bailey et al. 2015; Institute of Medicine Committee on Micronutrient Deficiencies, 1998). Pregnant women and children are particularly vulnerable to micronutrient deficiencies. A meta-analysis of 16 controlled clinical studies of 'multiple micronutrient powders' conducted in 6-month to 11-year old children living in developing countries found no evidence of significant effects on linear growth, despite improvements in micronutrient status (Salam et al., 2013). These disappointing results raise questions about what features of deficiency states we are failing to repair with current interventions, whether current protocols for dosing and duration of treatment are adequate, and whether unappreciated and unintended deleterious effects accompany such interventions. For example, the WHO-recommended dose of vitamin A for treatment of childhood deficiency meets the criterion for acute toxicity in humans (Penniston and Tanumihardjo, 2006), while iron supplementation may potentiate the risk for certain infections (e.g., malaria) (Soofi et al. 2013; Veenemans et al. 2011; Sazawal et al. 2006).

Recent studies have revealed a program of gut microbial community development, defined by the changing patterns of abundance of a group of age-discriminatory bacterial strains, that is executed during the first 2-3 years of postnatal life. This developmental program, which is shared among healthy biologically unrelated infants/children living in culturally and geographically distinct low income countries, is disrupted in infants and children with undernutrition, resulting in community configurations that appear younger (more immature) compared to those encountered in chronologically age-matched individuals with healthy growth phenotypes (Subramanian et al., 2014; Blanton et al., 2016a,b). Preclinical evidence indicates that this immaturity is not simply an effect of undernutrition but a contributing cause: recently weaned gnotobiotic mice colonized with immature gut microbiota samples from undernourished Malawian children manifest impaired growth compared to recipients of microbiota from chronologically-aged matched healthy donors,

even though animals in all treatment groups consumed the same amounts of a macro- and micronutrient deficient diet designed to resemble the diets of the microbiota donor population (Blanton et al., 2016a). Analysis of the microbiota of recipient mice identified bacterial strains that are growth discriminatory: they include a subset of the age-discriminatory strains. These observations suggest a testable hypothesis: namely, that various types of micronutrient deficiencies may disrupt various features of a developing microbiota. Moreover, such disruptions, occurring during a critical period of community assembly, may persistent, with resulting deleterious effects on host biology.

Earlier studies comparing germ-free animals and their conventionally-raised counterparts provided evidence that the gut microbiota can have beneficial effects in the face of micronutrient deficiencies (e.g., enhanced iron uptake and storage in rats and rabbit models; Reddy et al., 1965; 1972), or detrimental effects [increased mortality on vitamin A-deficient diets (Bieri et al., 1969; Rogers et al., 1971), and increased dietary zinc requirements (Smith et al., 1972; Reddy et al., 1972) in rats]. The specific microbes and underlying mechanisms responsible for these observed effects were not defined in these reports.

In the current study, we examine the effects of acute micronutrient deficiencies on members of the microbiota using gnotobiotic mice colonized with a large and phylogenetically diverse consortium of cultured and sequenced human gut bacterial strains, including strains representing species that are age- and/or growth-discriminatory in Random Forests-derived models of microbiota development. Mice were subjected to a diet oscillation that began with highly defined micronutrient-sufficient diet followed by a derived diet with one of four types of single micronutrient deficiency, or a diet representing combined deficiencies, followed by return to the original micronutrient sufficient diet. This model of acute deficiency allowed us to focus on primary microbiota effects rather than having to disentangle potentially cofounding effects of combined community and host deficiency states. Community DNA- and mRNA-level analysis, combined with *in vitro* genetic, biochemical and pharmacologic studies allowed us to characterize the mechanisms that underlie the pronounced effects of vitamin A deficiency on a growth-discriminatory bacterial species.

Results

The micronutrient sufficient diet and the derivative diets devoid of one or more micronutrients were all well-defined compositionally with protein represented only by amino acids to avoid the potentially confounding problem of having to vary protein type due to differences in their content of bound minerals (**Table S1**). Adult (8-9 week old) germ-free C57Bl/6J mice that had consumed a standard mouse chow, rich in plant polysaccharides and low in fat, since weaning were placed on the micronutrient-sufficient diet for four days prior to colonization. Mice then received a single oral gavage of a consortium of 92 sequenced human gut-derived bacterial type strains, containing 348,834 known or predicted protein-coding genes, encompassing the major phyla present in the human microbiota; 16 of these strains represented species corresponding to strains that had been identified as age- and/or growth-discriminatory in Random Forests-derived models of normal gut microbiota development (**Table S2**). Members of each treatment group (n=5 cohoused animals/group) were maintained on the micronutrient sufficient diet for 14 days, followed by a 21-day period of acute micronutrient deficiency, followed by a 14 day period of re-exposure to the micronutrient-sufficient diet. A control group was maintained on the micronutrient sufficient diet throughout the course of the experiment (**Figure 1A**). All diets were given *ad libitum*.

Short-read shotgun sequencing (COmmunity PROfiling by Sequencing; COPRO-Seq) of DNA prepared from fecal samples collected over time was used to define the efficiency and reproducibility of colonization within and across treatment groups, and the relative abundance of each community member as a function of diet. A group of 44 strains comprised a core group of organisms that was represented in the fecal microbiota of members of all treatment groups at the end of the first diet phase; the number of additional strains found in each treatment group was small (range 0-3) (**Table S3A,B**): this similarity in community membership across treatment groups at the end of this stage of the experiment was reflected in principal coordinates analysis (PCoA) of pairwise comparisons using the Bray-Curtis dissimilarity metric (**Figure 1B)**.

Dietary vitamin A deficiency has the greatest effect on community structure and meta-transcriptome

We applied mixed-effects linear models to log-transformed, rarefied COPRO-Seq data to identify organisms with significant interactions between treatment group and diet stage. We also performed least-squares means comparisons between mice in the control group monotonously fed the nutrient sufficient diet and those assigned to the experimental treatments (**Table 1**). Communities sampled at the end of the initial micronutrient sufficient diet phase (experimental day 14), 14 days after switch to the deficient diet (day 28) and 14 days after return to the sufficient diet (day 49) were included in the analyses. The results revealed that among the five acute dietary deficiency states tested, vitamin A had the greatest effect on community structure, significantly impacting the abundances of the largest number of organisms (**Table S3A-G, Table S4A-C**).

We subsequently used microbial RNA-Seq to characterize transcriptional responses to the various diets: data generated from samples collected from each mouse in each treatment group at the end of the micronutrient sufficiency phase (day 14), the end of the micronutrient deficiency phase (day 35), and 14 days after return to the sufficient diet (day 49) were compared; statistically significant differences in gene expression as a function of time/diet were identified using DESeq2 (see *Methods*); responsive genes were binned into KEGG Pathways and KEGG Orthology (KO) groups. Analogous to the COPRO-Seq analysis, animals consuming the micronutrient sufficient diet monotonously served as a reference control for temporal effects independent of diet transitions.

Table S5A-H describes the results of this community-wide (top-down) analysis for all treatment groups. Vitamin A deficiency elicited a larger number of significant alterations in the meta-transcriptome than any of the other acute deficiency states (summarized in **Table S5A**): the two top ranked KOs that incorporated transcripts whose expression changed significantly as a function of the presence and absence of vitamin A were K02014 (‘TonB dependent receptors’), K00936 (‘phosphotransferases with a nitrogenous group as acceptor’) (**Table S5B**).

The relative abundance of *B. vulgatus* increased significantly during the vitamin A deficiency phase and decreased significantly when mice were transitioned back to the sufficient diet: mixed effects linear modeling revealed that no other single micronutrient deficiency produced a statistically significant increase in its representation. The only other single micronutrient deficient state that affected its representation was iron but the change occurred in a direction opposite to those observed with vitamin A. (**Table 1**). The direction and specificity of the response to vitamin A deficiency was remarkable, as none of the other *Bacteroides* in the community exhibited this pattern (**Table S4**).

The specificity and distinctive breadth of *B. vulgatus*' responses to vitamin A availability were also evident in the microbial RNA-Seq dataset (see **Table S6A-G** for a KO-level summary of significant changes in its *in vivo* gene expression profile in response to diet oscillations involving vitamin A, iron, zinc, or folate, and combined deficiency, as well as in the control group monotonously fed the micronutrient sufficient diet, and **Table S7A-T** for a KO-level summary of transcriptional responses for each member of the gut community represented in the vitamin A treatment group). Acute dietary vitamin A deficiency did not produce a significant change in body weight in these adult animals: this was also true for all of the deficiency states (**Table S8**).

Identification of a member of the TetR family of transcriptional repressors that mediates the retinol sensitivity of *B. vulgatus*

To examine the mechanisms underlying the *in vivo* response of *B. vulgatus* ATCC 8482 to dietary vitamin A availability, we incubated the strain *in vitro*, under anaerobic conditions, in a defined medium, with or without supplementation of a range of concentrations of retinol, retinal, retinyl palmitate, all-trans retinoic acid or β-carotene; the diterpene alcohol geranylgeraniol was used as a control. Retinoid sensitivity was defined as the ratio between the time required to reach an OD_{600} threshold of 0.3 for treated cultures versus control cultures containing vehicle alone (0.2% DMSO). The concentration range of retinol (and other retinoids) used was based on previous reports of levels in small intestinal and fecal contents of mice and humans (Liu et al. 2008; Hernandez-Alvarez

et al. 2015). Treatment with 10 μM retinol completely inhibited the growth of *B. vulgatus*; retinal and retinyl palmitate produced significantly reduced levels of growth inhibition compared to retinol and geranylgeraniol had no significant effect (**Figure 2A,B, Table S9A**). A primary isolate of *B. vulgatus* recovered from a Malawian child, characterized as a growth-discriminatory strain in the gnotobiotic mouse experiments described in the *Introduction* (Blanton et al., 2016a), also exhibited marked, dose-dependent growth suppression in the presence of retinol (**Figure 2C, Table S9B**). Consistent with the responses documented *in vivo* to the dietary vitamin A oscillation where *B. dorei* exhibited increased abundance in the presence compared to absence of vitamin A (**Table S4**), retinol induced significantly less inhibition of the growth of this organism *in vitro* than *B. vulgatus* (**Figure 2B, Table S9B**).

Whole genome transposon mutagenesis (INsertion Sequencing, INSeq; Goodman et al., 2009; Wu et al., 2015) was subsequently used to identify the genetic determinants of the response of *B. vulgatus* ATCC 8482 to retinol. A library of 30,300 isogenic Tn mutants was generated (see *Methods*): 71% (2894) of the strain's predicted ORFs contained Tn mutants positioned within their proximal 80% (average of 10.5 Tn mutants/ORF represented in the library; 1 Tn/strain) (**Figure S1A**). Simulating the number of unique mutants required to cover all non-essential ORFs revealed that the INSeq library approached saturation (**Figure S1B**).

The library of Tn mutants was subjected to *in vitro* selection in the presence of 10 μM retinol. Aliquots were withdrawn from primary cultures during lag and stationary phases. An aliquot from the stationary phase culture was then re-inoculated into fresh medium containing 10 μm retinol for a second round of selection: log and stationary phase samples were withdrawn from these secondary cultures (n=3 replicate primary and secondary cultures; **Figure 3A**). The selected *B. vulgatus* libraries contained only four mutants (**Figure 3B**). These mutants map to two adjacent genes in the *B. vulgatus* ATCC 8482 genome; *BVU0240* encoding an homolog of *E. coli* AcrR (17% identity, 22% similarity), a member of the TetR family of transcription factors, and *BVU0241*, encoding a homolog of *E. coli* LpxA (33% identity, 35% similarity), a UDP-N-acetylglucosamine O-acyltransferase which functions as the first enzyme in the biosynthetic path-

way for the lipid A moiety of lipopolysaccharide (transfers (*R*)-2-hydroxymyristate from its acyl carrier protein thioester to the 3'OH of UDP-N-acetylglucosamine; Crowell et al. 1986). Control, DMSO-treated cultures displayed no selection for these mutants in either the primary or secondary cultures.

As shown in **Figure 3C**, the *acrR* ortholog is positioned in the middle of a locus containing 12 similarly-oriented ORFs. Three ORFs located upstream of *acrR* and three ORFs located immediately downstream each encode the orthologs of components of the *E. coli* AcrAB-TolC complex. AcrAB-TolC is the prototypic example of multidrug efflux systems from the Resistance-Nodulation-Cell Division (RND) superfamily (**Figure 3D**). Its AcrB component is a homotrimeric integral inner membrane transporter powered by a proton gradient. TolC is also a homotrimer and resides in the outer membrane. AcrA, a homohexamer, is a periplasmic adapter protein that bridges AcrB and TolC. Substrates are captured in the lower cleft region of AcrB (through a process determined in part by an associated small accessory protein AcrZ), transported through the binding pocket, the gate, and finally to the AcrA funnel that connects AcrB to TolC (Du et al. 2014, Kim et al. 2015).

Monocultures of each mutant strain exhibited a marked decrease in retinol sensitivity compared to wild-type (WT) (**Figure 3E**). To confirm that the *B. vulgatus* AcrR ortholog was a key regulator of the retinol sensitivity phenotype, we used the integrating expression vector pNBU2_tetQ to complement the mutant containing the Tn at genomic location 361472 (138 nucleotides downstream of the start of the AcrR ORF). To do so, the BVU0240 (AcrR) ORF and the 21 nt intergenic region between *BVU0240* and *BVU0241* were linked to the promoter of *rpoD* (*BVU2738*) (**Figure S2, Table S10** and *Methods*). The recombinant plasmid was amplified in *E. coli* S17 λpir, and conjugated into the *B. vulgatus acrR_361472::IN* (abbreviated *acrR::IN*) strain. PCR of erythromycin- and tetracycline-resistant transformants verified insertion at the *attBV* site positioned at the 3' end of *BVU2094* (one of two serine tRNAs in the *B. vulgatus* genome). Complementation of *acrR::IN* with the vector carrying *PrpoD_acrR* restored retinol sensitivity to wild-type levels,

while complementation of *acrR::IN* with the empty pNBU2_tetQ vector had no effect on retinol sensitivity (**Figure 2F**; **Table S9C,D**).

Characterizing the regulon controlled by AcrR

Having established that *acrR* (*BVU0240*) is a key genetic determinant of retinol sensitivity *in vitro*, we characterized its regulon. Triplicate cultures of the WT, *acrR::IN* and *lpxA_362422::IN* (abbreviated *lpxA::IN*) strains were grown to mid-log phase under control (0.2% DMSO) and treated (10 μM retinol/0.2% DMSO) conditions (since WT *B. vulgatus* does not grow in the presence of this concentration of retinol, microbial RNA-Seq could not be performed for this strain under this treatment condition). Expression of the *lpxA* ortholog (*BVU0241*) was completely ablated by the Tn insertion in its ORF. Low levels of expression of *acrR* was detectable in the *acrR::IN* mutant but all reads mapped to the area encompassed by the 5' 138 nucleotides of the gene, indicating that only truncated transcripts derived from the region of *BVU0240* upstream of the Tn insertion site at genome coordinate 361472 were being produced.

Analysis of the transcriptional profiles of untreated (DMSO control) cells identified 220 genes with statistically significant differences in their expression (DESeq2) in the *acrR::IN* mutant vs WT comparison, and 165 genes in the *lpxA::IN* mutant vs WT comparison with 92 genes common to both sets of differentially expressed genes (**Figure 4A**; note that the fold differences in expression of these 92 genes between the WT versus *acrR::IN* and the WT versus *lpxA::IN* mutants were highly correlated with Pearson's $r = 0.92$, $p<0.000001$) (**Table S11**). The putative 92 gene regulon included groups of genes belonging to KEGG pathways involved in (i) 'amino sugar and nucleotide sugar metabolism' (6 genes, downregulated in Tn mutants), 'cationic antimicrobial peptide (CAMP) resistance/beta-lactam resistance' (5 genes, upregulated except for BVU0238), 'sulfur metabolism/purine metabolism' (4 genes, upregulated), 'alanine, aspartate and glutamate metabolism' (3 genes, upregulated) (**Figure 4A, Table S11**). Transcription of the 12 gene locus containing *acrR* and *lpxA* was affected in similar ways by Tn mutagenesis of either gene: expression of upstream genes was significantly increased and expression of downstream genes signifi-

cantly decreased (DESeq2) (**Figure 4B**, **Table S11**). Together, these results support a conclusion that the AcrR encoded by *BVU0240* acts as a transcriptional repressor whose normal function can be disrupted either by direct insertional inactivation, or by polar effects of the Tn insertion in the upstream *BVU0241* (*lpxA*) gene.

Inspection of the RNA-Seq datasets generated from the fecal microbiota of mice in the vitamin A treatment group disclosed that 24 genes in the putative regulon identified from the *in vitro* analysis were differentially expressed *in vivo* (Pathways; see **Table S11**). However, none of the AcrAB-TolC locus components were defined as being differentially regulated *in vivo* by DESeq2.

Comparison of the genomes of other *Bacteroides* strains represented in the defined community, other human gut *Bacteroides*, and other members of the family Bacteroidaceae demonstrated that *acrR* orthologs are positioned in loci containing genes encoding components of multidrug efflux systems belonging to the Resistance-Nodulation-Cell Division (RND) superfamily (**Figure 5A, Table S12**). **Figure S3** presents a phylogenetic tree of AcrR orthologs identified in these organisms (note that *B. dorei* has the highest degree of similarity; **Table S12B**).

We employed comparative genomics (see *Methods*) of *B. vulgatus* ATCC 8482 and related organisms to identify a conserved 30-bp palindrome as a candidate AcrR-binding motif (**Figure 5B,C**). Genome scans with this motif allowed reconstruction of AcrR regulons, including orthologs of *BVU0244-BVU0233* (**Table S12A**). As noted above, in *B. vulgatus* ATCC 8482 this gene cluster encodes two homologous AcrAB-TolC efflux pumps; however, their respective components only share 20-27% amino acid identity. Interestingly, in *B. thetaiotaomicron* and several other *Bacteroides* genomes, the AcrR-associated gene cluster is broken into two separate loci, each encoding one paralog of the AcrAB-TolC efflux system and preceded by a candidate AcrR binding site (**Figure 5A**, **Table S12A**), suggesting co-regulation by AcrR orthologs in these genomes.

Genomic searches yielded one additional locus in *B. vulgatus* ATCC 8482 (*BVU0421-BVU0415*) that is preceded by a high-scoring candidate AcrR-binding site (**Figure 5B**). This additional candidate AcrR target operon contains genes encoding an uncharacterized outer membrane

protein (*oma87*), sodium/sulfate symporter (*slt*), 3'-phosphoadenosine 5'-phosphosulfate (*cysQ*), adenylylsulfate kinase (*cysC*), and sulfate adenylyltransferase (*cysDN*). The latter enzymes are involved in the sulfate assimilation pathway. In *E. coli*, the initial steps in assimilation of sulfate during cysteine biosynthesis include sulfate uptake and sulfate activation by formation of adenosine 5'-phosphosulfate, conversion to 3'-phosphoadenosine 5'-phosphosulfate, and reduction to sulfite (Wirtz et al., 2005).

We subsequently used *in vitro* DNA-binding assays to test the predicted AcrR binding site and determine whether retinol or filtered cell extracts from *B. vulgatus* affects binding. The predicted 30 nt binding site upstream of the orthologous AcrAB-TolC operon in *B. dorei* has a single nucleotide mutation located inside the non-conserved center of the AcrR binding motif. $AcrR_{BV}$ and $AcrR_{BD}$ differ by three amino acid substitutions. Two mutations are located in the N-terminal DNA-binding domain, whereas a single mutation is positioned inside the effector binding domain. We also noticed that the annotated *BVU0240* ORF in *B. vulgatus* is 24-nt shorter than its ortholog in *B. dorei,* which encodes an additional eight amino acid segment at its N-terminus. This N-terminal sequence is conserved in AcrR orthologs across all analyzed *Bacteroides* spp., suggesting its functional relevance and that the site of initiation of translation of the transcript arising from *BVU0240* may have been previously mis-annotated. Therefore, we expressed the the full length and 'truncated' version of BVU0240, as well as its *B. dorei* DSMZ 17855 ortholog (BACDOR_0022), each fused to a Smt3-His6 tag, in *E. coli*. The recombinant proteins, termed $AcrR_{BV}$, $AcrR^*_{BV}$ (truncated version) and $AcrR_{BD}$, were purified, their tag removed, and their ability to bind the predicted DNA operator upstream of *BVU0244* (*acrA*) tested. Fluorescence Polarization Assay (FPA) yielded K_d values for $AcrR_{BV}$ and $AcrR_{BD}$ interacting with the tested DNA fragment of 18.5 ± 7 nM and 25 ± 10 nM, respectively. The truncated $AcrR^*_{BV}$ protein did not interact with the same target DNA fragment. Moreover, no appreciable binding was observed with full-length $AcrR_{BV}$ protein and a negative control target DNA (representing the binding site of the unrelated *B. thetaiotaomicron* AraR regulator of arabinose catabolism in the upstream region of *BT0356* (Chang et

al., 2015) (**Figure 5D**). Retinol treatment (125 μM) had no effect on the binding of either purified AcrR ortholog to target DNA.

These results were independently confirmed using an Electrophoresis Mobility Shift Assay (EMSA). Both full-length proteins showed comparable concentration-dependent binding with a ~ 50% shift at ~ 0.5 μM while no effect was observed using $AcrR^*_{BV}$ or the nonspecific (negative control) DNA fragment (**Figure 5E**). Adding retinol at concentrations up to 125 μM had no effect on binding affinity in this assay. [The binding affinity (EC50) of $AcrR_{BV}$ for its target DNA sequence estimated by EMSA is ~20-fold higher compared to FPA results. FPA assesses a thermodynamic equilibrium constant (K_d), whereas EMSA is intrinsically non-equilibrium, depending on the dynamics of complex dissociation (k_{off}). We considered the EMSA results as a qualitative verification, with the FPA results providing a more accurate quantitative assessment of binding affinity].

Further evidence that the AcrAB-TolC efflux system affects retinol sensitivity and the effects of bile acids

We hypothesized that the AcrAB-TolC efflux system that was upregulated when expression of the *acrR* repressor was abrogated operated to reduce local toxic concentrations of retinol in either the periplasm or cytoplasm. To test this hypothesis more directly, we measured the efflux of retinol from cultures of WT *B. vulgatus* and the isogenic *acrR::IN* and *PrpoD_acrR* complemented *acrR::IN* mutants. Equal numbers of stationary cells were resuspended in PBS containing cysteine and 10 μM retinol. LC-MS quantitation of retinol in cell free supernatants harvested at various time points during a 2h incubation revealed a statistically significant increase in extracellular retinol in the *B. vulgatus acrR::IN* mutant (where the efflux machinery is transcriptionally upregulated) but not in the WT or complemented strains **(Figure 6A)**.

We proceeded to treat cultures of *B. dorei*, which unlike *B. vulgatus* is resistant to the growth inhibition produced by retinol, with phenylalanine-arginine β-naphthylamide (PAβN), a known inhibitor of multidrug efflux systems including AcrAB-TolC (Renau et al., 1999). Treat-

ment of *B. dorei* with 5 or 25 μg/mL PAβN in the absence of retinol did not produce a significant effect on growth relative to untreated cultures (**Figure 6B**). Addition of 5 and 25 μg/mL PAβN in the presence of 10 μM retinol produced a significant increase in retinol sensitivity (**Figure 6C**, **Table S13A**). Treatment of *B. vulgatus* with PAβN resulted in a modest but statistically significant inhibition of growth (**Figure 6B**; **Table S13A**). *B. vulgatus* cultures treated with retinol do not display observable growth by OD_{600} measurement, and as such were not further affected by inhibition of the efflux machinery with PAβN (**Figure 6C**). Together, these results support the notion that AcrAB-TolC functions to mediate resistance to the growth inhibitory effects of retinol.

AcrAB-TolC has also been reported to confer resistance to bile acids (Thanassi et al. 1997). Therefore, we tested the bile sensitivity of the WT and *acrR::IN* strains of *B. vulgatus,* WT *B. dorei* DSM 17855, and WT *B. fragilis* NCTC 9343 (a known bile acid-resistant organism), using oxgall-impregnated disks. WT *B. vulgatus* displayed the greatest sensitivity, in parallel with its retinol sensitivity. The bile acid sensitivity of *B. vulgatus acrR::IN* mutant (upregulated expression of AcrAB-TolC) was significantly lower than that of the isogenic WT strain and not significantly different from that of *B. dorei* (**Figure 6D**, **Table S13B**).

Intriguingly, UPLC-MS analysis of fecal bile acid metabolites disclosed a significant increase in the proportional representation of β-tauro-muricholic acid sulfate in the vitamin A deficient and multiple deficient groups compared to the control group monotonously fed the micronutrient-sufficient diet (**Table S14**). Together, these results suggest a testable hypothesis: namely that dietary retinol availability, bile acid metabolites generated through biotransformation by members of the gut microbiota, and the AcrAB-TolC efflux system interact to influence the fitness of *B. vulgatus* and either directly or indirectly (through changes in the abundances/expressed biological properties of organisms like *B. vulgatus*) other components of a developing or fully assembled gut

community.

Prospectus

Results obtained from these studies invite a number of follow-up analyses. As noted above, tests of the interactions between the efflux pump, retinol and bile acid metabolites whose concentrations are affected by dietary vitamin A availability can be performed using the WT, *acrR::IN* and complemented *acrR::IN* strains of *B. vulgatus* and WT *B. dorei*.

The mechanism by which retinol suppresses growth of *B. vulgatus* when the activity of the AcrAB-TolC efflux pump is markedly reduced remains unclear. High resolution 2D-LC-MS/MS proteomics has been performed on WT and *acrR::IN* strains, each grown to mid-log phase in the presence or absence of 1 μM retinol to determine whether any *B. vulgatus* proteins are covalently modified with retinol.

The mechanisms underlying the discordant sensitivities of WT *B. vulgatus* and *B. dorei* to retinol *in vitro* remain unexplained. This discordance is seen when monocultures are compared and when the two organisms are co-cultured in the presence of 10 μM retinol (resulting in the dominance of *B. dorei* by stationary phase in treated, but not untreated cultures) *(***Figure S4**). This discordance is mirrored by the opposing patterns of change in the relative abundances of each strain *in vivo* during the course of the dietary vitamin A oscillation. Low molecular weight cellular extracts (<3 kDa) prepared from WT strains of *B. vulgatus* and *B. dorei* harvested during log phase in the absence of retinol show negative (inhibitory) effects on binding of *B. vulgatus* AcrR and *B. dorei* AcrR to the AcrR target sequence (**Figure 6E**). Additional studies are needed to determine whether the different low molecular weight extracts, purified from the two different *Bacteroides* strains grown initially under permissive conditions and then exposed to different concentrations of retinol (and bile acid metabolites), produce different degrees of inhibition of $AcrR_{BD}$ and $AcrR_{BV}$ binding to their shared 30 nt target sequence, as judged by EMSA and/or FPA. Parallel qRT-PCR analysis of RNA isolated from these cells to define expression of AcrAB-TolC components, AcrR itself and other elements of the regulon (e.g., genes involved in sulfur metabolism) could also be

informative. Nonetheless, this observation suggests the existence of as yet unknown compounds that may operate as negative effectors (de-repressor) for these transcriptional regulators. Although the chemical nature of the de-repressing ligand(s) remain(s) unknown, strain-associated differences in levels (upon retinol treatment) may provide a mechanism for the observed discordant sensitivities of the two organisms.

Finally, these studies emphasize the importance of exploring the effects of applying specified dietary micronutrient deficiencies (vitamin A, various B vitamins, iron, zinc and other minerals) to gnotobiotic mice harboring (i) defined collections of cultured age- and growth-discriminatory human gut bacterial strains representing the different stages of assembly of the human gut microbiota, or (ii) intact uncultured normally developing microbiota from children with healthy growth phenotypes or immature microbiota from those with undernutrition. The results should not only allow dissection of the mechanisms by which micronutrients interact with community members and the products of their metabolism to shape microbiota and host development, but also may inform new approaches for more effectively treating (and ultimately preventing) the short and longer term sequelae of deficiency states.

Acknowledgements

We thank David O'Donnell, Maria Karlsson and Sabrina Wagner for their assistance with gnotobiotic mouse husbandry, Barb Mickelson at Envigo for her guidance in the design of the experimental diets, and Eric Martens at the University of Michigan for protocols and guidance regarding genetic manipulation of *B. vulgatus*. This work was supported in part by grants from the NIH (DK30292) and the Bill & Melinda Gates Foundation. Data deposition: COPRO-Seq, microbial RNA-Seq, and INSeq datasets have been deposited in the European Nucleotide Archive (ENA).

Materials and Methods

Bacterial strains and culture conditions

Reference type strains used in this study are listed **Table S2**. Strains were grown in Gut Microbiota Medium (GMM; Goodman et al., 2011) or Brain Heart Infusion agar (BHI, Becton-Dickinson, Maryland, USA) supplemented with 10% horse blood, under anaerobic conditions (atmosphere 5% H_2, 20% CO_2, 75% N_2) in a soft-sided plastic anaerobic chamber (Coy Laboratory Products, Michigan, USA). The identity of each strain was confirmed by sequencing full length 16S rRNA gene amplicons generated using the universal primers 8F and 1391R. Strains were arrayed into 96-well format and preserved in GMM containing 15% glycerol at -80°C. Additional manipulations of the arrayed collection were performed inside the anaerobic chamber using a Precision XS liquid-handling robot (Biotek Instruments, Inc.).

Primary human isolates of *Bacteroides vulgatus* (Blanton et al., 2016a) were revived from -80°C stocks and cultured anaerobically in BHI broth supplemented with L-cysteine (0.5g/L), L-histidine (0.2 mM), hematin (1.9 μM) and Vitamin K_3 (1 mg/L) (referred to as BHI+ broth) or on BHI-Blood plates. *Escherichia coli* S17 λpir was used for routine cloning and as a conjugation donor for genetic experiments involving *B. vulgatus*; it was grown in LB-Miller broth (BD Difco). Antibiotics were added to media as appropriate: ampicillin (100 μg/mL), erythromycin (25 μg/mL), tetracycline (2 μg/mL), and gentamicin (200 μg/mL).

Gnotobiotic animal husbandry

All experiments involving mice were performed using protocols approved by the Animal Studies Committee of the Washington University School of Medicine.

Diets - Experimental diets were custom designed and manufactured by Harlan Teklad/Envigo (Wisconsin, USA). Six diets were produced: four devoid of one of the micronutrients (vitamin A, iron, zinc, folic acid), one in which all four micronutrients were absent, and one where the levels of all of these micronutrients were sufficient. To design a consistent, defined base diet

for all experimental diets, a nutritionally-replete mixture of individual amino acids was used in place of complete protein. Custom vitamin and mineral mixes containing only the micronutrients appropriate to each diet were then added to the base diet to generate each experimental diet. Diets were measured into ~500 g portions and placed into 3 mm thick vacuum-sealed bags (Uline, Inc., Pleasant Praire, WI) and then placed in a second bag which was also vacuum-sealed. Diets were shipped overnight on ice for sterilization by gamma radiation (20 kGy-50 kGy; STERIS Corp, Mentor, OH). The nutritional characteristics of each irradiated diet were calculated based on diet formulation and are reported in **Table S1**.

Colonization of germ-free mice - A -80°C stock plate of the clonally arrayed culture collection was thawed in the anaerobic chamber. A 96-well, deep well plate (Thermo Scientific Nunc) was filled robotically with 960 µL of GMM broth. A 40 µL aliquot was withdrawn from each well of the clonally arrayed culture collection and inoculated into the recipient plate, which was then covered with an atmosphere-permeable seal (VWR). The inoculated plate was incubated under anaerobic conditions for 48 h at 37°C, after which time an aliquot of each well was assayed for growth by measuring OD_{600}. Equal volumes of each well culture were pooled, mixed, transferred to 1.8 mL crimp seal glass vials (Wheaton, NJ, USA) and sealed for transport to the gnotobiotic mouse facility. Vials were immediately fogged into gnotobiotic isolators and 500 µL of the pooled culture was introduced into each recipient germ-free mouse by oral gavage.

Adult male CF57BL/6J mice were maintained in a flexible plastic film gnotobiotic isolator and fed a nutritionally-sufficient standard diet (B&K autoclavable chow #7378000, Zeigler Bros Inc.) *ad libitum*. Four days prior to gavage of the defined 93-strain culture collection, all mice were transitioned to the nutritionally-sufficient replete experimental diet. On experimental day 0, mice received 500 µL of the strain mixture (via a single oral gavage administered through a flexible plastic tube, attached to a syringe).

All mice were maintained on a strict light cycle (lights on at 0600h, off at 1800h). Each experimental group consisted of 5 mice housed in a single cage in a single gnotobiotic isolator. All

diets were provided *ad libitum*. All animals in all treatment groups were observed on a daily basis and weighed weekly. Autoclaved bedding (Aspen woodchips; manufacturer) was changed weekly and at the beginning of each diet oscillation.

The timing of fecal sampling for COPRO-Seq and microbial RNA-Seq analyses is described in **Figure 1A**. All fecal samples were collected from individual mice into 2 mL screw cap tubes (Axygen, CA, USA). Once sampling of the five animals in an isolator had been completed, tubes were removed promptly and snap-frozen in liquid $N_{2,}$ after which time they were transferred to a -80^{o}C freezer.

Community Profiling by Sequencing (COPRO-Seq)

The microbial community structure in each fecal sample was analyzed by COPRO-Seq as previously described (McNulty et al., 2013). Briefly, DNA was isolated by subjecting each fecal pellet to bead-beading in a mixture containing 500 μL Buffer A (200 mM NaCl, 1200 mM Tris, 20 mM EDTA), 210 μL 20% SDS, 500 μL phenol:chloroform:isoamyl alcohol (25:24:1, pH 7.9, Ambion) and 250 μL of 0.1 mm zirconium beads (BioSpec Products, OK, USA) (3 min 2 mL screw cap tubes (Axygen)) using Mini-Beadbeater-8 (Biospec). The aqueous phase was collected after centrifugation at 4^{o}C for 3 min at 8000 x g, and nucleic acids were purified with Qiaquick columns (Qiagen) and eluted into 10 mM Tris.

COPRO-Seq libraries were prepared by first sonicating 100 μL of a 5 ng/μL solution of DNA from each fecal sample [Bioruptor Pico (Diagenode, Jew Jersey, USA);10 cycles of 30 sec on / 30 sec off at 4^{o}C]. Fragmented DNA was cleaned up in MinElute 96 UF PCR Purification plates (Qiagen). The fragments were blunt-ended, an A-tail was added, and the reaction products ligated to Illumina paired-end sequencing adapters containing sample-specific 8 bp in-line barcodes. Size selection was performed (1% agarose gels); 250-350 bp fragments were excised and the DNA purified by MinElute Gel Extraction (Qiagen). Adapter-linked fragments were enriched by a 20-cycle PCR using Illumina PCR Primers PE 1.0 and 2.0 followed by MinElute PCR Purification (Qiagen) and if agarose gels indicated adapter dimers further size-selected by AMPure XP

SPRI bead cleanup (Beckman Coulter, California, USA). Libraries were pooled and sequenced using Illumina MiSeq or HiSeq instrument (unidirectional 50 nt reads).

Sequence data was de-multiplexed and mapped to the reference genomes of community members, plus three "distractor" genomes (*B. fragilis* NCTC 9343, *Clostridium perfringens* ATCC 13124, and *Shigella* sp. D9). The proportion of reads mapping to the "distractor" genomes was used to set a minimum threshold cutoff indicating the presence/absence of an organism in the community on a per-sample basis. Normalized counts for each bacterial strain in each sample were used to produce a relative abundance table (summarized in **Table S3**). Prior to statistical analyses, the table was further filtered to exclude organisms not present at 0.1% relative abundance in >25% of samples across all samples collected. Taxonomy information for each strain was added, and the table was converted to BIOM format (McDonald et al., 2012).

To identify bacterial taxa that whose relative abundances were influenced by the micronutrient deficiency treatments, we rarefied the abundance table to 7,000 reads per sample and used linear mixed-effects models of log-transformed abundances (plus one pseudo-count). For each taxon, models were generated for each of the five dietary micronutrient deficiencies, including the micronutrient sufficient group as a control in each model. Each model included experimental stage (end of first sufficient diet phase at experimental day 14; 14 days after initiation of the micronutrient deficient diets; 14 days after return to the sufficient diet), treatment group (deficiency versus control) and their interaction as fixed effects, with individual mice treated as a random effect. A significant interaction term was considered evidence of a potentially interesting influence of the micronutrient deficiency, and tests of differences of least-squares means between the control and deficiency groups in each experimental stage, followed by p-value adjustments using Holm's method, were used to further explore the effects of the experimental treatments.

In addition, relative abundances before and after diet oscillation were compared using the group_significance.py script in QIIME version 1.9.0 (Caporaso et al., 2010). A followup analysis was performed in R (version 3.2.3; R Core Team, 2015); (i) relative abundance data and associated

metadata files were read into R, and the change in relative abundance for each organism within an individual mouse between two diet phases was calculated; (ii) these values were compared across experimental groups to identify changes in relative abundance that were significantly different from relative abundance responses in other experimental groups. For all univariate analyses, both nonparametric and parametric statistical tests were performed and the results compared.

Microbial RNA-Seq

Cultures of wild-type *B. vulgatus* and isogenic mutants were diluted 1:100 from overnight cultures into 5 mL of fresh medium containing 1 μM or 10 μM retinol or 0.2% DMSO as control, and grown to mid-log phase (OD_{600} 0.4-0.6) under anaerobic conditions in sealed Balch tubes. Once cultures reached mid-log phase, they were treated with RNAProtect Bacteria Reagent (Qiagen), vortexed, and incubated at room temperature for 5 minutes. Cultures were then transferred to clean 15 mL tubes, centrifuged for 10 min at 3023 x g, supernatants were decanted, and the pellets stored at -80°C. Pellets were thawed and resuspended in 500 μL of Buffer A immediately prior to total RNA extraction.

Microbial RNA-Seq was performed as previously described (Rey et al., 2010; McNulty et al., 2011). Following acid phenol extraction, precipitation in isopropanol, and two rounds of DNAse treatment, each followed by cleanup using a MEGAClear column (Ambion). RNA integrity was confirmed by gel electrophoresis and PCR-based checks for genomic DNA contamination were performed. 23S rRNA, 16S rRNA, 5S rRNA and tRNA was removed [Ribo-Zero Kit (Illumina)] and purified bacteria mRNA precipitated with ethanol in the presence of GlycoBlue (Ambion) to aid/guide complete resuspension in nuclease-free H_2O. Double-stranded cDNA was synthesized using random hexamers and Superscript II (Invitrogen). Illumina library preparation was performed as described above for COPRO-Seq; however, size selection was performed in the 200-300 bp range. Libraries were subjected to sequencing first on the Illumina MiSeq platform for quality control purposes, after which library balance adjustments were made where necessary and

final sequencing at greater depth was performed using the Illumina HiSeq platform (50 nt unidirectional reads).

Data analysis - The pipeline we employed for processing short-read metatranscriptomic data is described in Rey et al. (2010). Briefly, sequence data were demultiplexed and bowtie version 1.1.0 (Langmead et al., 2009) was used to map reads to the genomes of community members. Raw counts were subsetted, normalized, and analyzed using DESeq2 (Love et a. 2014) in R 3.2.3 employing two complementary strategies ('top-down' and 'bottom-up'). To analyze data at the community level (top-down view of the meta-transcriptome), raw count data for each comparison was filtered at a low abundance threshold of ≥ 3 raw reads and for consistent representation in biological replicates (present in ≥ 2 samples in both micronutrient sufficient and deficient diet groups compared or present in all samples in one group and in none of the other), then imported into R. Size factors and dispersions were estimated in DESeq2; significant differential expression was defined using the Wald test based on negative binomial model-fitting. To obtain a strain-level view of transcriptional responses (bottom-up analysis), RNA-Seq data were subsetted by strain, filtering for low abundance and sample representation performed as above, and the resulting dataset analyzed in R using DESeq2. Rarefaction was used to determine the fraction of expressed protein-coding sequences in each organism that was detected across all RNA-Seq samples. Examination of the saturation characteristics of per-strain rarefaction curves across all samples allowed us to stratify organisms by predicted transcriptome saturation. Strains that colonized gnotobiotic mice (by COPRO-Seq analysis) but for which saturation was low (*Bacteroides finegoldii* DSM 17565, *Bacteroides ovatus* ATCC 8483, *Bifidobacterium adolescentis* L2-32, *Enterobacter cancerogenus* ATCC 35316, *Megamonas funiformis* DSM 19343, *Parabacteroides distasonis* ATCC 8503, and *Proteus penneri* ATCC 35198) were excluded from the bottom-up analysis (all transcriptomic data was included in the community-level analysis).

Functional annotation of differentially expressed genes - The general strategy and bioinformatic tools used for functional analysis of RNA-Seq data are described in an earlier publication (McNulty et al., 2011). Predicted protein-coding genes in the genomes of community members

were annotated by BLASTP query (e-value threshold of 1E-05) against the Kyoto Encyclopedia of Genes and Genomes (KEGG) database (release 4 January 2016). Annotation results were used to match coding sequence locus tags to KEGG Orthology (KO) identifiers. KO lookup tables for each genome were used to annotate transcriptional data, which were then used to determine the representation of KEGG General Categories, Pathways, Functions and Enzyme Commission numbers in each microbial RNA-Seq dataset.

Phenotypic screen for the effects of various retinoids on growth of *Bacteroides spp.*

Stocks (50 mM) of retinol, retinal, retinoic acid, retinyl palmitate, ß-carotene, and geranylgeraniol (Sigma-Aldrich) were prepared in dimethyl sulfoxide under low-light conditions and stored in N_2-purged amber vials at -80°C. Bacterial strains were struck from -80°C glycerol stocks onto BHI-blood plates containing antibiotics where appropriate and grown for 48 h at 37°C under anaerobic conditions. Single colonies were picked into BHI+ broth and grown overnight under anaerobic conditions at 37°C. Cultures were diluted to an OD_{600} of 0.05 in fresh BHI+ broth and grown to mid-log phase. A *Bacteroides* defined medium (BDM) was prepared by mixing equal volumes of a 2x concentrate of the carbohydrate-free medium stock with a 2x concentrated carbon source solution, as described previously (McNulty et al., 2013). Either retinoids or DMSO (carrier control) were mixed at a 25% overblend concentration into appropriate volumes of BDM, after which 150 µL of each treated medium was aliquoted into wells of a 96-well plate (Techno Plastic Products AG) using a liquid-handling robot housed in the Coy chamber. Mid-log test cultures were subsequently diluted 1:25 into 1 mL BDM/0.2% v/v DMSO in deep-well plates; 50 µL of the diluted cultures were transferred to recipient wells in the test plate by robot, yielding 1x treatment and 1:100 final dilutions of the bacterial strains. Test plates were sealed with optically clear film (Axygen UC500) and transferred to a plate stacker-reader system housed in the anaerobic chamber (BioTek Eon and Biostack 4). For data collection from individual plates, each plate was placed directly in the Eon plate reader and incubated at 37°C with OD_{600} values determined at 15 min intervals. For multiplate data collection, the anaerobic chamber was heated to 37°C and plates were placed in

the plate-handling robot and draped with laboratory diapers to achieve low-light conditions; OD_{600} measurements were performed for each plate at 15 minute intervals.

For multidrug efflux inhibitor studies, triplicate cultures were prepared as described above for retinoid sensitivity testing and treated with phenylalanine-arginine β-naphthylamide (PAβN, Sigma-Aldrich) at 0, 5, or 25 μg/mL in combination with 0 or 10 μM retinol in 200 μL BDM volumes. Plates were sealed and OD_{600} tracked as above for single plates.

At the conclusion of each experiment, data were exported to text file and in-house perl scripts were used to plot growth rate, the time at which each growth curve crossed a user-defined OD_{600} threshold, and the maximum OD_{600}. Curve parameters were normalized to corresponding values from control cultures containing 0.2% DMSO before comparison between strains. Statistical analyses were performed in Prism 6.0 (GraphPad Software).

***In vitro* competition experiments**

Cultures of wildtype *B. vulgatus* ATCC 8482 and *B. dorei* DSMZ 17855 were grown overnight to stationary phase in BHI+ at 37°C under standard anaerobic conditions. Cultures were diluted to OD_{600} ~ 0.05 in fresh medium and allowed to grow to mid-log phase, at which time roughly equal quantities of viable cells [$1.3x10^5 \pm 3.6x10^4$ CFU for single organism controls; $2.19x10^5 \pm 2.7x10^4$ total mixed cfu for competitions) were pelleted by centrifugation, and resuspended in 10 mL BDM in triplicate balch tubes. Serial dilutions of pre-treatment cultures were plated on BHI-Blood agar plates and incubated 24-36 hrs at 37°C under anaerobic conditions to define cfu/mL. Either 10 μM retinol or 0.2% v/v DMSO as carrier control was added to each culture, which was then capped, sealed, and incubated at 37°C outside the anaerobic chamber. Optical density (OD_{600}) measurements were taken over time to track the growth of each culture. When individual cultures reached stationary phase, one mL samples were withdrawn aseptically from each tube using a sterile syringe and needle. A 100 μL fraction of each sample was used for serial dilutions and plating in order to define the number of viable organisms (cfu/mL titers); the remainder was pelleted by

centrifugation. The percentage of *B. vulgatus* and *B. dorei* in mixed-culture samples was independently defined by COPRO-Seq analysis of DNA purified from the cell pellet.

INSeq-based identification of *B. vulgatus* mutants that affect retinoid sensitivity

Bacteroides vulgatus ATCC 8482 taxon-specific barcodes were introduced into the INSeq mutagenesis vector (pSAM_Bt) by PCR amplification, using the primer pairs described in **Table S10**. Amplification conditions were as follows: initial denaturation at 94 °C for 2 min, followed by 25 cycles of denaturation (94°C for 15 sec), annealing (58°C for 30 sec), and amplification (58°C for 90 sec). Vector DNA was digested with KpnI and BamHI, and the linear product ligated to the amplicon product of the PCR, yielding the barcoded transposon mutagenesis vector.

Whole genome transposon mutagenesis of *B. vulgatus* ATCC 8482 was performed using a published protocol (Wu et al., 2015). Aliquots of the mutant library were inoculated into BDM containing retinol (10 μM) or 0.2 % DMSO. Triplicate cultures (250 mL each; starting OD_{600} of 0.05) were incubated anaerobically at 37°C. Aliquots were removed in lag phase phase and after selected mutants reached stationary phase. Additionally, a stationary phase aliquot from the primary culture was used to inoculate 250 mL of fresh selection medium. The resulting secondary cultures were sampled in mid-log phase (OD_{600} 0.4-0.6) and at stationary phase.

DNA was isolated from all cultures/time points, and the abundance and genome location of mutants in input, control, and selected samples were determined. The *mariner* Tn contains two engineered MmeI sites at both of its ends. DNA was digested with MmeI (which cuts 20 bp distal to its recognition site), yielding products with flanking genomic sequence tags at both ends. Ampure XP bead-based and gel-based size selection is used to isolate and purify the products: custom, indexed Illumina adapters were ligated to these fragments which were then sequenced (Illumina HiSeq platform; 50 nt reads). INSeq reads were mapped to the *B. vulgatus* genome and analyzed (Wu et al., 2015) to obtain the identity and abundance of each Tn mutant present in the input library and the selected or control libraries.

Retinol-resistant Tn mutants were isolated by plating dilutions of cryopreserved, station-

ary-phase cultures on BHI-blood containing 25 μg/mL erythromycin. Colony PCR using primer pairs that spanned inserted Tn borders (one genome location-specific primer and one transposon-specific primer in each pair) were used to confirm the identities of mutants. Confirmed colonies were grown overnight in BHI+ and archived as 15% glycerol stocks at -80°C. Retinoid sensitivity experiments were performed using monocultures of isolated Tn mutant strains.

Complementation of *B. vulgatus* Tn mutants

Tn mutants of *B. vulgatus* were complemented using the genomic insertion vector pNBU2_tetQ (Martens et al., 2008). The coding sequences of *acrR* (*BVU0240*), *lpxA* (*BVU0241*), or both genes were amplified by PCR with Phusion HF Master Mix (New England Biolabs, Massachusetts, USA) from purified genomic DNA from wild-type *B. vulgatus*. To drive constitutive expression of complemented genes, a 300 bp region upstream of the *B. vulgatus* rpoD gene (PrpoD) was also amplified by PCR. The pNBU2_tetQ backbone was digested with XbaI and PstI; Gibson Assembly (New England Biolabs) was used to assemble PrpoD and the appropriate *B. vulgatus* coding sequence(s) into the digested vector. Assembled vectors were transformed into *E. coli* S17 λpir and the assemblies confirmed by junction-spanning PCR. Vectors were mobilized from *E. coli* donor to the corresponding *B. vulgatus* recipient by conjugation. Briefly, overnight cultures of both donor and recipient were inoculated into rich media with antibiotics where appropriate and grown for 16-20 h at 37°C (*E. coli*, aerobically with shaking at 225 rpm; *B. vulgatus*, anaerobically without shaking). Stationary phase cultures were then serially diluted into fresh medium, incubated for 4 h at 37°C. Cultures of donor and recipient cells with approximately equal optical densities were pelleted by centrifugation, resuspended in 1 mL of fresh medium, and plated on BHI-blood agar. After a 24 h aerobic incubation, the surface of each plate was scraped, resuspended in 5 mL BHI+ liquid, and plated on BHI+ agar with tetracycline (2 μg/mL). After a 48 h incubation under anaerobic conditions, colonies were picked, re-struck on BHI+ agar with tetracycline, and the site of insertion and orientation of introduced gene verified by PCR and sequencing. Confirmed complemented Tn mutants carrying either the empty pNBU2_tetQ vector or *B. vulgatus* sequences of interest were subjected to retinoid sensitivity assays as described above.

Transcription factor binding site analyses

Analysis of Bacteroides TetR regulons **-** We applied an integrative comparative genomics approach to reconstruct the AcrR regulon in *Bacteroides* species (as implemented in the RegPredict Web server, http://regpredict.lbl.gov) (Novichkov et al., 2010). This approach combines identification of candidate regulator binding sites with cross-genomic comparison of regulons and functional context analysis of candidate target genes (Rodionov et al., 2007). The upstream regions of *BVU0240* and its orthologs in 11 *Bacteroides* genomes (representing a non-redundant set of species excluding closely related strains) were analyzed employing a DNA motif recognition program (the "Discover Profile" procedure implemented in RegPredict) to identify a conserved palindromic DNA motif. After construction of a position-weight matrix for the candidate AcrR binding motif, we searched for additional AcrR-binding sites in the analyzed *Bacteroides* genomes. Finally, we performed a consistency check or cross-species comparison of the predicted AcrR regulons. Scores of candidate binding sites were calculated as the sum of positional nucleotide weights. The score threshold was defined as the lowest score observed in the training set. Sequence logo for the derived DNA binding motif was drawn using the WebLogo package (Crooks et al., 2004).

Cloning, expression and protein purification of B. vulgatus and B. dorei AcrR-like regulators **-** Genes encoding orthologous AcrR-like regulators from *B. vulgatus* (BVU0240, $AcrR_{BV}$) and *B. dorei* (BACDOR_00223, $AcrR_{BD}$) were amplified by PCR from genomic DNA using two sets of specific primers containing BamHI and HindIII restriction sites (**Table S10**). A truncated variant of $AcrR_{BV}$ protein ($AcrR^*_{BV}$) that lacks eight N-terminal amino acids was cloned using an alternative forward primer (**Table S10**). This "truncated variant" corresponds to an alternative translational start of this protein as currently reflected in GenBank (WP_008782083.1).

The full length AcrR orthologs from *B. vulgatus* and *B. dorei* and the the truncated $AcrR^*_{BV}$ variant were cloned into the pSMT3 expression vector, and the recombinant proteins were expressed with an N-terminal His6-Smt3-tag in *E. coli* BL21/DE3 under control of the T7 promoter (Mossessova et al., 2000). The engineered constructs encode fusion proteins with a N-terminal

Smt3 polypeptide (SUMO ortholog), which is known to assist in protein folding and can be selectively removed by treatment with SUMO protease (Ulp1; Mossessova and Lima, 2000). Cells were grown in LB medium (50 mL) to an OD_{600} of ~1.0 and protein expression was induced with 0.2 mM isopropyl-β-D-thiogalactopyranoside (IPTG). Cell were harvested after 18 h of additional shaking at 20°C.

The recombinant $AcrR_{BV}$, $AcrR^*_{BV}$ and $AcrR_{BD}$ proteins were purified using a rapid one-step mini-column protocol on Ni-NTA agarose (Qiagen). Briefly, the harvested cells were re-suspended in 20 mM HEPES buffer (pH 7) containing 100 mM NaCl, 0.03% Brij-35, 2 mM β-mercaptoethanol and 2 mM phenylmethylsulfonyl fluoride (Sigma-Aldrich). Cells were then lysed by incubation with lysozyme (1 mg/mL) for 30 min at 4°C, followed by a freeze-thaw cycle and sonication. For purification of the soluble fraction after centrifugation, Tris-HCl buffer (pH 8) was added to the supernatant (50 mM), which was loaded onto a Ni-NTA agarose mini-column (0.3 mL). After washing with the starting buffer containing 1 M NaCl and 0.3% Brij-35, bound proteins were eluted with 0.3 mL of the starting buffer containing 300 mM imidazole. Protein size and purity (>90) were verified by SDS PAGE. Protein concentration was determined by Quick Start Bradford Protein Assay kit (Bio-Rad). The N-terminal His6-Smt3-tag was cleaved off the purified proteins by digestion with Ulp1 protease (overnight incubation at 4°C in a reaction mixture containing 0.07 mg/mL of the protease).

DNA binding assays - Interactions between the purified recombinant transcription factors and their predicted DNA-binding sites were assayed using two techniques: electrophoretic mobility shift assay (EMSA) and fluorescence polarization assay (FPA). Single-stranded labeled and unlabeled DNA oligonucleotides were synthesized (**Table S10**). A 40 bp oligo with a fragment of the promoter region of the *BVU_0244* gene contained the predicted 30 bp AcrR-binding site (upper case characters). For EMSA, we used 5′-biotin-labeled DNA fragments, while FPA employed DNA fragments 3′-labeled with 6-carboxyfluorescein (the double-stranded labeled DNA fragments were obtained by annealing the labeled oligonucleotides with unlabeled complementary oligonucleotides at a 1:10 ratio). As a negative control, we used a 41-bp DNA fragment from the

BT0356 gene containing the verified binding site of an unrelated transcriptional regulator, AraR, from *B. thetaiotaomicron* (Chang et al., 2015).

For EMSA, the target DNA fragment (0.25 nM) was mixed with increasing concentrations of the purified tag-free $TetR_{BV}$ and $TetR_{BD}$ proteins in a total reaction volume of 20 μL. The binding buffer contained Tris-HCl 20 mM (pH 8.0), KCl 150 mM, $MgCl_2$ 5 mM, DTT 1 mM, 0.05% NP-40, 2.5% glycerol. After a 25 min incubation at 37ºC, the reaction mixture was subjected to electrophoresis on native 5% polyacrylamide gels in 0.5X TB at room temperature (100 min, 90 V). The DNA was electrophoretically transferred onto a Hybond-N^+ membrane (Pierce) and fixed by UV cross-linking. Biotin-labeled DNA was detected with the LightShift chemiluminescent EMSA kit (Pierce).

The effects of retinol and low molecular weight cell extracts from *Bacteroides vulgatus* ATCC 8482 and *Bacteroides dorei* DSM 17855 were tested by their addition to the EMSA incubation mixture. Low molecular weight cell extracts were prepared from 5 mL cultures grown in BDM to OD_{600} = 0.5. Cells were pelleted by centrifugation, resuspended in 1 mL of lysis buffer (50 mM Tris-HCl pH 8.0, 0.2 mM NaCl, 0.03% Brij-35 and 1 mM DTT), and lysed by freeze-thaw, followed by sonication for 1 min on ice. Debris were removed by centrifugation (13,000 rpm for 50 min at 4ºC). The resulting supernatants were subjected to ultrafiltration [Amicon microcentrifuge filter units; 3 kDa cutoff (EMD Millipore)] to remove biopolymers.

For FPA, fluorescence-labeled double-stranded DNA fragments (3 nM) were incubated with the increasing concentrations of the purified tag-free $TetR_{BV}$ and $TetR_{BD}$ proteins in a 100 μL reaction mixture in 96-well black plates (VWR). The binding buffer contained 20 mM Tris-HCl (pH 7.5) and 100 mM NaCl and the incubation was conducted for 20 min at 24°C. Herring sperm DNA (1 μg) was added to the reaction mixture as a non-specific competitor DNA to suppress non-specific binding. FPA measurements were made using a Beckman multimode plate reader (DTX 880) with excitation and emission filters set at 495 and 520 nm. The fluorescence polarization values were determined as previously described (Ravcheev et al., 2012).

Bile sensitivity assays

Cultures of *B. vulgatus* WT, *B. vulgatus acrR*::IN, *B. dorei* WT, and *B. fragilis* ATCC 25285 (bile-resistant control organism) were picked into supplemented BHI cultures and grown to stationary phase at 37°C under anaerobic conditions. Culture density was measured by optical density and cultures were diluted to OD_{600} = 0.5. Sterile cotton-tipped applicators were used to swab each culture (triplicate for each organism) onto the surface of a BHI-Blood plate; sterile forceps were then used place an oxgall-impregnated disk (Remel, Kansas, USA) in the center of each plate. Plates were incubated at 37°C anaerobically for 24 h. The diameter of zone of inhibition (ZOI) was measured in triplicate for each plate using a digital caliper. Mean ZOI was calculated for replicate measurements for each plate.

Targeted mass spectrometry-based assays of retinoids *in vitro*

Aliquots of cultures of WT *B. vulgatus* WT, *B. vulgatus acrR*::IN, and the *B. vulgatus acrR*::IN::*acrR* complemented mutant were diluted into supplemented BHI medium and grown to stationary phase at 37°C under anaerobic conditions. Cultures were then diluted to an OD_{600} of 0.5 in 10 mL PBS/0.2% w/v cysteine and retinol was added to a final concentration of 10 μM. At indicated timepoints 500 μL of each culture was removed to a 1.5 mL tube, spun in a microcentrifuge (Eppendorf 5430) for 3 min at 20,817 x g. The supernatant was withdrawn and transferred to a 1 mL sample vial (Waters, MA, USA), and deuterated (D5) retinol (Toronto Research Chemicals, Ontario, Canada) was added to a final concentration of 10 μM as a spike-in control. Cell pellets from the initial centrifugation were resuspended in 500 μL PBS by vortexing; the mixture was centrifuged for an additional 3 min at 20,817 x g and the supernatant decanted. The resulting washed cell pellets were subjected to 3 cycles of freeze/thaw at -80°C and on ice, respectively, then resuspended in 500 mL methanol by vortexing for 30 s. Cell debris were pelleted by centrifugation for 3 min at 20,817 x g, supernatants were transferred to a fresh 1.8 mL glass vial, and then evaporated to dryness using a Speedvac (Savant SPD1010, Thermo Scientific, MA, USA). Dried material was resuspended in 100 μL 10% methanol by vortexing: a 90 μL aliquot was mixed with 10 μL of D5-

retinol stock (100 μM) to achieve a final D5-retinol concentration of 10 μM. Mass spectrometry analyses were performed using an Acquity I Class UPLC system (Waters, MA, USA) coupled to an LTQ-Orbitrap Discovery (Thermo Scientific, MA, USA). Mobile phases for positive ionization were (A) 0.1% formic acid in water and (B) 0.1% formic acid in acetonitrile. Retinol quantification was achieved by comparison of measured values to standard curves generated from stocks of retinol and D5-retinol.

UPLC-MS analysis of fecal bile acids was performed using protocols described in an earlier report (Dey et al., 2015).

References

Allen L.H. B vitamins in breast milk: relative importance of maternal status and intake, and effects on infant status and function. *Adv Nutr. 3*, 362-369 (2012).

Bailey, R L, K P West Jr, and R E Black. The Epidemiology of Global Micronutrient Deficiencies. *Ann Nutr Metabol 66*, 22–33 (2015).

Bhutta Z.A., Das J.K., Rizvi A., Gaffey M.F., Walker N., Horton S., Webb P., Lartey A., Black R.E. Lancet Nutrition Interventions Review Group; Maternal and Child Nutrition Study Group. Evidence-based interventions for improvement of maternal and child nutrition: what can be done and at what cost? *Lancet 382*, 452-77 (2013).

Black, R.E. Risk of childhood undernutrition related to small-for-gestational age and preterm birth in low- and middle-income countries. *Int J Epidemiol. 42*, 1340-55 (2013).

Blanton, L.V., Charbonneau, M.R., Salih, T., Barratt, M.J., Venkatesh, S., Ilkaveya, O., Subramanian, S., Manary, M.J., Trehan, I., Jorgensen, J.M., Fan, Y., Henrissat, B., Leyn, S.A., Rodionov, D.A., Osterman, A.L., Maleta, K.M., Newgard, C.B., Ashorn, P., Dewey, K.G., and Gordon, J.I. Gut bacteria that prevent growth impairments transmitted by microbiota from malnourished children, *Science 351*, aad3311 (2016).

Blanton, L.V., Barratt, M.J., Charbonneau, M.R., Ahmed, T., and Gordon, J.I. Childhood undernutrition, the gut microbiota, and microbiota-directed therapeutics. *Science 352*, 1533. aad9359 (2016).

Bieri, J. G., McDaniel, E. G., & Rogers, W. E. Survival of germfree rats without vitamin A. *Science*, *163*, 574–575. (1969).

Crooks, G. E., Hon, G., Chandonia, J.-M., & Brenner, S. E. WebLogo: a sequence logo generator. *Genome Res*, *14*, 1188–1190 (2004).

Caporaso, J. G., Kuczynski, J., Stombaugh, J., Bittinger, K., Bushman, F. D., Costello, E. K., et al. QIIME allows analysis of high-throughput community sequencing data. *Nature Methods*, *7*, 335–336 (2010).

Chang, C., Tesar, C., Li, X., Kim, Y., Rodionov, D. A., and Joachimiak, A. A novel transcriptional regulator of L-arabinose utilization in human gut bacteria. *Nucleic Acids Res*, *43*, 10546–10559 (2015).

Crowell, D. N., Anderson, M. S., and Raetz, C. R. Molecular cloning of the genes for lipid A disaccharide synthase and UDP-N-acetylglucosamine acyltransferase in *Escherichia coli*. *J Bacteriol 168*, 152–159 (1986).

Dey, N., Wagner, V.E., Blanton, L.V., Cheng, J., Fontana, L., Haque, R., Ahmed, T., and Gordon, J.I. Regulators of gut motility revealed by a gnotobiotic model of diet-microbiome interactions related to travel. *Cell 163*, 95-107 (2015).

Du, D., Wang, Z., James, N. R., Voss, J. E., Klimont, E., Ohene-Agyei, T., et al. Structure of the AcrAB-TolC multidrug efflux pump. *Nature 509*, 512–515.(2014).

Goodman, A.L., McNulty, N.P., Zhao, Y., Leip, D., Mitra, R.D., Lozupone, C.A., Knight, R., and Gordon, J.I. Identifying genetic determinants needed to establish a human gut symbiont in its habitat. *Cell Host Microbe 6*, 279-289 (2009).

Hernandez-Alvarez, E., Pérez-Sacristán, B. I., Blanco-Navarro, I., Donoso-Navarro, E., Silvestre-Mardomingo, R. A., and Granado-Lorencio, F. Analysis of microsamples of human faeces: a non-invasive approach to study the bioavailability of fat-soluble bioactive compounds. *Eur. J. Nutr*, *54*, 1371–1378 (2015).

Institute of Medicine (US) Committee on Micronutrient Deficiencies, Howson, C. P., Kennedy, E. T., and Horwitz, A. Prevention of Micronutrient Deficiencies: Tools for Policymakers and Public Health Workers (1998).

Kim, J.-S., Jeong, H., Song, S., Kim, H.-Y., Lee, K., Hyun, J., and Ha, N.-C. Structure of the tripartite multidrug efflux pump AcrAB-TolC suggests an alternative assembly mode. *Molecules and Cells 38*, 180–186 (2015).

Langmead, B., Trapnell, C., Pop, M., and Salzberg, S.L. Ultrafast and memory-efficient alignment of short DNA sequences to the human genome. *Genome Biology*, *10*, R25 (2009)

Liu, L., Tang, X.-H., and Gudas, L. J. Homeostasis of retinol in lecithin: retinol acyltransferase gene knockout mice fed a high retinol diet. *Biochem Pharm*, *75*, 2316–2324 (2008).

Love, M. I., Huber, W., and Anders, S. Moderated estimation of fold change and dispersion for RNA-seq data with DESeq2. *Genome Biology*, *15*, 550 (2014).

Martens, E. C., Chiang, H. C., and Gordon, J. I. Mucosal glycan foraging enhances fitness and transmission of a saccharolytic human gut bacterial symbiont. *Cell Host and Microbe*, *4*, 447–457 (2008).

McNulty, N, Yatsunenko, T, Hsiao, A., Faith, J., Muegge, B., Goodman, A., Henrissat, B., Oozeer, R., Cools-Portier, S., Gobert, G., Chervaux, C., Knights, D., Lozupone, C., Knight, R., Duncan, A.E., Bain, J.R., Muehlbauer, M.J., Newgard, C.B., Heath, A.C., and Gordon, J.I. The impact of a consortium of fermented milk strains on the gut microbiome of gnotobiotic mice and monozygotic twins. *Science Translational Medicine 3*, 106ra106 (2011).

McNulty, N.P., Wu, M., Erickson, A.R., Martens, E.C., Pudlo, N.A., Muegge, B., Henrissat, B., Hettich, R.L., and Gordon, J.I. Effects of diet on resource utilization by a defined model human gut microbiota containing *Bacteroides cellulosilyticus* WH2, a symbiont with an extensive glycobiome, *PLoS Biol 11*, e1001637 (2013).

Novichkov, P. S., Rodionov, D. A., Stavrovskaya, E. D., Novichkova, E. S., Kazakov, A. E., Gelfand, M. S., et al. RegPredict: an integrated system for regulon inference in prokaryotes by comparative genomics approach. *Nucleic Acids Research*, *38* (Web Server issue), W299–307 (2010).

Mossessova E. and Lima C.D. Ulp1-SUMO crystal structure and genetic analysis reveal conserved interactions and a regulatory element essential for cell growth in yeast. *Mol Cell 5*, 865–876. (2000).

Papathakis, P. C., Singh, L. N., and Manary, M. J. How maternal malnutrition affects linear growth and development in the offspring. *Mol Cell Endo* S0303-7207(16)30025-9. doi (2016).

Penniston, K. L., and Tanumihardjo, S. A. The acute and chronic toxic effects of vitamin A. *Am J Clin Nutr*, *83*, 191–201 (2006).

R Core Team. R: A language and environment for statistical computing. R Foundation for Statistical Computing, Vienna, Austria. URL https://www.R-project.org/. (2015).

Ravcheev, D. A., Li, X., Latif, H., Zengler, K., Leyn, S. A., Korostelev, Y. D., et al. Transcriptional regulation of central carbon and energy metabolism in bacteria by redox-responsive repressor Rex. *J Bacteriol*, *194*, 1145–1157 (2012).

Rodionov, D. A. Comparative genomic reconstruction of transcriptional regulatory networks in bacteria. *Chem Rev*, *107*, 3467–3497. (2007)

Rogers, W. E., Bieri, J. G., & McDaniel, E. G. Vitamin A deficiency in the germfree state. *Federation Proceedings*, *30*(6), 1773–1778. (1971).

Ramakrishnan, U., Grant, F.K., Goldenberg, T., Bui, V., Imdad, A., Bhutta, Z.A. Effect of multiple micronutrient supplementation on pregnancy and infant outcomes: a systematic review *Paediatr. Perinat. Epidemiol*., *26* (Suppl. 1) 153–167 (2012).

Reddy, B. S., Pleasants, J. R., Zimmerman, D. R., & Wostmann, B. S. Iron and copper utilization in rabbits as affected by diet and germfree status. *J Nutr 87*, 189–196 (1965).

Reddy, B. S., Pleasants, J. R., & Wostmann, B. S. Effect of intestinal microflora on iron and zinc metabolism, and on activities of metalloenzymes in rats. *J Nutr 102*, 101–107 (1972).

Renau, T. E., Léger, R., Flamme, E. M., Sangalang, J., She, M. W., Yen, R., et al. Inhibitors of Efflux Pumps in *Pseudomonas aeruginosa* Potentiate the Activity of the Fluoroquinolone Antibacterial Levofloxacin. *J Med Chem*, *42*, 4928–4931 (1999).

Rey, F., Faith, J., Bain, J., Muehlbauer, M., Stevens, R., Newgard, C., and Gordon, J.I. Dissecting the *in vivo* metabolic potential of two human gut acetogens. *J. Biol. Chem***.** *285*, 22082-22090 (2010).

Salam. R.A., MacPhail, C., Das, J.K., Bhutta, Z.A. Effectiveness of Micronutrient Powders (MNP) in women and children. *BMC Public Health 13*, *Suppl* 3, S22 (2013).

Sazawal, S., Black, R. E., Ramsan, M., Chwaya, H. M., Stoltzfus, R. J., Dutta, A., et al. Effects of routine prophylactic supplementation with iron and folic acid on admission to hospital and mortality in preschool children in a high malaria transmission setting: community-based, randomised, placebo-controlled trial. *Lancet*, *367*(9505), 133–143. (2006).

Smith, J. C., McDaniel, E. G., McBean, L. D., Doft, F. S., and Halsted, J. A. Effect of microorganisms upon zinc metabolism using germfree and conventional rats. *J Nutr 102*, 711–719 (1972).

Soofi, S., Cousens, S., Iqbal, S. P., Akhund, T., Khan, J., Ahmed, I., et al. Effect of provision of daily zinc and iron with several micronutrients on growth and morbidity among young children in Pakistan: a cluster-randomised trial. *Lancet*, *382*(9886), 29–40. (2013).

Subramanian, S., Huq, S., Yatsunenko, T., Haque, R., Mahfuz, M., Alam, M.A., Benezra, A., DeStefano, J., Meier, M.F., Muegge, B.D., Barratt, M.J., Zhang, Q., Province, M.A., Petri, W.A., Ahmed, T., and Gordon, J.I. Persistent gut microbiota immaturity in malnourished Bangladeshi children. *Nature 509*, 417-421 (2014).

Thanassi, D. G., Cheng, L. W., & Nikaido, H. Active efflux of bile salts by Escherichia coli. *J Bacteriol. 179*, 2512–2518 (1997).

Veenemans, J., Milligan, P., Prentice, A. M., Schouten, L. R. A., Inja, N., van der Heijden, A. C., et al. Effect of supplementation with zinc and other micronutrients on malaria in Tanzanian children: a randomised trial. *PLoS Medicine*, *8*(11), e1001125. (2011).

Wirtz, M., and Droux, M. Synthesis of the sulfur amino acids: cysteine and methionine. *Photosynthesis Res*, *86*, 345–362. (2005).

Wu, G., Imhoff-Kunsch, B., and Girard, A.W. Biological mechanisms for nutritional regulation of maternal health and fetal development. *Paediatr Perinat Epidemiol*. *26 Suppl 1*, 4–26 (2012).

Wu, M., McNulty, N.P., Rodionov, D.A., Khoroshkin, M.S., Griffin, N.W., Cheng, J., Latreille, P., Kerstetter, R.A., Terrapon, N., Henrissat, B., Osterman, A.L., and Gordon, J.I. Genetic determinants of *in vivo* fitness and diet responsiveness in multiple human gut *Bacteroides*, *Science 350*, aac5992 (2015).

Figure Legends

Figure 1. The effect of dietary micronutrient deficiency on the configuration of a defined human gut microbiota established in gnotobiotic mice. (**A**) Experimental design. (**B**) PCoA of pairwise comparisons of fecal microbiota using Bray Curtis dissimilarity metric and COPRO-Seq datasets. Fecal samples were obtained from mice in the indicated treatment groups at the indicated time points.

Figure 2. The distinct retinol sensitivity phenotypes of *B. vulgatus* and *B. dorei in vitro*. (**A**) Growth curves of *B. vulgatus* and *B. dorei* in defined medium with and without various retinoids. The horizontal dashed line indicates the threshold used for calculating time-to-log phase measurements. (**B,C**) Bar plots indicating mean (± SEM) retinoid sensitivity, calculated as time-to-log phase for treated cultures versus time-to-log phase for vehicle alone (DMSO) control cultures.

Figure 3. Selection of retinol-resistant *B. vulgatus* Tn mutants. (**A**) Experimental design. The mutant library was inoculated into defined medium containing 10 μM retinol or 0.2% v/v DMSO (three cultures per treatment). In the first round of selection, mutants were allowed to grow to stationary phase and were then passaged to fresh medium and subjected to a second round of selection. Aliquots were withdrawn at lag and stationary phases from the primary cultures and at log and stationary phase of the secondary cultures. The site of insertion of the Tn was defined in the retinol-resistant mutants using INseq. (**B**) Fractional abundance of Tn mutants in retinol-selected *B. vulgatus* libraries. The left portion of the panel indicates the abundance of each selected mutant in the input library. Each set of four bars shown in the right portion of the panel indicates the abundance of the Tn mutants at the indicated growth phases from both passages. (**C**) Schematic of the *B. vulgatus* locus containing the retinol-resistant mutants identified from screening the Tn library. Annotation is based on the NCBI reference assembly NC_009614.1. The genomic location of each selected Tn mutant is indicated by a downward pointing arrow annotated with the corresponding color from panel B and the corresponding genome coordinate for the site of Tn insertion. (**D**) Schematic of components comprising the *E. coli* AcrAB-TolC effux system (taken from http://2013.

igem.org/Team:Ciencias-UNAM/Project). (**E**) Retinol sensitivity of *B. vulgatus* Tn mutants grown in monoculture in defined medium treated with 1 μM, 5 μM, and 10 μM retinol versus 0.2% v/v DMSO as control. Mean values ± SEM of the ratio between treated and control cultures for each strain are shown. The sensitive *B. vulgatus* WT and resistant *B. dorei* WT strains are shown as positive and negative controls, respectively. (**F**) Retinol sensitivity of WT, *acrR*::IN (genome location 361472) mutant strain, the complemented *B. vulgatus acrR*::IN + pNBU_*PrpoD_acrR* strain and a control *B. vulgatus acrR*::IN361472 strain containing the empty vector.

Figure 4. Characterization of the *acrR* regulon. (**A**) Summarized KEGG pathways and functions of differentially expressed genes identified by comparing log phase RNA-Seq data from untreated cultures of mutant *acrR*::IN361472 and *lpxA*::IN strains to WT *B. vulgatus*. DESeq2-based analysis identified a shared set of 92 differentially-expressed genes emanating from the two insertion mutatns. The proportional representation of hits to the top four KEGG pathways versus all other KEGG pathways is indicated by the horizontal bar plot; up- or downregulation of expression of genes in the comparison of WT to mutant in the indicated pathway is indicated by arrows. (**B**) Transcript counts, normalized by DESeq2, for each gene in the putative *BVU0244-BVU0233* operon. Bars indicate mean ± SEM values for *B. vulgatus* WT and *BVU0240::361472IN* and *BVU041*::IN strains under untreated and 10 μM retinol-treated conditions. Significant differential expression between indicated conditions was defined by DESeq2.

Figure 5. Measuring interactions between the AcrR transcription factor and its target DNA binding site. (**A**) Predicted AcrR-regulated operons in the genomes of Bacteroides species. Boxes indicate clusters of co-regulated genes. Filled black circles indicate predicted AcrR binding sites. (B) Sequences of predicted AcrR binding sites. (**C**) Consensus binding site motif. (**D,E)** Fluorescence Polarization Assay (FPA) and Electrophoresis Mobility Shift Assay (EMSA) of the specificity and affinity of the binding of $AcrR_{BV}$, $AcrR^*_{BV}$ and $AcrR_{BD}$ with predicted target DNA sequences.

Figure 6. Role of the AcrAB-TolC efflux pump in regulating *B. vulgatus* retinol sensitivity. **(A)** Retinol efflux assay. Stationary phase cultures of WT, *acrR::IN*, and pNBU2_*PrpoD-acrR* complemented *acrR::IN* strains were resuspended in PBS plus cysteine and treated with 10 μM retinol. Samples were collected over time. Retinol in cell-free supernatants (CFS) was quantified by LC-MS. (**B,C**) Retinol sensitivity of WT *B. dorei* and *B. vulgatus* strains treated with increasing concentrations of phenylalanine-arginine β-naphthylamide (PAβN), a chemical inhibitor of multi-drug efflux systems. Data shown are mean (± SEM) values for retinol sensitivity (treated/control). (**D**) Bile sensitivity of WT and *acrR::IN* strains of *B. vulgatus*, WT B. *dorei*, and WT *B. fragilis* (bile-resistant control). Data shown represent the diameter of zone of inhibition (mm) around an oxgall-impregnated disc.

Figures

Figure 1.

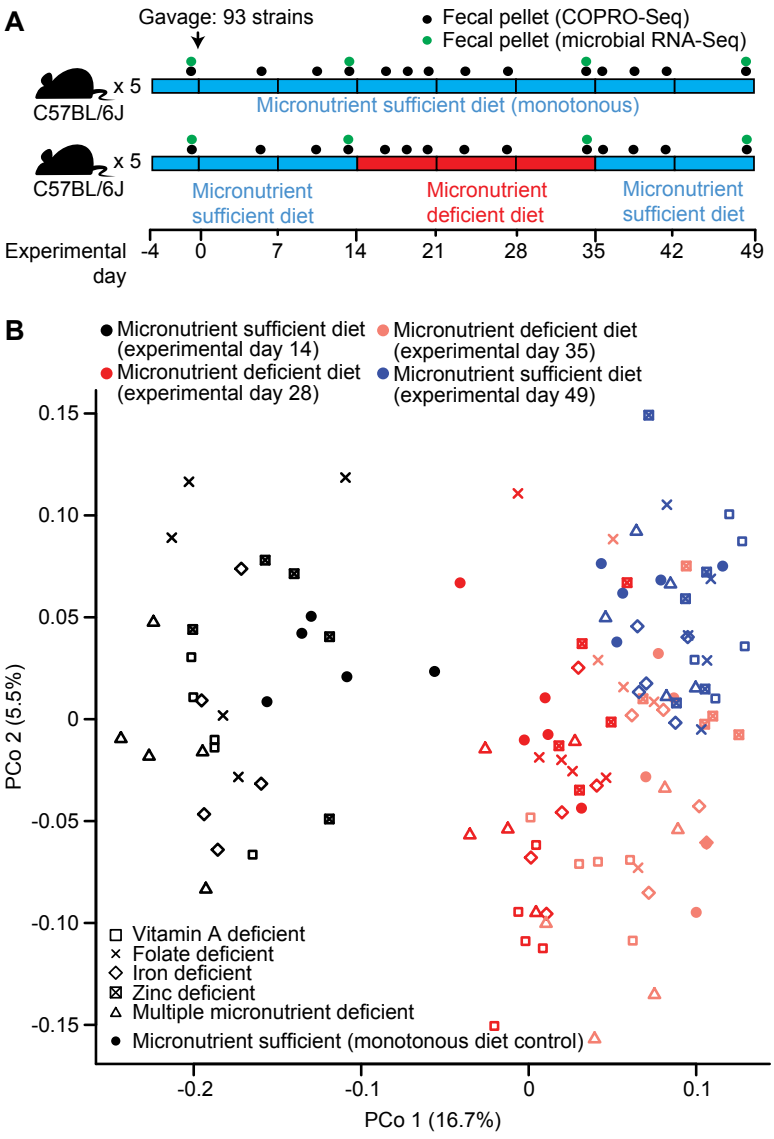

Figure 2.

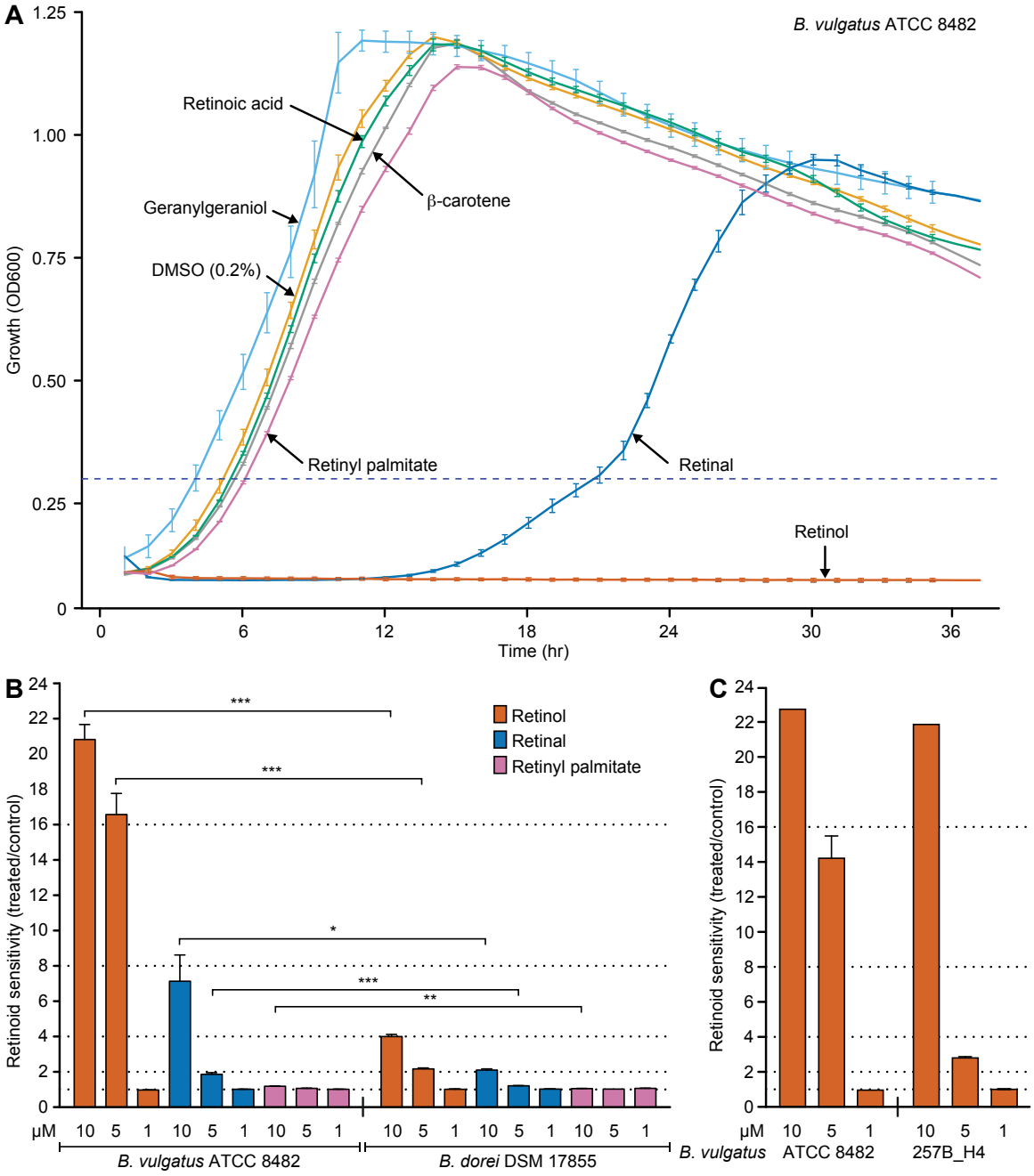
A
B. vulgatus ATCC 8482
Retinoic acid
Geranylgeraniol
DMSO (0.2%)
β-carotene
Retinyl palmitate
Retinal
Retinol
Growth (OD600)
Time (hr)
B
Retinol
Retinal
Retinyl palmitate
Retinoid sensitivity (treated/control)
μM
B. vulgatus ATCC 8482
B. dorei DSM 17855
C
Retinoid sensitivity (treated/control)
μM
B. vulgatus ATCC 8482
257B_H4

Figure 3.

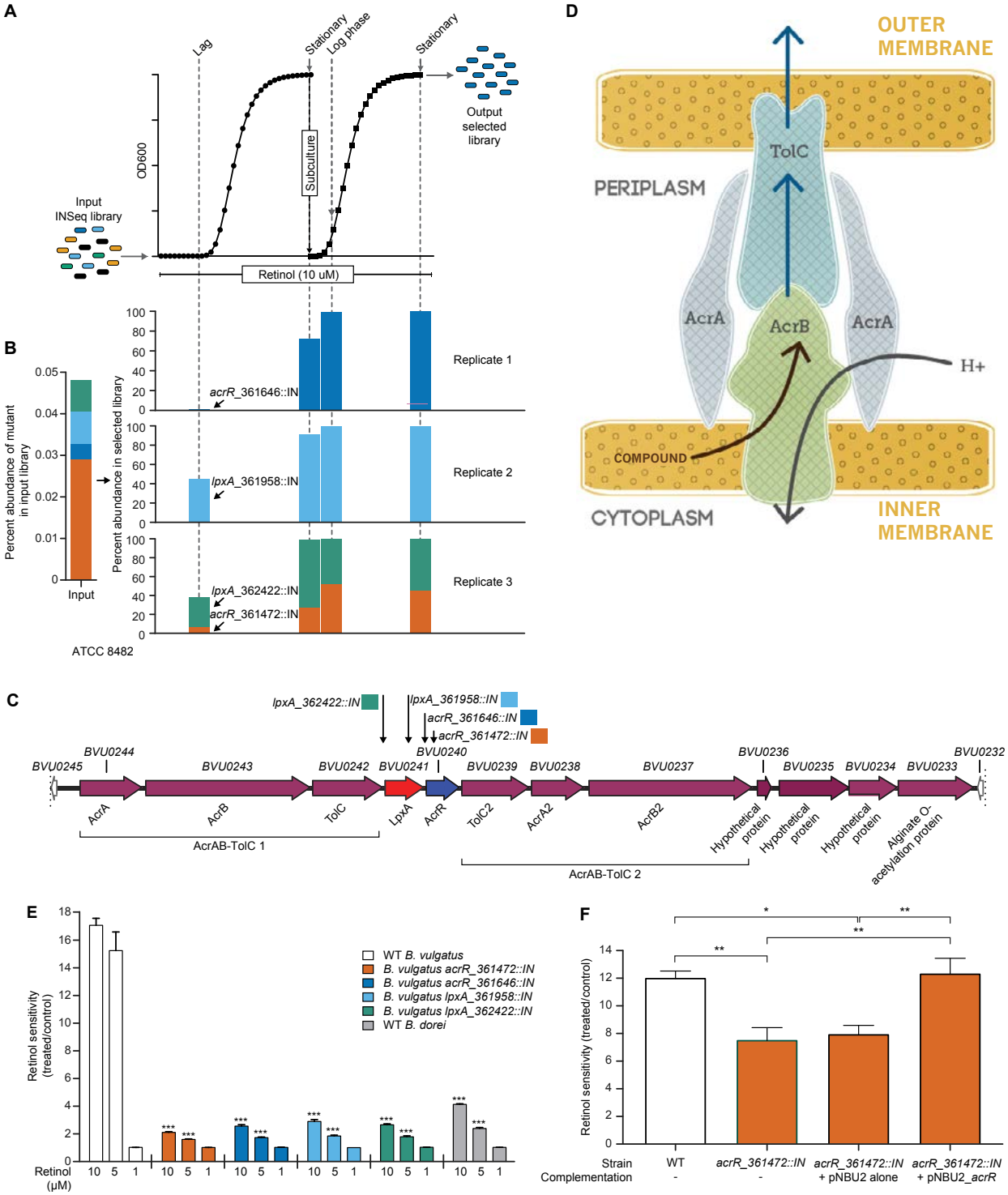
A
Lag
Stationary
Log phase
Stationary
OD600
Subculture
Output selected library
Input INSeq library
Retinol (10 uM)
B
Percent abundance of mutant in input library
Input
Percent abundance in selected library
acrR_361646::IN
lpxA_361958::IN
lpxA_362422::IN
acrR_361472::IN
Replicate 1
Replicate 2
Replicate 3
ATCC 8482
C
lpxA_362422::IN
lpxA_361958::IN
acrR_361646::IN
acrR_361472::IN
BVU0244
BVU0245
BVU0243
BVU0242
BVU0241
BVU0240
BVU0239
BVU0238
BVU0237
BVU0236
BVU0235
BVU0234
BVU0233
BVU0232
AcrA
AcrB
TolC
LpxA
AcrR
TolC2
AcrA2
AcrB2
Hypothetical protein
Hypothetical protein
Hypothetical protein
Alginate O-acetylation protein
AcrAB-TolC 1
AcrAB-TolC 2
D
OUTER MEMBRANE
TolC
PERIPLASM
AcrA
AcrB
AcrA
H+
COMPOUND
CYTOPLASM
INNER MEMBRANE
E
Retinol sensitivity (treated/control)
WT B. vulgatus
B. vulgatus acrR_361472::IN
B. vulgatus acrR_361646::IN
B. vulgatus lpxA_361958::IN
B. vulgatus lpxA_362422::IN
WT B. dorei
Retinol (μM)
10 5 1
F
Retinol sensitivity (treated/control)
Strain
Complementation
WT
-
acrR_361472::IN
-
acrR_361472::IN
+ pNBU2 alone
acrR_361472::IN
+ pNBU2_acrR

Figure 4.

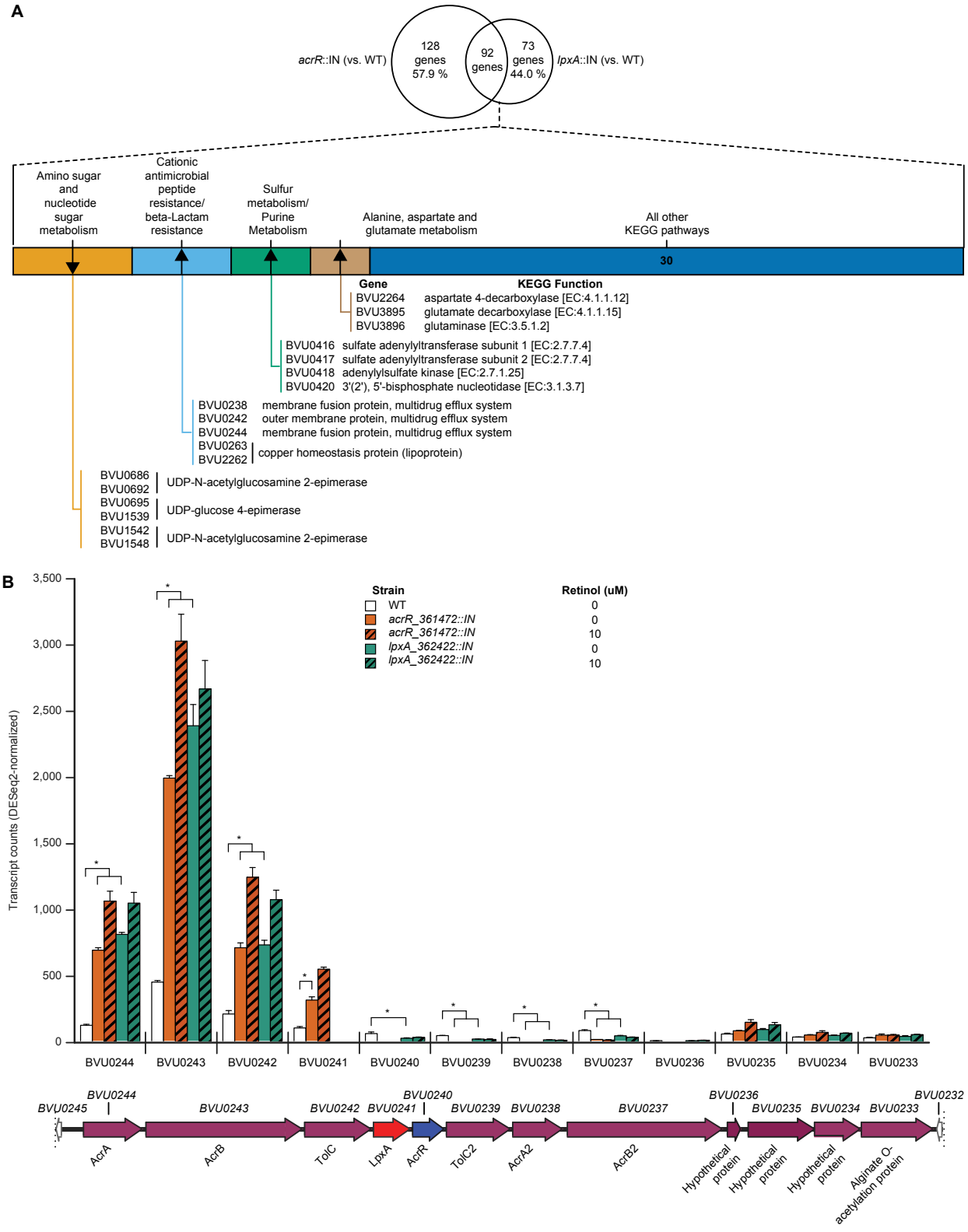
A
acrR::IN (vs. WT)
128 genes 57.9 %
92 genes
73 genes 44.0 %
lpxA::IN (vs. WT)
Amino sugar and nucleotide sugar metabolism
Cationic antimicrobial peptide resistance/ beta-Lactam resistance
Sulfur metabolism/ Purine Metabolism
Alanine, aspartate and glutamate metabolism
All other KEGG pathways
30
Gene
KEGG Function
BVU2264 aspartate 4-decarboxylase [EC:4.1.1.12]
BVU3895 glutamate decarboxylase [EC:4.1.1.15]
BVU3896 glutaminase [EC:3.5.1.2]
BVU0416 sulfate adenylyltransferase subunit 1 [EC:2.7.7.4]
BVU0417 sulfate adenylyltransferase subunit 2 [EC:2.7.7.4]
BVU0418 adenylylsulfate kinase [EC:2.7.1.25]
BVU0420 3'(2'), 5'-bisphosphate nucleotidase [EC:3.1.3.7]
BVU0238 membrane fusion protein, multidrug efflux system
BVU0242 outer membrane protein, multidrug efflux system
BVU0244 membrane fusion protein, multidrug efflux system
BVU0263 BVU2262 copper homeostasis protein (lipoprotein)
BVU0686 BVU0692 UDP-N-acetylglucosamine 2-epimerase
BVU0695 BVU1539 UDP-glucose 4-epimerase
BVU1542 BVU1548 UDP-N-acetylglucosamine 2-epimerase
B
Transcript counts (DESeq2-normalized)
3,500
3,000
2,500
2,000
1,500
1,000
500
0
Strain
Retinol (uM)
WT 0
acrR_361472::IN 0
acrR_361472::IN 10
lpxA_362422::IN 0
lpxA_362422::IN 10
BVU0244
BVU0243
BVU0242
BVU0241
BVU0240
BVU0239
BVU0238
BVU0237
BVU0236
BVU0235
BVU0234
BVU0233
BVU0245
BVU0232
AcrA
AcrB
TolC
LpxA
AcrR
TolC2
AcrA2
AcrB2
Hypothetical protein
Hypothetical protein
Hypothetical protein
Alginate O-acetylation protein

Figure 5.

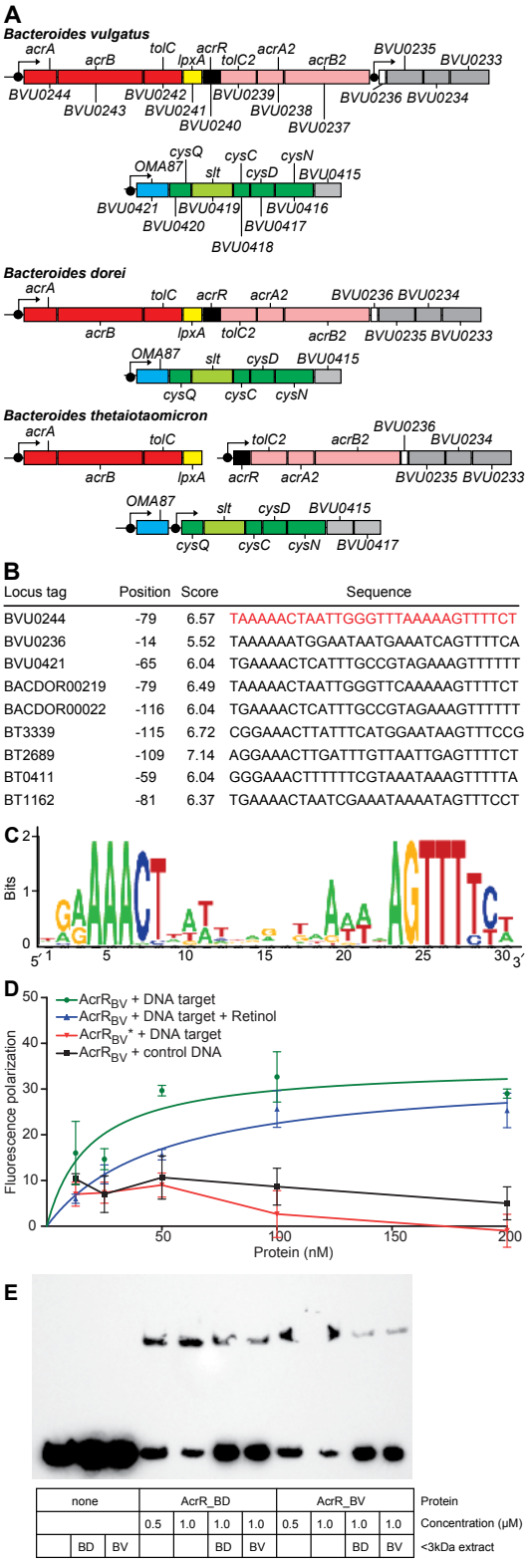
A
Bacteroides vulgatus
acrA
acrB
tolC
acrR
lpxA
tolC2
acrA2
acrB2
BVU0235
BVU0233
BVU0244
BVU0243
BVU0242
BVU0241
BVU0240
BVU0239
BVU0238
BVU0237
BVU0236
BVU0234
cysQ
OMA87
slt
cysC
cysD
cysN
BVU0415
BVU0421
BVU0420
BVU0419
BVU0418
BVU0417
BVU0416
Bacteroides dorei
Bacteroides thetaiotaomicron
B
Locus tag Position Score Sequence
BVU0244 -79 6.57 TAAAAACTAATTGGGTTTAAAAAGTTTTCT
BVU0236 -14 5.52 TAAAAAATGGAATAATGAAATCAGTTTTCA
BVU0421 -65 6.04 TGAAAACTCATTTGCCGTAGAAAGTTTTTT
BACDOR00219 -79 6.49 TAAAAACTAATTGGGTTCAAAAAGTTTTCT
BACDOR00022 -116 6.04 TGAAAACTCATTTGCCGTAGAAAGTTTTTT
BT3339 -115 6.72 CGGAAACTTATTTCATGGAATAAGTTTCCG
BT2689 -109 7.14 AGGAAACTTGATTTGTTAATTGAGTTTTCT
BT0411 -59 6.04 GGGAAACTTTTTTCGTAAATAAAGTTTTTA
BT1162 -81 6.37 TGAAAACTAATCGAAATAAAATAGTTTCCT
C
Bits
D
AcrR_BV + DNA target
AcrR_BV + DNA target + Retinol
AcrR_BV* + DNA target
AcrR_BV + control DNA
Fluorescence polarization
Protein (nM)
E
none
AcrR_BD
AcrR_BV
Protein
Concentration (μM)
BD
BV
<3kDa extract

Figure 6.

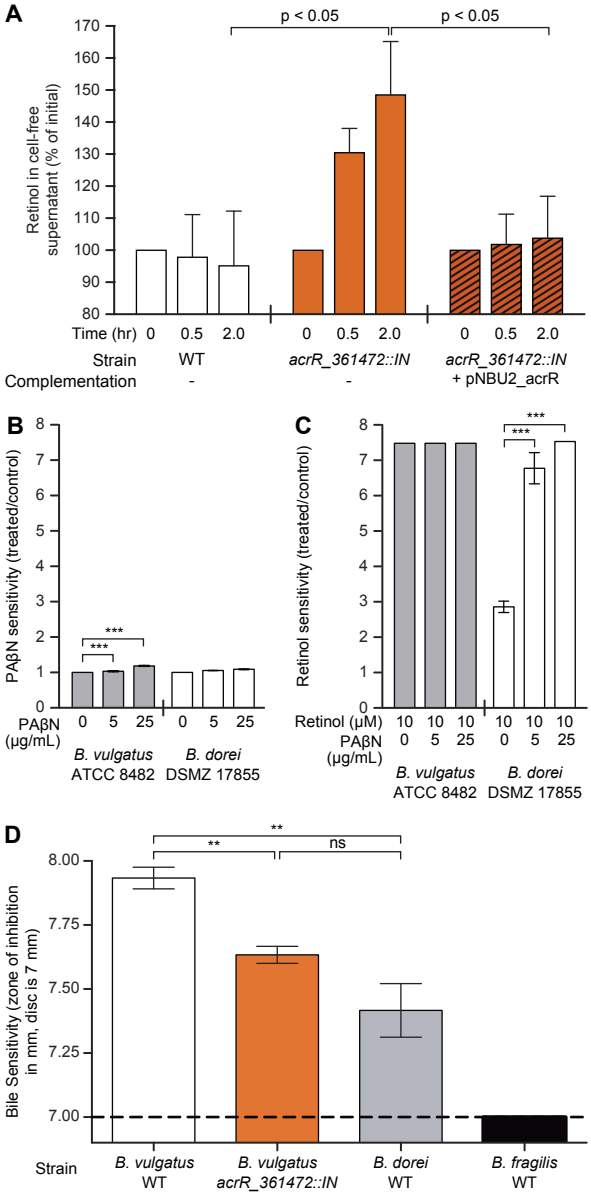
A
p < 0.05
p < 0.05
Retinol in cell-free supernatant (% of initial)
Time (hr) 0 0.5 2.0 0 0.5 2.0 0 0.5 2.0
Strain WT acrR_361472::IN acrR_361472::IN
Complementation - - + pNBU2_acrR
B
PAβN sensitivity (treated/control)
PAβN (μg/mL) 0 5 25 0 5 25
B. vulgatus ATCC 8482
B. dorei DSMZ 17855
C
Retinol sensitivity (treated/control)
Retinol (μM) 10 10 10 10 10 10
PAβN (μg/mL) 0 5 25 0 5 25
B. vulgatus ATCC 8482
B. dorei DSMZ 17855
D
Bile Sensitivity (zone of inhibition in mm, disc is 7 mm)
ns
Strain
B. vulgatus WT
B. vulgatus acrR_361472::IN
B. dorei WT
B. fragilis WT

Table 1. Influences of micronutrient deficiencies on the relative abundances of specific taxa.

OTU ID	Vitamin A deficiency			Iron deficiency			Zinc deficiency			Folate deficiency			Multiple micronutrient deficiency		
	Stage x Diet	Sufficient (Day 14)	Deficient (Day 28)	Sufficient (Day 49)	Stage x Diet	Sufficient (Day 14)	Deficient (Day 28)	Sufficient (Day 49)	Stage x Diet	Sufficient (Day 14)	Deficient (Day 28)	Sufficient (Day 49)	Stage x Diet	Sufficient (Day 14)	Deficient (Day 28)	Sufficient (Day 49)	Stage x Diet	Sufficient (Day 14)	Deficient (Day 28)	Sufficient (Day 49)
Akkermansia_muciniphila_ATCC_BAA-835	0.032	0.715	0.665	0.002	0.289	0.481	0.660	0.122	0.290	0.792	0.759	0.067	0.150	0.484	0.432	0.003	0.929	0.815	0.980	0.761
Anaerotruncus_colihominis_DSM_17241	0.846	0.262	0.713	0.331	0.572	0.267	0.723	0.886	0.135	0.007	0.831	0.014	0.823	0.790	0.289	0.712	0.071	0.313	0.075	0.185
Bacteroides_caccae_ATCC_43185	0.506	0.064	0.724	0.419	0.093	0.192	0.060	0.570	0.356	0.040	0.678	0.768	0.498	0.400	0.926	0.760	0.206	0.221	0.253	0.293
Bacteroides_cellulosilyticus_DSM_14838	0.669	0.144	0.394	0.781	0.923	0.952	0.662	0.949	0.797	0.834	0.476	0.943	0.032	0.133	0.018	0.426	0.440	0.311	0.780	0.455
Bacteroides_dorei_DSM_17855	2.0E-05	2.9E-05	2.2E-08	0.365	0.379	0.732	0.106	0.431	8.8E-05	2.5E-06	0.217	0.299	0.396	0.108	0.518	0.757	0.022	0.004	3.4E-04	0.954
Bacteroides_eggerthii_DSM_20697	0.004	0.027	0.854	0.191	0.550	0.450	0.540	0.947	0.392	0.411	0.356	0.603	0.319	0.662	0.867	0.242	0.071	0.178	0.538	0.936
Bacteroides_finegoldii_DSM_17565	0.968	0.711	0.637	0.506	0.293	0.203	0.569	0.635	0.875	0.705	0.910	0.691	0.210	0.430	0.889	0.057	0.579	0.900	0.284	0.400
Bacteroides_intestinalis_DSM_17393	0.027	0.417	0.879	0.003	0.025	0.193	0.959	0.019	0.332	0.693	0.286	0.222	0.145	0.439	0.991	0.049	0.072	0.204	0.110	0.132
Bacteroides_ovatus_ATCC_8483	0.378	0.422	0.552	0.260	0.558	0.334	0.627	0.508	0.420	0.759	0.287	0.424	0.925	0.587	0.996	0.747	0.879	0.653	0.927	0.823
Bacteroides_thetaiotaomicron_3731	0.216	0.955	0.251	0.040	0.141	0.686	0.115	0.444	0.508	0.579	0.374	0.852	0.214	0.671	0.166	0.050	0.592	0.612	0.773	0.425
Bacteroides_thetaiotaomicron_7330	0.004	0.011	0.053	0.267	0.210	0.098	0.577	0.174	0.252	0.043	0.821	0.830	0.275	0.123	0.796	0.846	0.442	0.889	0.626	0.362
Bacteroides_thetaiotaomicron_VPI-5482	0.368	0.639	0.295	0.020	0.649	0.954	0.475	0.549	0.937	0.448	0.212	0.313	0.771	0.118	0.361	0.078	0.556	0.719	0.264	0.968
Bacteroides_uniformis_ATCC_8492	0.037	0.031	0.211	0.261	0.057	0.784	0.021	0.237	0.340	0.089	0.701	0.733	0.024	0.037	0.220	0.079	0.114	0.533	0.019	0.425
Bacteroides_vulgatus_ATCC_8482	0.001	0.343	0.003	0.011	0.001	0.364	4.7E-05	6.9E-05	0.013	0.316	0.521	0.001	0.114	0.426	0.164	0.269	7.9E-05	0.028	0.006	0.001
Bacteroides_WH2	0.635	0.094	0.452	0.093	0.951	0.583	0.890	0.843	0.374	0.948	0.553	0.188	0.034	0.002	0.197	0.855	0.261	0.162	0.833	0.101
Bacteroides_xylanisolvens_XB1A	0.487	0.161	0.824	0.835	0.005	0.404	0.003	0.043	0.557	0.277	0.903	0.363	0.144	0.567	0.032	0.878	0.822	0.789	0.453	0.899
Bifidobacterium_adolescentis_L2-32	0.505	0.891	0.196	0.931	0.479	0.787	0.153	0.466	0.139	0.451	0.069	0.549	0.727	0.631	0.171	0.681	0.326	0.227	0.134	0.872
Blautia_hansenii_DSM_20583	0.003	0.554	1.0E-04	0.946	0.018	0.850	0.001	0.078	0.155	0.504	0.018	0.915	0.669	0.786	0.842	0.361	0.100	0.519	0.008	0.818
Citrobacter_youngae_ATCC_29220	0.733	0.356	0.946	0.817	0.507	0.905	0.494	0.437	0.028	0.012	0.240	0.542	0.580	0.025	0.128	0.290	0.034	0.421	0.088	0.045
Clostridium_asparagiforme_DSM_15981	0.001	0.116	0.005	0.013	0.009	0.008	0.186	0.322	1.2E-04	2.8E-06	0.504	0.180	0.228	0.100	0.502	0.808	0.091	0.011	0.634	0.079
Clostridium_bolteae_ATCC_BAA-613	0.011	0.492	0.005	0.146	0.005	0.155	0.001	0.678	0.158	0.061	0.435	0.213	0.171	0.171	0.233	0.587	0.038	0.003	0.479	0.152
Clostridium_hathewayi_DSM_13479	0.299	0.895	0.347	0.050	0.441	0.098	0.337	0.009	0.034	4.7E-06	1.3E-05	0.044	0.008	0.011	0.799	0.027	0.140	0.519	0.407	0.225
Clostridium_hylemonae_DSM_15053	0.292	1.000	0.818	0.046	0.241	1.000	0.104	0.023	0.011	1.000	0.608	0.001	0.069	1.000	0.079	0.002	0.213	1.000	0.367	0.169
Clostridium_leptum_DSM_753	0.993	0.640	0.526	0.566	0.465	0.313	0.750	0.278	0.155	0.779	0.133	0.302	0.163	0.873	0.021	0.850	0.383	0.681	0.159	0.444
Clostridium_nexile_DSM_1787	0.174	0.029	0.904	0.890	0.257	0.026	0.001	0.149	0.941	0.387	0.354	0.624	0.280	0.118	0.689	0.988	0.098	0.009	0.771	0.265
Clostridium_ramosum_DSM_1402	0.131	0.821	0.047	0.920	0.177	0.639	0.094	0.806	0.189	0.762	0.072	0.473	0.615	0.365	0.906	0.435	0.012	0.010	0.341	0.703
Clostridium_scindens_ATCC_35704	0.693	0.901	0.660	0.467	0.159	0.223	0.133	0.533	0.376	0.713	0.898	0.125	0.517	0.543	0.090	0.847	0.841	0.733	0.885	0.528
Clostridium_sporogenes_ATCC_15579	0.202	0.258	0.485	0.074	0.057	0.196	0.513	0.040	0.333	1.000	0.112	0.696	0.282	0.871	0.607	0.114	0.047	0.080	0.664	0.129
Clostridium_symbiosum_DSM_934	0.881	0.151	0.045	0.051	0.008	0.002	0.927	0.149	0.277	0.012	0.453	0.389	0.791	0.525	0.471	0.139	0.053	0.000	0.693	0.098
Collinsella_aerofaciens_ATCC_25986	0.002	0.018	0.170	0.033	0.001	0.002	0.572	0.190	0.099	0.015	0.598	0.543	0.047	0.001	0.051	0.982	0.129	0.243	0.173	0.858
Collinsella_intestinalis_DSM_13280	0.006	0.005	0.038	0.892	0.935	0.665	0.883	0.533	0.016	0.482	0.002	0.876	0.047	0.032	0.173	0.577	0.117	0.505	0.234	0.099
Collinsella_stercoris_DSM_13279	0.064	0.172	0.375	0.041	0.099	0.792	0.009	0.038	0.732	0.967	0.472	0.301	0.818	0.402	0.251	0.726	0.585	0.832	0.267	0.935
Coprococcus_comes_ATCC_27758	0.042	3.4E-04	0.418	0.501	0.077	0.090	0.102	0.843	0.005	0.057	0.036	0.009	0.064	0.093	0.074	0.808	0.251	0.109	0.012	0.788
Desulfovibrio_piger_GOR1	0.428	0.080	0.205	0.995	0.622	0.734	0.148	0.771	0.071	0.180	0.044	0.945	0.283	0.610	0.071	0.682	0.561	0.900	0.820	0.256
Edwardsiella_tarda_ATCC_23685	0.036	0.154	0.574	0.044	0.198	0.516	0.036	0.005	0.083	0.430	0.079	0.063	0.506	0.227	0.951	0.999	0.855	0.815	0.355	0.778
Enterobacter_cancerogenus_ATCC_35316	0.129	0.794	0.026	0.785	1.1E-04	0.505	0.031	0.001	0.113	0.192	0.004	1.000	2.5E-04	0.058	0.002	0.001	0.176	0.121	0.025	0.751
Escherichia_fergusonii_ATCC_35469	0.188	0.831	0.018	0.290	0.374	0.635	0.084	0.836	0.102	0.803	0.041	0.810	0.007	0.212	0.004	0.307	0.249	0.388	0.290	0.416
Fusobacterium_varium_ATCC_27725	0.523	0.936	0.851	0.250	0.208	0.117	0.497	0.864	0.703	0.813	0.753	0.539	0.344	0.569	0.148	0.532	0.799	0.816	0.563	0.557
Holdemania_filiformis_DSM_12042	0.955	0.411	0.659	0.630	0.660	0.977	0.340	0.807	0.566	0.510	0.751	0.246	0.959	0.817	0.877	0.887	0.361	0.167	0.885	0.043
Megamonas_funiformis_DSM_19343	0.002	0.004	0.009	0.196	0.016	0.039	0.046	0.979	0.130	0.367	0.102	0.311	0.493	0.726	0.355	0.606	0.003	2.9E-05	0.639	0.295
Parabacteroides_distasonis_ATCC_8503	0.142	0.849	0.109	0.011	0.077	0.842	0.007	0.842	0.900	0.113	0.034	0.040	0.649	0.689	0.387	0.597	0.465	0.661	0.688	0.190
Parabacteroides_johnsonii_DSM_18315	0.423	0.291	0.834	0.446	0.238	0.729	0.177	0.026	0.455	0.874	0.897	0.138	0.674	0.967	0.344	0.869	0.299	0.206	0.376	0.592
Parabacteroides_merdae_ATCC_43184	0.061	0.905	0.112	0.001	0.449	0.417	0.446	0.458	0.056	0.949	0.124	0.001	0.062	0.860	0.007	0.007	0.092	0.955	0.588	0.004
Proteus_penneri_ATCC_35198	0.308	0.207	0.747	0.395	0.405	0.831	0.541	0.110	0.518	0.820	0.496	0.369	0.413	0.504	0.280	0.400	0.626	0.224	0.944	0.344
Ruminococcus_gnavus_ATCC_29149	0.003	0.801	0.037	0.007	0.269	0.012	0.082	0.648	0.512	0.966	0.830	0.209	0.265	0.509	0.308	0.473	0.146	0.226	0.221	0.839
Ruminococcus_gnavus_GM2_1	9.8E-11	7.6E-15	5.1E-15	0.436	2.1E-05	3.8E-09	2.1E-04	0.698	0.001	3.2E-06	0.360	0.747	0.024	0.002	0.692	0.861	1.5E-10	2.5E-13	0.928	0.473
Ruminococcus_torques_ATCC_27756	0.188	0.605	0.543	0.040	0.137	0.695	0.410	0.016	0.347	0.651	0.711	0.033	0.953	0.740	0.946	0.658	0.193	0.708	0.188	0.032
Subdoligranulum_variabile_DSM_15176	0.016	0.735	0.003	0.869	0.013	0.108	0.020	0.643	0.055	0.037	0.693	0.183	0.059	0.019	0.197	0.455	0.122	0.704	0.031	0.686

P-values from linear mixed-effects of models of OTU relative abundances are presented. Within each micronutrient deficiency, the "Stage x Diet" column provides the FDR-corrected *P*-value for the interaction term between experimental stage and diet (micronutrient sufficient vs. deficient). The following three columns under each deficiency category present *P*-values (corrected by Holm's method) for comparisons of least-squares means between the mouse group fed the micronutrient sufficient diet and the group fed the deficient diet within each experimental stage.

Color key: Significant interaction in model | OTU more prevalent in SUFFICIENT group | OTU more prevalent in DEFICIENT group

Supplemental Materials

Supplemental Figure Legends

Figure S1. Characterization of the *B. vulgatus* INSeq library. (**A**) Distribution of transposon mutants in the genome of *B. vulgatus* ATCC 8482. Key; Track 1 (innermost circle), plot of GC skew for the genome using a sliding window size of 10kb (yellow, GC skew > 0; purple, GC skew < 0); Track 2 (middle circle), genes with transposon insertions are depicted in light grey; Track 3 (outermost circle), all genes in the genome are shown with those represented in polysaccharide utilization locus (PULs) colored green, components of capsular polysaccharide synthesis (CPS) loci colored red, and all others colored light grey. (**B**) Estimating the saturation of *B. vulgatus* ATCC 8482 transposon mutant libraries by *in silico* simulation.

Figure S2. Recombinant vector used to complement *B. vulgatus acrR::IN* mutant

Figure S3. Maximum likelihood phylogenetic tree of BVU0240/AcrR orthologs identified in human gut-associated *Bacteroides* and other members of the family Bacteroidaceae. Multiple sequence alignments were generated using ClustalX and exported in PHYLIP format. PhyML was used to generate the maximum likelihood tree, with bootstrap support (out of 100) indicated for a given node.

Figure S4. *In vitro* competition involving *B. vulgatus* and *B. dorei*. Plating was performed at early log (EL) phase of each culture, immediately before treatment with either 10 μM retinol or 0.2% v/v DMSO, and again when cultures reached stationary phase. Mean values ± SEM are shown.

Supplemental Figures

Figure S1.

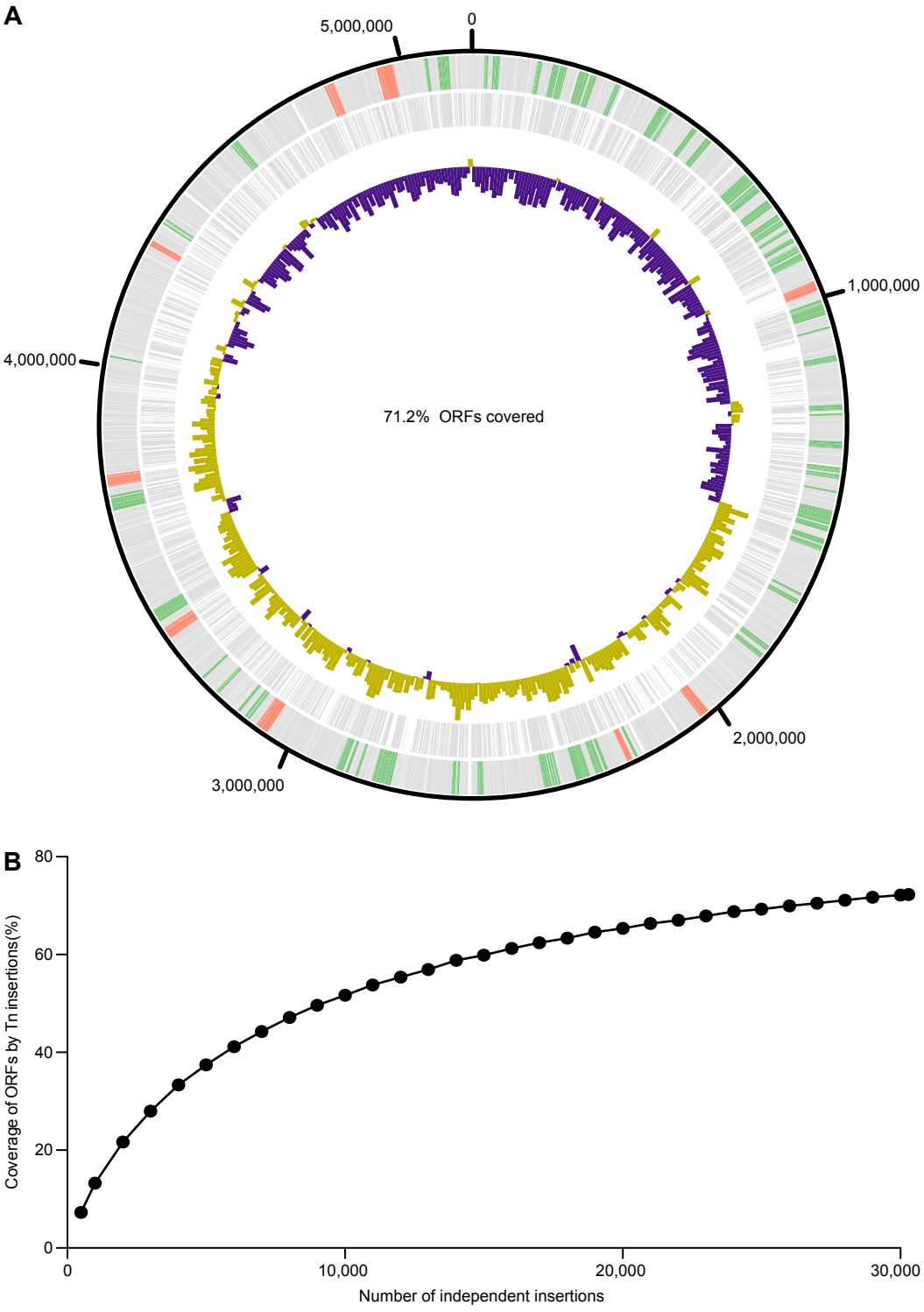

Figure S2.

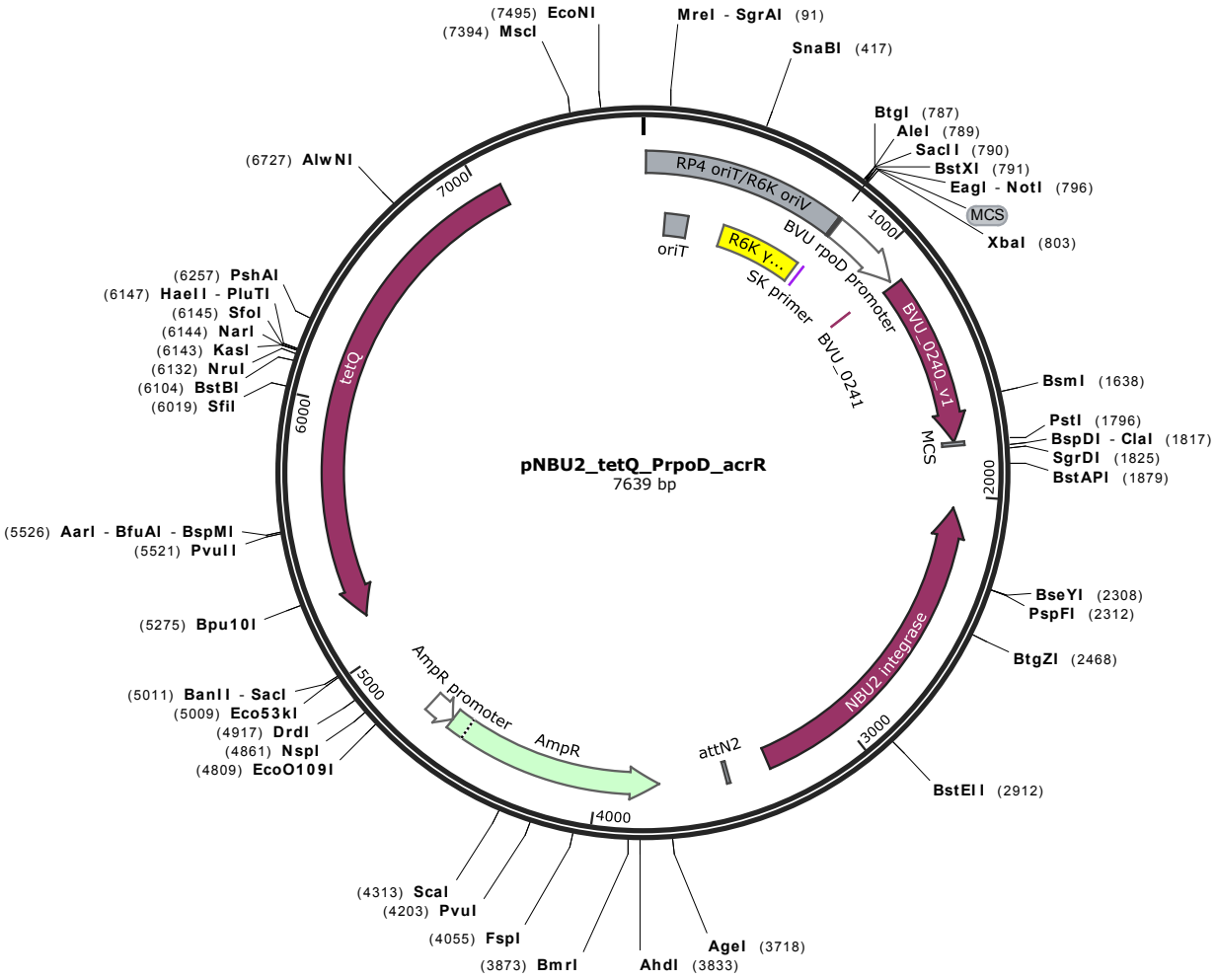
pNBU2_tetQ_PrpoD_acrR
7639 bp
(7495) EcoNI
(7394) MscI
MreI - SgrAI (91)
SnaBI (417)
BtgI (787)
AleI (789)
SacII (790)
BstXI (791)
EagI - NotI (796)
MCS
XbaI (803)
(6727) AlwNI
7000
RP4 oriT/R6K oriV
1000
oriT
R6K γ...
SK primer
BVU rpoD promoter
BVU_0241
BVU_0240_v1
MCS
BsmI (1638)
PstI (1796)
BspDI - ClaI (1817)
SgrDI (1825)
BstAPI (1879)
2000
(6257) PshAI
(6147) HaeII - PluTI
(6145) SfoI
(6144) NarI
(6143) KasI
(6132) NruI
(6104) BstBI
(6019) SfiI
6000
tetQ
(5526) AarI - BfuAI - BspMI
(5521) PvuII
(5275) Bpu10I
BseYI (2308)
PspFI (2312)
BtgZI (2468)
(5011) BanII - SacI
(5009) Eco53kI
(4917) DrdI
(4861) NspI
(4809) EcoO109I
5000
AmpR promoter
AmpR
attN2
NBU2 integrase
3000
BstEII (2912)
4000
(4313) ScaI
(4203) PvuI
(4055) FspI
(3873) BmrI
AhdI (3833)
AgeI (3718)

Figure S3.

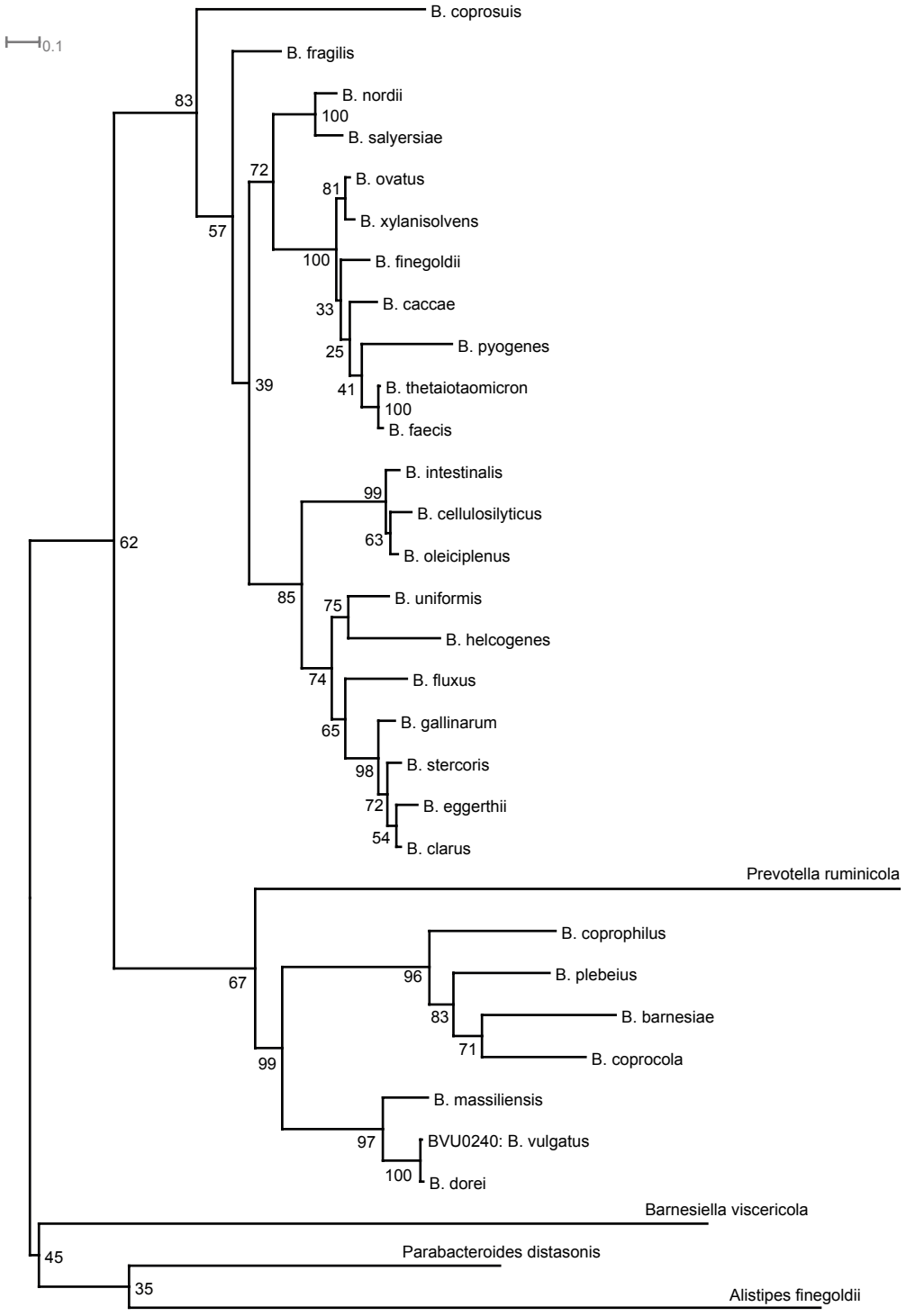
0.1
B. coprosuis
B. fragilis
B. nordii
B. salyersiae
B. ovatus
B. xylanisolvens
B. finegoldii
B. caccae
B. pyogenes
B. thetaiotaomicron
B. faecis
B. intestinalis
B. cellulosilyticus
B. oleiciplenus
B. uniformis
B. helcogenes
B. fluxus
B. gallinarum
B. stercoris
B. eggerthii
B. clarus
Prevotella ruminicola
B. coprophilus
B. plebeius
B. barnesiae
B. coprocola
B. massiliensis
BVU0240: B. vulgatus
B. dorei
Barnesiella viscericola
Parabacteroides distasonis
Alistipes finegoldii
83
100
72
81
57
100
33
25
41
39
100
99
63
62
85
75
74
65
98
72
54
67
96
83
71
99
97
100
45
35

Figure S4.

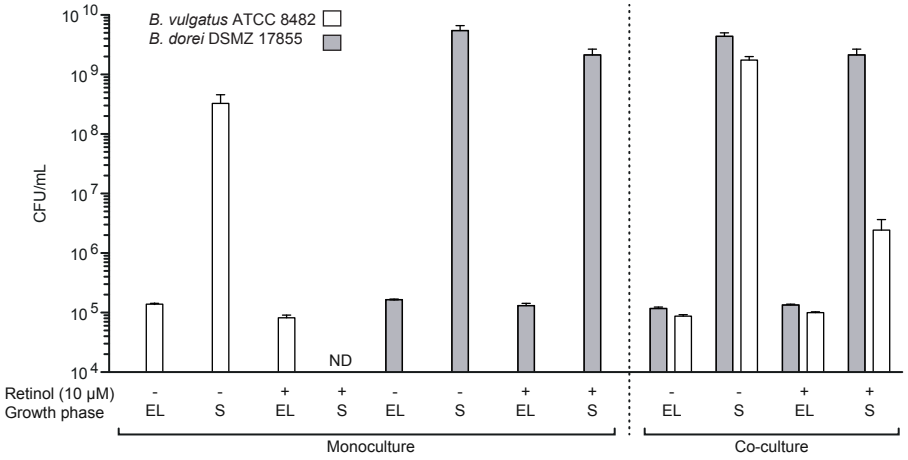

EL = Early log (pre-treatment)
S = Stationary phase

Supplemental Tables

Table S1. Nutritional characteristics of experimental micronutrient deficient and sufficient diets

(A) Diet formulation for micronutrient sufficient and micronutrient deficient defined experimental diets

(B) Micronutrient composition of defined experimental diets

Table S2. 92 sequenced human gut-derived bacterial strains

Table S3: COPRO-Seq analysis of community composition

(A) Relative abundance of strains associated with all treatment groups as measured at the end of the first sufficient diet phase (experimental day 14)

(B) Relative abundance of strains associated with some, but not all treatment groups as measured at the end of the first sufficient diet phase (experimental day 14)

(C) Relative abundance of strains associated with all treatment groups as measured in the micronutrient deficient diet phase (experimental day 28)

(D) Relative abundance of strains associated with some, but not all treatment groups as measured in the micronutrient deficient diet phase (experimental day 28)

(E) Relative abundance of strains associated with all treatment groups as measured in the micronutrient deficient diet phase (experimental day 35)

(F) Relative abundance of strains associated with some, but not all treatment groups as measured in the micronutrient deficient diet phase (experimental day 35)

(G) Relative abundance of strains associated with all treatment groups as measured in the second micronutrient sufficient diet phase (experimental day 49)

Table S4. Identification of community members that exhibit significant changes in their

abundance as a function of diet treatment and/or time

(A) Comparisons between day 14 (all mice on micronutrient sufficient diet) and day 28 (all mice except control on micronutrient deficient diets as indicated), two-group Kruskal-Wallis (KW) tests, false discovery rate corrected p-values where indicated

(B) Comparisons between day 14 (all mice on micronutrient sufficient diet) and day 35 (all mice except control on micronutrient deficient diets as indicated), two-group Kruskal-Wallis (KW) tests, false discovery rate corrected p-values where indicated

(C) Comparisons between day 14 (all mice on micronutrient sufficient diet) and day 49 (all mice on micronutrient sufficient diet), two-group Kruskal-Wallis (KW) tests, false discovery rate corrected p-values where indicated

Table S5. Microbial RNA-Seq analysis of changes in community metatranscriptome as a function of diet treatment with grouping of transcripts into KEGG Orthology (KO) groups

(A) Number of genes with significant differences in their expression as a function of diet treatment and/or time (DESeq2)

(B) KEGG Orthology group-summarized, differentially-expressed genes, vitamin A deficient treatment group

(C) KEGG Orthology group-summarized, differentially-expressed genes, iron deficient treatment group

(D) KEGG Orthology group-summarized, differentially-expressed genes, zinc deficient treatment group

(E) KEGG Orthology group-summarized, differentially-expressed genes, folate deficient treatment group

(F) KEGG Orthology group-summarized, differentially-expressed genes, multiple deficient treatment group

(G) KEGG Orthology group-summarized, differentially-expressed genes, micronutrient sufficient group (monotonous diet)

(H) Differentially-expressed genes in fecal microbiota of members of the different treatment groups, referenced to monotonous micronutrient sufficient diet control group, summarized at the level of KEGG Pathways.

Table S6. Microbial RNA-Seq analysis of changes in *B. vulgatus* gene expression as a function of diet treatment with grouping of transcripts into KEGG Orthology (KO) groups

(A) Number of genes with significant differences in their expression as a function of diet treatment and/or time (DESeq2)

(B) KEGG Orthology group-summarized, differentially-expressed genes, vitamin A deficient treatment group

(C) KEGG Orthology group-summarized, differentially-expressed genes, iron deficient treatment group

(D) KEGG Orthology group-summarized, differentially-expressed genes, zinc deficient treatment group

(E) KEGG Orthology group-summarized, differentially-expressed genes, folate deficient treatment group

(F) KEGG Orthology group-summarized, differentially-expressed genes, multiple deficient treatment group

(G) KEGG Orthology group-summarized, differentially-expressed genes, micronutrient sufficient group (monotonous diet)

Table S7. Strain level RNA-Seq analysis of the effects of vitamin A on gene expression (summarized at the level of KEGG Orthology (KO) groups)

(A) Number of genes with significant differences in their expression as a function of strain, diet

treatment and/or time (DESeq2)

(B) *B. dorei* DSMZ 17855 KEGG Orthology group-summarized, differentially-expressed genes

(C) *P. merdae* ATCC 43184 KEGG Orthology group-summarized, differentially-expressed genes

(D) *B. thetaiotaomicron* 7330 KEGG Orthology group-summarized, differentially-expressed genes

(E) *B. intestinalis* DSM 17393 KEGG Orthology group-summarized, differentially-expressed genes

(F) *B. thetaiotaomicron* VPI-5482 KEGG Orthology group-summarized, differentially-expressed genes

(G) *B. uniformis* ATCC 8492 KEGG Orthology group-summarized, differentially-expressed genes

(H) *B. cellulosilyticus* WH2 KEGG Orthology group-summarized, differentially-expressed genes

(I) *B. eggerthi* DSM 20697 KEGG Orthology group-summarized, differentially-expressed genes

(J) *C. intestinalis* DSM 13280 KEGG Orthology group-summarized, differentially-expressed genes

(K) *A. colhiminis* DSM 17241 KEGG Orthology group-summarized, differentially-expressed genes

(L) *C. nexile* DSM 1787 KEGG Orthology group-summarized, differentially-expressed genes

(M) *R. gnavus* ATCC 29149 KEGG Orthology group-summarized, differentially-expressed genes

(N) *C. symbiosum* DSM 934 KEGG Orthology group-summarized, differentially-expressed genes

(O) *C. aerofaciens* ATCC 25986 KEGG Orthology group-summarized, differentially-expressed genes

(P) *B. hansenii* DSM 20583 KEGG Orthology group-summarized, differentially-expressed genes

(Q) *C. asparagiforme* DSM 15981 KEGG Orthology group-summarized, differentially-expressed

genes

(R) *C. scindens* ATCC 35704 KEGG Orthology group-summarized, differentially-expressed genes

(S) *R. torques* ATCC 27756 KEGG Orthology group-summarized, differentially-expressed genes

(T) *E. fergusonii* ATCC 35469 KEGG Orthology group-summarized, differentially-expressed genes

Table S8. Mouse weights as a function of diet treatment and time

Table S9. In vitro retinoid sensitivities of Bacteroides strains

(A) *B. vulgatus* ATCC 8482 and *B. dorei* DSMZ 17855

(B) *B. vulgatus* ATCC 8482 and a primary *B. vulgatus* isolate from a Malawian child

(C) *B. vulgatus* ATCC 8482, *B. vulgatus* Tn mutants, and *B. dorei* DSMZ 17855

(D) *B. vulgatus* (ATCC 8482), *B. vulgatus* Tn mutants, and complemented *B. vulgatus* Tn mutants.

Table S10. Strains, Primers, and Plasmids used in this study

Table S11. RNA-Seq analysis of *B. vulgatus* WT and Tn mutants (DESeq2)

Table S12. Characterization of *acrR* regulons in human gut Bacteroides strains

(A) Orthologs of components of B. vulgatus *acrR* regulon in other Bacteroides

(B) Conservation of BVU0240 (*acrR*) orthologs

(C) AcrR binding site predictions in Bacteroides

Table S13. Effects of bile acids and a pharmacologic inhibitor of AcrAB-TolC on growth of WT and mutant strains of *B. vulgatus* and WT human gut Bacteroides strains

(A) Effects of pharmacologic inhibition of AcrAB-TolC by Phenylalanine-Arginine β-Naphthylamide (PAβN) on growth and retinol sensitivity

(B) Bile acid sensitivity

Table S14. UPLC-MS analysis of the effects of micronutrient deficiency on fecal bile acid metabolites

Chapter 3

Future directions

Introduction

The work described in this dissertation has revealed an interaction between vitamin A, a dietary micronutrient of global health significance, and members of the human gut microbiota. Expanding the defined community concept to capture the strain diversity of the human gut microbiota and the application of COPRO-Seq, microbial RNA-Seq, INSeq, genetic complementation, transcription factor binding and mass spectrometry-based analyses provides an experimental framework for future studies. At least three major areas need to be explored further: (1) additional mechanistic characterization of the interactions between vitamin A and human gut *Bacteroides*; (2) advancing experimental and computational approaches for analyzing the responses of large defined human gut microbial communities, installed in gnotobiotic models, to specific micronutrient deficiencies, and (3) translating knowledge gained from these preclinical studies to proof of concept/proof of mechanism studies in humans.

Further mechanistic characterization of bacterial responses to micronutrients

Vitamin A resistance mechanisms, toxicity, and interspecies variation in sensitivity

Several outstanding questions/issues arise from the work described in Chapter 2: (1) confirm and expand our understanding of the role of multidrug efflux as a determinant of resistance to vitamin A; (2) identify the intracellular targets of retinol and its mechanism of toxicity, and (3) investigate the determinants of differential sensitivity in *B. vulgatus* and other human gut bacterial taxa to retinol, including the role of microbial metabolites of bile acids.

While transcriptional and genetic analyses implicate the AcrAB-TolC efflux machinery in vitamin A resistance *in vitro*, and to some extent, *in vivo*, additional work is needed to directly measure the physical movement of retinoid movement from the cytoplasm or periplasm to the extracellular environment to validate our predictions. Retinoids can be effectively quantified by mass-spectrometric techniques. Once protocols are optimized, quantitative efflux studies should be performed using wild-type *B. vulgatus* strains and corresponding *acrR*::IN and *lpxA*::IN mu-

tants with retinol in the presence and absence of varying concentrations of the bile acid metabolites we have identified in the microbiota of animals treated with the specified dietary micronutrient manipulations; the results should be correlated with vitamin A sensitivity (see below).

The mechanism of retinol-mediated killing of *B. vulgatus* remains unknown. Two lines of evidence provide hypotheses that can be tested. Bile acids possess similar chemical properties to retinoids, are known to physically associate with retinoids *in vivo* to facilitate their epithelial absorption, and have relatively well-studied mechanisms of toxicity in bacteria; i.e., they induce membrane damage and destabilize macromolecules through detergent-like effects (reviewed in Begley et al., 2005). I have identified consistently higher *in vitro* sensitivity to bile acids in the wild-type *B. vulgatus* strain compared to the wild-type *B. dorei* strain. Moreover, the mutant *B. vulgatus acrR*::IN strain (in which expression of the AcrAB-TolC efflux machinery is upregulated) exhibits reduced bile sensitivity compared to the corresponding isogenic wild-type strain. This profile of bile acid sensitivity parallels the profile of retinol sensitivity in these organisms. Therefore, I hypothesize that retinol may exert its toxicity via bile-like mechanisms, e.g. membrane damage. This hypothesis is further supported by the observation that the multidrug efflux system identified as regulated by the key determinant of retinol resistance (the *B. vulgatus* AcrR) is also a key determinant of bile acid resistance in other organisms (Lacroix et al. 1996; Prouty et al. 2004; Thanassi et al., 1997).

A second hypothesis regarding the mechanism of retinol toxicity is that an altered profile of proteins that are post-translationally, covalently modified with retinol (Kubo et al. 2005; Genchi and Olson 2001) leads to toxicity. Protein retinoylation is thought to have important consequences for cell fate in eukaryotic lineages (Breitman et al., 1980; Breitman et al., 1981; Myhre et al. 1996); however, it is unclear how retinoylation affects protein structure or enzymatic activity (Takahashi and Breitman 1991) or if it occurs in bacteria. Improvements in mass-spectrometry-based proteomics are providing new insights into the types and protein targets of bacterial post-translational modifications (PTMs; Cain et al., 2014). In eukaryotes, retinoylation relies on formation of an ester or thioester bond, an observation that helps guide expectations of which amino acids may be

modified by this PTM in bacteria. Analyzing high resolution proteomic datasets generated from cultures of wild-type and *acrR*::IN *B. vulgatus* strains exposed to varying levels of retinol for peptide fragments shifted from their expected mass by an amount that could reflect retinoylation represents a first pass approach to determine if this PTM occurs in Bacteroides. If retinoylation is observed, knowledge of the function of the targeted bacterial proteins could help delineate mechanisms of toxicity.

It will be important to identify the determinants of the differential responses of *B. vulgatus* strains and *B. dorei* to retinol *in vitro* and *in vivo*. The studies described in Chapter 2 indicate that retinol is not a direct ligand of the AcrR homologs of either organism. As implied above, comparable studies need to be performed with bile acid species identified by UPLC-MS of cecal and fecal samples obtained from gnotobiotic mice harboring the defined community and subjected to the diet oscillation, namely tauro-β-muricholic acid, β-muricholic acid, and deoxycholic acid (molecular weights all < 550 Da), to determine whether these compounds serve as AcrR ligands in this system. Intriguingly, we have found that the *in vitro* DNA-binding activity of this transcription factor is affected by an as yet unidentified < 3 kDa factor present in cellular extracts of both organisms. Identifying the bioactive compound in this fractionated extract may provide clues as to the nature of primary signals that regulate this locus, and how regulation of this locus differs between *B. vulgatus* and *B. dorei*.

If differences in vitamin A resistance cannot be attributed to differential regulation of the activity of the AcrAB-TolC system or its associated AcrR transcription factor by retinol/bile acid metabolites, other aspects of efflux regulation may differentiate the species. For example, the AcrAB system in *E. coli* is subject to an additional layer of regulation by the cell-stress-sensitive transcription factors MarA and MarR (Multiple antibiotic resistance Activator and Regulator/Repressor, respectively) (George and Levy 1983; Barbosa and Levy 2000; Keeney et al. 2007). To date, my preliminary BLASTP-based searches for MarA and MarR in the *B. vulgatus* and *B. dorei* genomes have produced several candidate MarA, but no MarR orthologs in either species. In *B. vulgatus*, transcripts from three of four candidate *marA* genes (*BVU0079, BVU0737*, and *BVU3088*) were

detectable in WT and *acrR*::IN but no differential expression was observed between the strains or treatment with retinol). *In vitro* experiments assaying the transcriptional responses of *B. dorei marA* candidates to retinol treatment and genetic tests are needed to evaluate whether predicted *B. dorei marA* orthologs are involved in regulating retinol sensitivity phenotypes

In *E. coli*, a conserved protein AcrZ is activated by MarA, physically associates with the AcrB component of the efflux pump, and enhances efflux of specific antibiotics (Hobbs et al. 2012; Du et al. 2014). Preliminary BLASTP queries for *Bacteroides* AcrZ homologs have also failed to detect orthologs.

Detailed comparative genomic analyses coupled to detailed assays of the retinol sensitivities of different strains of *B. vulgatus* in the presence/absence or various bile acid metabolites may provide insights about the mechanisms underlying their discordant retinol sensitivity phenotypes as well as the discordant sensitivity phenotypes of various human gut-derived Bacteroides, including *B. dorei*. Finally, while the studies described in Chapter 2 implicate AcrAB-TolC-mediated efflux as a contributor to vitamin A resistance in *B. vulgatus*, differential sensitivities may also involve efflux-independent mechanisms.

Expanding host-side exploration of bacteria-vitamin A interactions

The experiments described in my thesis were intended to investigate the effects of micronutrient deficiency on members of the gut microbiota and did not focus on the host. By design, no attempts were made to induce deficiency in host cell lineages. Mouse models of vitamin A deficiency rely on long-term exposure to deficient diets (periods of >10 months or more) or intergenerational transfer of deficiency by exposure of pregnant dams to vitamin A deficient diets, followed by weaning of their offspring onto the same deficient diets (Moore and Holmes 1971; McCarthy and Cerecedo 1952). These intergenerational deficiency models present challenges when using gnotobiotic models, as the effects of nutritional status on bacterial colonization must be considered in order to provide reasonably-equivalent initial microbial populations for subsequent experimentation. An alternative strategy is based on the observation that *in vitro*, retinol was the most potent

retinoid inhibitor of the growth of *B. vulgatus*; however, free retinol is relatively uncommon in dietary ingredients. The metabolism of dietary vitamin A requires processing of retinyl esters by host retinyl ester hydrolases (REHs) secreted into the intestinal lumen or associated with the epithelial brush border (membrane-associated phospholipase B1); the resulting retinol is then transported across the epithelium (Stipanuk and Caudill 2013; Reboul 2013). Stable or inducible knockouts of these host genes in mice re-derived germfree would provide a model where retinol levels could be manipulated in a more typical diet context and in an otherwise healthy host. A challenge of this approach is that vitamin A metabolites have broad effects on a variety of host functions; thus, any disruption of vitamin A metabolism could disrupt essential processes and lead to unanticipated off-target effects.

As suggested by the *in vitro* experiment described in Chapter 2, retinol-sensitive bacteria may arise based on an inability to export cell-associated retinol. Retinol-resistant bacteria may be efflux sufficient, or may achieve resistance by an as yet unidentified chemical transformation of retinol that generates a derivative of reduced toxicity. Follow-up studies in the gnotobiotic animals colonized with defined bacterial communities consisting of retinol-sensitive or -resistant taxa and subjected to dietary vitamin A manipulations could identify situations in which sensitive bacteria affect vitamin A availability to the host by either sequestration, or by actively transforming it to a form with altered bioavailability/bioactivity.

Observations from both the *in vivo* and *in vitro* studies support a model of the interactions between *B. vulgatus* and vitamin A illustrated in **Figure 1**. In the context of a diet replete with vitamin A, retinol liberated from the retinyl esters by brush border or luminal host enzymes interacts with bile acid species generated by the host and transformed by microbial metabolism as part of its absorptive process. This liberated, bile-associated retinol interacts with *B. vulgatus* and other Bacteroides such as *B. dorei* in the distal small intestine and proximal colon (as hypothesized above, an additional level of interaction may occur at the level of the efflux pump). *In vitro* retinol sensitivity and competition assays suggest that *B. vulgatus* is inhibited or killed by this interaction, whereas *B. dorei* is much less sensitive, thus allowing *B. dorei* to thrive in the presence of vitamin

A. Under circumstances of vitamin A deficiency, the balance between *B. vulgatus* and *B. dorei* is not tipped in favor of *B. dorei*. A related hypothesis based on the greater concentration of free or bile-associated vitamin A in the small intestine compared to colon is that the spatial distribution of these two organisms along the length of the gut may also be affected by the presence of vitamin A. A decreasing retinol gradient from the small intestine to more distal regions of the gut due to incomplete absorption (under vitamin A sufficient diet conditions) may favor resistant organisms like *B. dorei* over sensitive organisms like *B. vulgatus*.

The effects of other micronutrient deficiencies on the model gut microbiota

Dietary folate deficiency induced the second largest effect on the structure of the model community (17 organisms) and its expressed meta-transcriptome, though the transcriptional effect was manifest primarily when animals were returned to a folate-sufficient diet after experiencing folate deficiency. The ability to synthesize folate is a common feature of human gut bacterial taxa. In the context of dietary folate deficiency, organisms capable of producing this vitamin should exhibit a fitness advantage; however, other members of the microbiota that are incapable of *de novo* synthesis can "salvage" folate either in its intact form or by the less well characterized transport of pterin and *p*-aminobenzoate-glutamate precursors (de Crécy-Lagard et al. 2007). In support of this view, organisms that displayed positive responses to folate deficiency generally belong to taxa that are capable of *de novo* folate biosynthesis (as defined by KEGG or SEED-based in silico metabolic reconstructions). None of these organisms possessed annotated folate transporters: however, many possessed transport and utilization proteins for aminobenoyl-glutamate. A more complete analysis is needed of folate precursor synthetic and transport capabilities in the folate-responsive organisms identified from during the course of this thesis.

Only four organisms displayed significant decreases in abundance in response to folate deficiency. Based on a SEED subsystem analysis (http://rast.nmpdr.org/seedviewer.cgi) only one member of this group, *C. aerofaciens*, is predicted to rely on salvage for acquisition of folate or folate precursors (specifically, 7,8-dihydropteroate). As bacterial folate biosynthesis is much more

common than salvage, one prediction is that a salvage-dependent organism would be negatively impacted by folate deficiency.

Fewer organisms were affected by iron and zinc deficiency (13 and 14 responsive species, respectively). Bacteria possess sophisticated systems for siderophore-mediated or direct acquisition of complexed or free iron and zinc, suggesting a possible competitive interaction between host and microbiota for these metals. Interestingly, earlier studies in gnotobiotic animals, discussed in Chapter 1, suggested beneficial roles for bacteria in iron metabolism and detrimental roles for bacteria in zinc metabolism. In our system, responses to both mineral deficiencies were similar for a number of Bacteroides and Clostridia, both in terms of direction and magnitude.

Desulfovibrio piger GOR1 displayed a significant increase in its relative abundance between when animals were switched to an Fe-deficient diet: this increase abundance was 'reversed' when mice were returned to the Fe-sufficient diet. This organism reduces sulfate as a component of its terminal anaerobic respiration; in other environments related organisms can reduce ferric iron directly (as electron acceptor) or indirectly (via reduced sulfate) (Tebo and Obraztsova 1998; Lovley et al. 1993). The observed response in *D. piger* to Fe-deficiency seem paradoxical: we would expect that under iron-restricting conditions respiration would be slowed (assuming sulfate is available) and fitness reduced, not increased. Unfortunately, functional annotation of differentially-expressed genes in *D. piger* GOR1 via KEGG only yielded genes of unknown function.

Technical considerations

Community structure analyses - COPRO-Seq

The studies described in this thesis provide evidence that model communities composed of ~50 diverse bacteria are amenable to structural analysis using scalable, shotgun-sequencing methods like COPRO-Seq. These shotgun sequencing methods avoid the bias introduced by primer selection and PCR in 16S rRNA amplicon analyses. COPRO-Seq relies on the availability of draft quality or complete genome sequences; its reliance on identification of unique regions in each member

genome of the assayed community provides the essence of the power of the method and its capacity to resolve strain-level differences in response to different perturbations. Our ability to culture bacterial strains from biospecimens obtained from individual donors with biological phenotypes of interest provides an opportunity to generate "personal, clonally-arrayed, sequenced culture collections" that capture organisms that have co-evolved in a single gut habitat and reflect the environmental exposures that the donor has experienced in his/her lifetime (Goodman et al. 2011; Blanton et al. 2016; Charbonneau et al. 2016). High-throughput culturing and genome sequencing efforts have recently identified an important taxonomic issue: disagreement between 16S rRNA-based, whole genome-based, and phenotypic identification is an increasingly common problem for newly-isolated strains. Achieving a well-supported consensus about assembly strategies, identification of genome contaminants, taxonomic identification, and gene prediction/annotation is essential to unite the diverse datatypes associated with high-throughput culturing and genome sequencing efforts. With well-characterized culture collections, the limitations of COPRO-Seq are reduced mainly to the quantity of sequencing a research group is willing to devote to their analyses of community composition and structural variation.

Community metatranscriptome analyses - Microbial RNA-Seq

The same efforts to generate and annotate draft quality genome sequences for COPRO-Seq also enable microbial RNA-Seq analyses of defined communities. Microbial transcriptional analyses need to consider gene boundaries, operon structures, and RNAs arising from regions of the genome that are not predicted to encode proteins. Following from this, the "search space" for assigning reads to genes to identify transcript enrichment and by inference the biological meaning of transcriptional responses represents a major bioinformatics challenge. This challenge can be addressed using at least two approaches. The first method, typically applied to intact uncultured community samples, relies on brute force by increasing sequencing depth. Although this method is enabled by decreases in sequencing costs, it is still costly at the scale that is often required. In addition, larger datasets require additional computational resources to process. A second strategy

relies on directly reducing the search space by (i) utilizing defined communities of cultured organisms for which genome sequences are available, (ii) improving gene annotations, and (iii) carefully curating transcriptomic datasets. High fidelity gene annotations, in addition to predicting gene function, enable researchers to shrink the search space down to portions of the genome that represent protein-coding sequences. Reads assigned to non-coding regions should not be discarded, as information can be used to refine gene boundaries (as a component of gene calling and annotation operations) and study small RNA biology. Carefully curating metatranscriptomic datasets during analysis helps reduce search space post-facto, as it can allow researchers to set inclusion criteria for organisms in metatranscriptomic analyses based on depth and quality of coverage. Even with the significant level of transcriptomic sequencing pursued in Chapter 2, some organisms in the defined community were not present at high enough abundance, or did not contribute sufficiently to the community metatranscriptome, to be reliably assayed. We approached identification of such organisms by rarefying metatranscriptome data and examining the degree to which plotted curves approached saturation (saturation indicating a theoretically complete coverage of an organism's transcribed genome). This expressed transcriptome "coverage" analysis was used to set inclusion criteria for organisms with "high," "mid," or "low" level coverage. Only organisms with high or mid-level coverage were considered in our bottom-up analyses, though all detectable transcripts were considered in top-down analyses. These types of considerations help to reduce errors introduced by statistical analysis of poorly-assayed transcriptomes.

Linking gnotobiotic micronutrient deficiency models to real-world global health outcomes

This dissertation sought to build on three key elements - highly-defined experimental diets deficient in specific micronutrients, defined model communities, and gnotobiotic mouse models – to characterize the effects of micronutrient deficiency on the gut microbiota. Clearly, micronutrient deficiencies present an immense global health challenge and studies reviewed in Chapter 1 indicate that gut microbes have both beneficial and detrimental roles in affecting host micronutrient status. A valuable next set of experiments would be to further study personal culture collections

generated from children, living in areas of the world with a high burden of undernutrition, who do or do not exhibit micronutrient deficiencies of interest. Preliminary evidence suggests that a *B. vulgatus* strain obtained from a culture collection generated from a fecal sample from healthy Malawian infant exhibits *in vitro* vitamin A sensitivity on par with the type strain *B. vulgatus* included in the large, defined community analyzed in Chapter 2. Experiments designed to examine the effects of vitamin A deficiency on the fitness of this primary *B. vulgatus* isolate in the context of members of its native community would help connect results obtained in this dissertation to more directly human relevant microbial communities. This type of model could be expanded to include a COPRO-Seq analysis of this same community but supplemented with a consortium of sequenced *B. vulgatus* isolates from multiple donors with and without micronutrient deficiency to define their relative fitness under conditions of vitamin A sufficiency or deficiency.

A second strategy to link the work described in Chapter 2 to micronutrient deficiencies in the developing world would be to correlate dietary micronutrient content, with a focus on vitamin A, with human fecal microbiota profiles obtained from clinical sites where deficiencies are endemic. To do so, we could leverage our lab's ongoing partnership members of with the Bill & Melinda Gates Foundation-supported MAL-ED consortium ("The Interactions of Malnutrition & Enteric Infections: Consequences for Child Health and Development") and a large repository of biospecimens (fecal and serum) that had been serially collected from members of birth cohorts living in five different low income countries. While these analyses could focus on vitamin A and *Bacteroides*, these could be expanded to include other taxa affected by the single micronutrient deficient states examined in Chapter 2. If correlations between microbial abundance and vitamin A status and Bacteroides in these samples are identified, culture collections could be generated for additional analyses in gnotobiotic mice and *in vitro*.

Finally, results from this work suggests that administration of micronutrient supplements may have unintended and unanticipated effects on the gut microbiota. The composition of multiple micronutrient supplements is carefully controlled with regard to iron in areas of the world where malaria is endemic (Soofi et al. 2013; Veenemans et al. 2011). However, supplements intended

to treat vitamin A deficiency generally contain levels of vitamin A that significantly exceed recommended daily doses. Given that (i) these doses may affect the composition of the developing human gut microbiota, and (ii) gnotobiotic mouse models have been used recently to provide preclinical proof of concept that impaired development of the gut microbiota ('microbiota immaturity') in children with undernutrition is causally related to their impaired growth and metabolism (Blanton et al. 2016), it may be informative to test the effects of administering different doses of dietary micronutrients to gnotobiotic recipients of transplanted intact uncultured microbiota from these children.

References

Barbosa, T M, and S B Levy. 2000. "Differential Expression of Over 60 Chromosomal Genes in Escherichia Coli by Constitutive Expression of MarA.." *Journal of Bacteriology* 182 :3467–74.

Begley, M, C G M Gahan, and C Hill. 2005. "The Interaction Between Bacteria and Bile.." *FEMS Microbiology Reviews* 29: 625–51. doi:10.1016/j.femsre.2004.09.003.

Blanton, L V, M R Charbonneau, T Salih, M J Barratt, S Venkatesh, O Ilkaveya, S Subramanian, et al. 2016. "Gut Bacteria That Prevent Growth Impairments Transmitted by Microbiota From Malnourished Children.." *Science* 351: aad3311. doi:10.1126/science.aad3311.

Breitman, T R, S E Selonick, and S J Collins. 1980. "Induction of Differentiation of the Human Promyelocytic Leukemia Cell Line (HL-60) by Retinoic Acid.." *Proceedings of the National Academy of Sciences of the United States of America USA* 77 (5). 2936–40.

Breitman, T R, S J Collins, and B R Keene. 1981. "Terminal Differentiation of Human Promyelocytic Leukemic Cells in Primary Culture in Response to Retinoic Acid.." *Blood* 57: 1000–1004.

Cain, J A, N Solis, and S J Cordwell. 2014. "Beyond Gene Expression: the Impact of Protein Post-Translational Modifications in Bacteria.." *Journal of Proteomics* 97: 265–86. doi:10.1016/j.jprot.2013.08.012.

Charbonneau, M R, D O'Donnell, L V Blanton, S M Totten, J C C Davis, M J Barratt, J Cheng, et al. 2016. "Sialylated Milk Oligosaccharides Promote Microbiota-Dependent Growth in Models of Infant Undernutrition.." *Cell* 164 (5): 859–71. doi:10.1016/j.cell.2016.01.024.

de Crécy-Lagard, V, B El Yacoubi, R Díaz de la Garza, A Noiriel, and A D Hanson. 2007. "Comparative Genomics of Bacterial and Plant Folate Synthesis and Salvage: Predictions and Validations.." *BMC Genomics* 8: 245. doi:10.1186/1471-2164-8-245.

Du, D, Z Wang, N R James, J E Voss, E Klimont, T Ohene-Agyei, H Venter, W Chiu, and B F Luisi. 2014. "Structure of the AcrAB-TolC Multidrug Efflux Pump.." *Nature* 509: 512–15. doi:10.1038/nature13205.

Genchi, G, and J A Olson. 2001. “Retinoylation of Proteins in Cell-Free Fractions of Rat Tissues in Vitro.” *Biochimica Et Biophysica Acta (BBA) - Molecular and Cell Biology of Lipids* 1530 : 146–54. doi:10.1016/S1388-1981(00)00175-X.

George, A M, and S B Levy. 1983. “Amplifiable Resistance to Tetracycline, Chloramphenicol, and Other Antibiotics in Escherichia Coli: Involvement of a Non-Plasmid-Determined Efflux of Tetracycline..” *Journal of Bacteriology* 155: 531–40.

Goodman, A L, G Kallstrom, J J Faith, A Reyes, A Moore, G Dantas, and J I Gordon. 2011. “Extensive Personal Human Gut Microbiota Culture Collections Characterized and Manipulated in Gnotobiotic Mice..” *Proceedings of the National Academy of Sciences USA* 108: 6252–57. doi:10.1073/pnas.1102938108.

Hobbs, E C, X Yin, B J Paul, J L Astarita, and G Storz. 2012. “Conserved Small Protein Associates with the Multidrug Efflux Pump AcrB and Differentially Affects Antibiotic Resistance..” *Proceedings of the National Academy of Sciences USA* 109 :16696–701. doi:10.1073/pnas.1210093109.

Keeney, D, A Ruzin, F McAleese, E Murphy, and P A Bradford. 2007. “MarA-Mediated Overexpression of the AcrAB Efflux Pump Results in Decreased Susceptibility to Tigecycline in Escherichia Coli.” *The Journal of Antimicrobial Chemotherapy* 61: 46–53. doi:10.1093/jac/dkm397.

Kubo, Y, M Wada, T Ohba, and N Takahashi. 2005. “Formation of Retinoylated Proteins From Retinoyl-CoA in Rat Tissues..” *Journal of Biochemistry* 138 : 493–500. doi:10.1093/jb/mvi145.

Lacroix, F J, A Cloeckaert, O Grépinet, C Pinault, M Y Popoff, H Waxin, and P Pardon. 1996. “Salmonella Typhimurium acrB-Like Gene: Identification and Role in Resistance to Biliary Salts and Detergents and in Murine Infection..” *FEMS Microbiology Letters* 135: 161–67.

Lovley, D R, E E Roden, E J P Phillips, and J C Woodward. 1993. “Enzymatic Iron and Uranium Reduction by Sulfate-Reducing Bacteria.” *Marine Geology* 113: 41–53.

McCarthy, P T, and L R Cerecedo. 1952. “Vitamin A Deficiency in the Mouse..” *The Journal of Nutrition* 46: 361–76. doi:10.1002/mnfr.201600031.

Moore, T, and P D Holmes. 1971. “The Production of Experimental Vitamin a Deficiency in Rats and Mice..” *Laboratory Animals* 5: 239–50.

Myhre, A M, N Takahashi, R Blomhoff, T R Breitman, and K R Norum. 1996. “Retinoylation of Proteins in Rat Liver, Kidney, and Lung in Vivo..” *Journal of Lipid Research* 37: 1971–77.

Prouty, A M, I E Brodsky, S Falkow, and J S Gunn. 2004. “Bile-Salt-Mediated Induction of Antimicrobial and Bile Resistance in Salmonella Typhimurium..” *Microbiology (Reading, England)* 150 (Pt 4): 775–83. doi:10.1099/mic.0.26769-0.

Reboul, E. 2013. “Absorption of Vitamin a and Carotenoids by the Enterocyte: Focus on Transport Proteins.” *Nutrients* 5: 3563–81. doi:10.3390/nu5093563.

Soofi, S, S Cousens, S P Iqbal, T Akhund, J Khan, I Ahmed, A K M Zaidi, and Z A Bhutta. 2013. “Effect of Provision of Daily Zinc and Iron with Several Micronutrients on Growth and Morbidity Among Young Children in Pakistan: a Cluster-Randomised Trial..” *Lancet* 382: 29–40. doi:10.1016/S0140-6736(13)60437-7.

Stipanuk, M H, and M A Caudill. 2013. *Biochemical, Physiological, and Molecular Aspects of Human Nutrition*. Elsevier Health Sciences.

Takahashi, N, and T R Breitman. 1991. “Retinoylation of Proteins in Leukemia, Embryonal Carcinoma, and Normal Kidney Cell Lines: Differences Associated with Differential Responses to Retinoic Acid..” *Archives of Biochemistry and Biophysics* 285: 105–10.

Tebo, B M, and A Y Obraztsova. 1998. “Sulfate-Reducing Bacterium Grows with Cr (VI), U (VI), Mn (IV), and Fe (III) as Electron Acceptors.” *FEMS Microbiology Letters*.

Thanassi, D G, L W Cheng, and H Nikaido. 1997. “Active Efflux of Bile Salts by Escherichia Coli..” *Journal of Bacteriology* 179. American Society for Microbiology (ASM): 2512–18.

Veenemans, J, P Milligan, A M Prentice, L R A Schouten, N Inja, A C van der Heijden, L C C de Boer, et al. 2011. “Effect of Supplementation with Zinc and Other Micronutrients on Malaria in Tanzanian Children: a Randomised Trial..” *PLoS Medicine* 8: e1001125. doi:10.1371/journal.pmed.1001125.

Figure Legend

Figure 1. An *in vivo* model of interactions between *B. vulgatus* and vitamin A. (**A**) Under vitamin A sufficient conditions retinol is released from dietary retinyl esters by the activity of host enzymes and interacts with bile and *B. vulgatus*. *In vitro* data suggests that *B. vulgatus* is inhibited or killed by this interaction, whereas *B. dorei* (or other retinol-resistant organisms) thrive in the presence of vitamin A. (**B**) Under vitamin A deficient conditions, the balance between vitamin A sensitive (*B. vulgatus*) and resistant (*B. dorei*, other organisms) is not tipped in favor of resistant organisms. See Chapter 2 for further mechanistic discussion.

Figure

Figure 1.

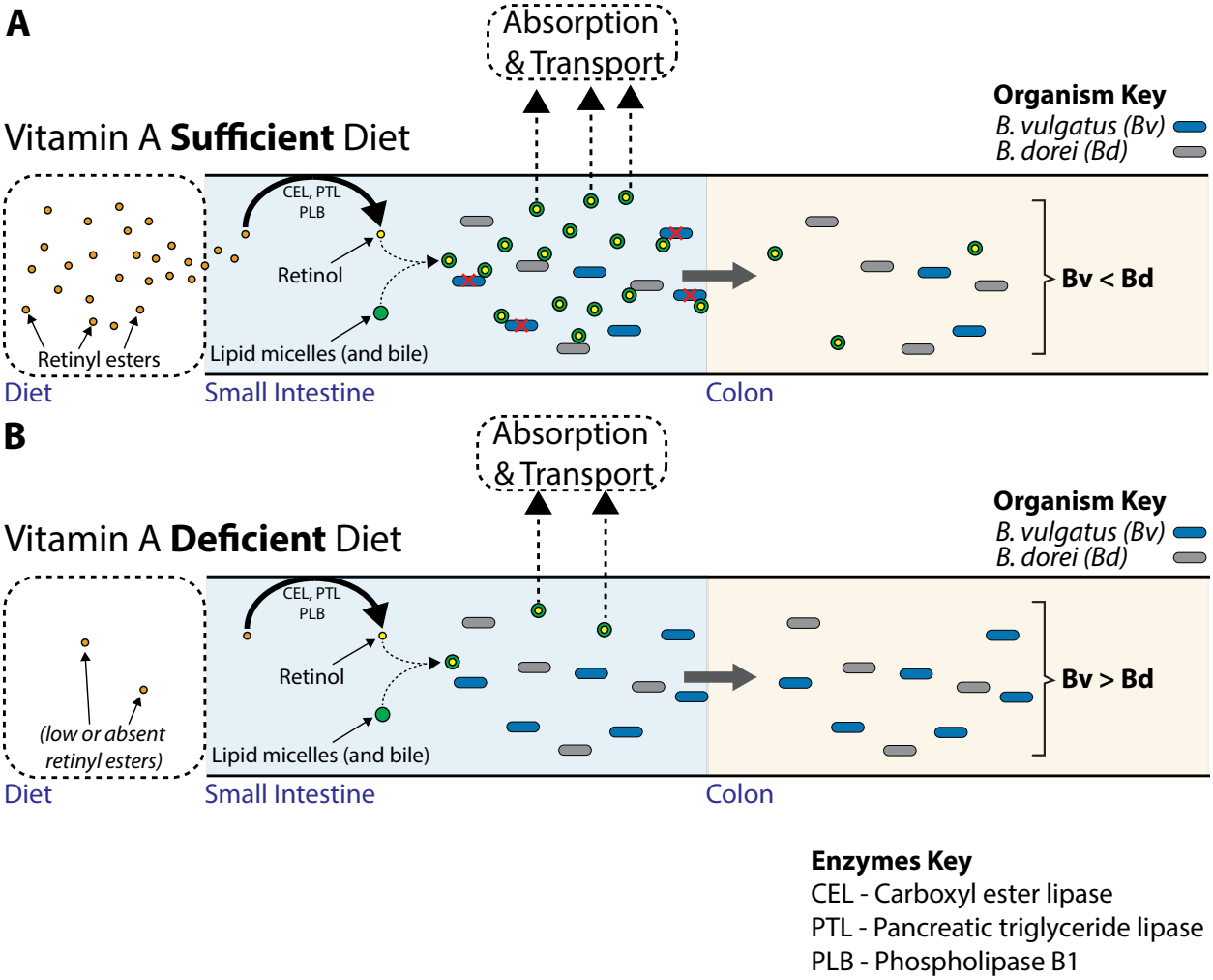

Enzymes Key
CEL - Carboxyl ester lipase
PTL - Pancreatic triglyceride lipase
PLB - Phospholipase B1